Australian Government
Geoscience Australia

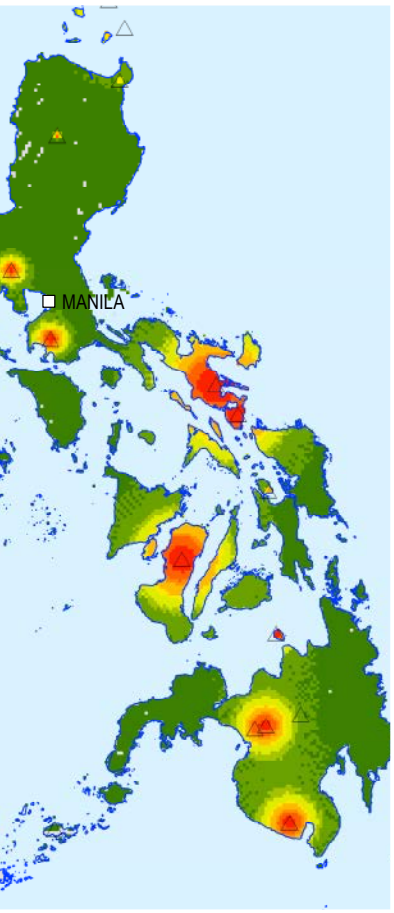

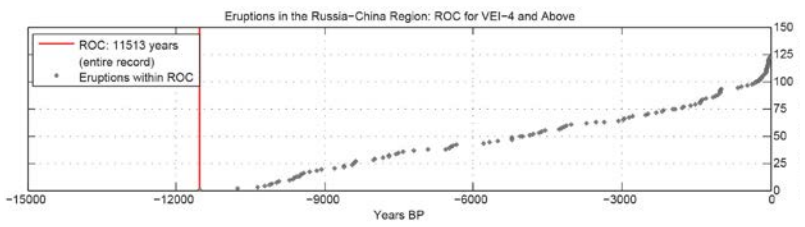

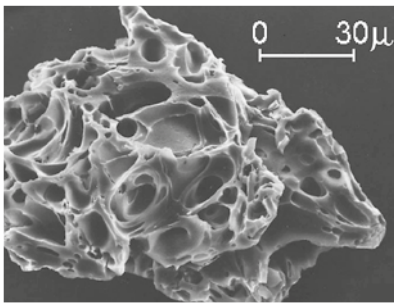

Record 2014/36 | **GeoCat** 81611

Emulating volcanic ash fall for multi-scale analysis:

Development of the VAPAHR tool and application to the Asia-Pacific region for the United Nations Global Assessment Report 2015

Bear-Crozier, A. N.[1], Miller, V.[1], Newey, V.[1], Horspool, N.[1] and Weber, R.[1]

Emulating volcanic ash fall for multi-scale analysis:

Development of the VAPAHR tool and application to the Asia-Pacific region for the United Nations Global Assessment Report 2015

GEOSCIENCE AUSTRALIA
RECORD 2014/36

Bear-Crozier, A. N.[1], Miller, V.[1], Newey, V.[1], Horspool, N.[1] and Weber, R.[1]

Australian Government
Geoscience Australia

1. Geoscience Australia

Department of Industry
Minister for Industry: The Hon Ian Macfarlane MP
Parliamentary Secretary: The Hon Bob Baldwin MP
Secretary: Ms Glenys Beauchamp PSM

Geoscience Australia
Chief Executive Officer: Dr Chris Pigram
This paper is published with the permission of the CEO, Geoscience Australia

ISSN 2201-702X (PDF)

ISBN 978-1-925124-36-1 (PDF)

GeoCat 81611

Bibliographic reference: Bear-Crozier, A. N., Miller, V., Newey, V., Horspool, N. and Weber, R. 2014. *Emulating volcanic ash fall for multi-scale analysis: Development of the VAPAHR tool and application for the Asia-Pacific region for the United Nations Global Assessment Report 2015*. Record 2014/36. Geoscience Australia, Canberra. http://dx.doi.org/10.11636/Record.2014.036

Corrigenda

- Nomenclature for equation (2) previously incorrect has been corrected; page 16.
- Nomenclature for equation (4) previously incorrect has been corrected; page 17.

Contents

Acronyms

Acronym	Description of Acronym
AEP	Annual Exceedance Probability
ALPE	Ash Load Prediction Equation
ARI	Annual Recurrence Interval
CAPRA	Central American Risk Assessment Capability
CIMNE	International Centre for Numerical Methods in Engineering
CPU	Central Processing Unit
EQRM	Earthquake Risk Model
GA	Geoscience Australia
GAR	Global Assessment Report
GED	Global Exposure Database
GEM	Global Earthquake Model
GMPE	Ground Motion Prediction Equation
GVM	Global Volcano Model
GVP	Global Volcanism Program
HFA	Hyogo Framework for Action
MER	Mass Eruption Rate
NCI	National Computing Infrastructure
NGI	Norwegian Geotechnical Institute
PGA	Peak Ground Acceleration
PSHA	Probabilistic Seismic Hazard Analysis
PTHA	Probabilistic Tsunami Hazard Analysis
PVAHA	Probabilistic Volcanic Ash Hazard Analysis
ROC	Record of Completeness
UNISDR	United Nations International Strategy for Disaster Reduction
UNODRR	United Nations Office for Disaster Risk Reduction
VAPAHR	Volcanic Ash Probabilistic Assessment tool for Hazard and Risk
VEI	Volcano Explosivity Index

Glossary

Term	Description of term
Caldera	A caldera is a large, usually circular depression at the summit of a volcano formed when magma is withdrawn or erupted from a shallow underground magma reservoir (Source: USGS).
Disaggregation	To divide into constituent parts (i.e. the factors which contribute to the hazard at a particular site by VEI, source, type etc.).
Distal	Distant from volcanic source.
Isopach Map	Volcanic ash thickness contour map.
Lapilli	Rock fragments between 2 and 64 mm (0.08-2.5 in) in diameter that were ejected from a volcano during an explosive eruption (Source: USGS).
Large Cone	Steep, conical volcanoes built by the eruption of viscous lava flows, tephra, and pyroclastic flows (also known as stratovolcanoes or composite volcanoes; Source: USGS).
Lava Dome	Volcanic domes are rounded, steep-sided mounds built by very viscous magma (Source: USGS).
Plinian	Plinian eruptions are large explosive events that form enormous dark columns of tephra and gas high into the stratosphere (>11km; (Source: USGS).
Proximal	Close to volcanic source.
Pyroclasts	Fragmented magma ejected from a volcano during an explosive eruption (see also Tephra; (Source: USGS).
Shield	Shield volcanoes are characterised by broad, gentle slopes, built by the eruption of fluid basalt lava (Source: USGS).
Small Cone	Small, steep-sided, conical-shaped hills of volcanic fragments that accumulate around and downwind from a vent (also known as cinder cones; (Source: USGS).
Strombolian	Strombolian eruptions are characterized by the intermittent explosion or fountaining of magma from a single vent or crater (Source: USGS).
Sub-Plinian	Sub-Plinian eruptions are explosive eruptions of intermediate in size/volume between Vulcanian and Plinian style eruptions (Source: USGS).
Tephra	Tephra is a general term for fragments of volcanic rock and lava regardless of size that are blasted into the air by explosions or carried upward by hot gases in eruption columns or lava fountains (Source: USGS).
Viscosity	The resistance to flow of magma.
Vulcanian	A vulcanian eruption is a moderate-sized explosive eruption that ejects new lava fragments that do not take on a rounded shape during their flight through the air (Source: USGS).

List of Figures

List of Tables

Acknowledgments

The authors gratefully acknowledge the financial support for this project provided by Australian Aid (Department of Foreign Affairs and Trade) The authors also greatly acknowledge L. Metz and T. Kuske for their constructive reviews and A. Jones (GA), J. Schneider (GA) and A. Simpson (GA/GFDRR) for their invaluable guidance and support in the development of this methodology and report and J. Walker (GA) for overseas travel logistical support.

Executive Summary

Background

The management of natural hazard risk is central to ensuring the sustainability of communities and economic activity within a country (Maqsood et al., 2014). This risk is particularly high in some developing nations as a result of the nature of local building stock, the size of human populations and a high natural hazard. This risk is manifested in severe events which inflict considerable damage, loss of life, socio-economic disruption and place acute demands on emergency services. Ultimately, these often devastating consequences can only be addressed with the uptake of effective and targeted disaster risk reduction strategies based on reliable risk information. Consistent information of this kind can enable decision makers to identify, quantify and manage risk with the objective of reducing it at a national scale.

The Global Assessment Report on Disaster Risk Reduction (GAR) seeks to provide a progressively improving evidence base on natural hazard risks globally and to measure the uptake of strategies to reduce these. It is a biennial global assessment of disaster risk reduction and is a comprehensive review and analysis of the natural hazards that are affecting humanity. The assessment includes the results of probabilistic risk assessments across a range of hazards that quantitatively integrate severe hazard likelihood, community exposure and the vulnerability of the assets of value. The GAR forms part of the United Nations International Strategy for Disaster Reduction (UNISDR) and contributes to achieving the Hyogo Framework for Action (HFA). The report is produced through collaboration and consultation with a wide range of stakeholders and draws upon academic and research institutions, technical organisations and specialists engaged in natural hazard risk analysis and assessment. Geoscience Australia (GA) has been one of these collaborators since April 2012.

Geoscience Australia participated in a review of the GAR13 report in late 2012 and concluded that the approach taken for assessing global probabilistic risk was pragmatic. As part of a review of the GAR13 report, GA highlighted an opportunity for the inclusion of volcanic risk in future assessments of the Asia-Pacific region. GA has developed probabilistic volcanic ash hazard assessments for a number of regional countries through a range of strategies. On this basis the opportunity for GA to develop a multi-scale probabilistic volcanic ash hazard assessment applicable to the Asia-Pacific region has been taken forward utilising funding from Australian Aid and the UN. This report describes the ensuing research activity and its outcomes in support of GAR15. It complements other GA activities for GAR15 supported by Australian Aid in tsunami, vulnerability and earthquake hazard analysis.

The GAR Risk Modelling Approach

The GAR risk modelling approach has been developed progressively by the United Nations Office for Disaster Risk Reduction (UNODRR) in Geneva and the International Centre for Numerical Methods in Engineering (CIMNE) in Barcelona (Maqsood et al., 2014). The UNODRR has led the development of the series of GARs and serves as its secretariat. The approach taken for the GARs has been practical in the adopted spatial resolution and in its utilisation of data developed and maintained by others. For GAR15 the resolution of exposure is coarse at a typical tile size of 5km by 5km, reducing to 1km by

1km in coastal regions exposed to riverine flooding and tsunami. The definition of the exposure information in each tile draws on several information sources with the building construction mix based on the global exposure definition developed and maintained by the World Agency of Planetary Monitoring and Earthquake Risk Reduction (WAPMERR) in Geneva. This framework categorises the building stock into vulnerability classes and is effectively the primary definition of building vulnerability classes used in GAR15.

The GAR approach to attributing vulnerability entails defining up to four resistance levels for each of the GAR15 building classes and mapping these to a national exposure database on the basis of the development level of the country, the size of its communities and the local hazard that may have influenced building resistance. Finally, these risk elements of exposure and vulnerability have been integrated into a risk modelling approach that has been implemented on the Central American Platform for Risk Assessment (CAPRA).

Probabilistic Volcanic Ash Hazard Assessment (PVAHA) and the Volcanic Ash Probabilistic Assessment tool for Hazard and Risk (VAPAHR)

The volcanic ash hazard work reported herein is compatible with the GAR approach to risk modelling adopted by the UN. The first objective was to develop a framework for multi scale Probabilistic Volcanic Ash Hazard Analysis (PVAHA) by adapting Probabilistic Seismic Hazard Analysis (PSHA), considered the global standard for developing seismic hazard information for volcanic ash. The second objective was to develop the Volcanic Ash Probabilistic Assessment tool for Hazard and Risk (VAPAHR) as a mechanism to facilitate PVAHA at multiple spatial scales. The final objective was to implement the PVAHA framework and the VAPAHR tool and provide a broad overview of regional scale volcanic ash hazard for the Asia-Pacific to inform a partial volcanic ash risk assessment for the GAR15 and more generally for prioritising areas for more detailed local-scale hazard assessments.

VAPAHR outputs have been designed to be compatible with and incorporated into risk models such as the CAPRA/CIMNE risk-modelling platform (CIMNE et al., 2013). PVAHA outputs from this study were designed to be integrated with vulnerability and exposure information for buildings across the Asia-Pacific region (at the 5 x 5km resolution; (De Bono, 2013)) using the CAPRA risk engine to provide a partial assessment of volcanic ash risk. The VAPAHR tool simplified the process of tailoring outputs for this application (e.g. scale and setting of return periods). However the tool can be configured to run at 1 x 1km resolution if needed for integration with global population datasets.

Outcomes

In the Asia-Pacific region, 276 source volcanoes were included, each characterised by their magnitude-frequency relationships. Sites for analysis within the Asia-Pacific region were limited to land-based locations within 500km of a volcanic vent. This PVAHA developed for the Asia-Pacific region using VAPAHR highlights the degree of volcanic ash hazard across the region as a function of return period. The Indonesian Island Arc system exhibits the greatest volcanic ash hazard in the entire Asia-Pacific region for all observable return periods, with the other volcanic arc systems across the region, particularly Japan, the Philippines, Papua New Guinea (PNG), the Kamchatka peninsula (Russia), and the north island of New Zealand, exhibiting increased volcanic ash hazard at the longer return periods. This PVAHA, which employed all available eruption data for the Asia-Pacific region,

allows us to quickly gauge the relative ash hazard across the region and identify volcanic sources and sites that should be prioritised for more detailed analysis. Results were disaggregated for sites of interest (e.g. Jakarta, Indonesia; Manila, the Philippines; Port Moresby, Papua New Guinea and Tokyo, Japan) in order to demonstrate how this multi-scale event-based approach allows for the rapid dissemination and disaggregation of results to identify priority areas subject to high volcanic ash hazard and the broader implications of this for disaster risk reduction efforts. This PVAHA was delivered to the CAPRA team and integrated with vulnerability and exposure information using the CAPRA risk engine to provide a partial assessment of volcanic ash risk for the Asia-Pacific region, the results of which will be presented as part of GAR15.

Recommendations for future research

The PVAHA methodology presented here is fully customisable and can be modified to reflect advances in our understanding of the dynamics of volcanic ash dispersal, improvement of statistical analysis techniques for historical eruptive events and ever increasing capabilities in high-performance computing. There is no limit to the number of ash dispersal models which could be used and this allows multiple competing hypotheses on models and parameters to be incorporated into the analysis.

This first step towards a fully probabilistic model of volcanic ash hazard for the Asia-Pacific region will be refined through the incorporation of updated eruption data when manifested and the inclusion of finer resolution meteorological models. In this manner, we can move towards a better understanding of the relative volcanic ash hazard in the Asia-Pacific region that can be updated quickly and easily as new information becomes available.

The VAPAHR tool currently addresses hazard, however the modular nature of the tool also supports a framework for risk analysis. For example, a python module for damage (i.e. building damage, infrastructure damage or agricultural crop damage), containing vulnerability functions for volcanic ash could be developed and integrated into the VAPAHR tool. Through integrating the hazard module (presented here) with a damage module, the conditional probability of damage (or loss in dollars) for an exposed element could be calculated for a given threshold of volcanic ash load. The resulting damage curves could be integrated with an exposure data module (e.g. population density, building footprints and crop extents) for the region of interest and the potential impact of events could be quantified in a risk framework.

1 Introduction

The GAR is a biennial global assessment of disaster risk reduction and is a comprehensive review and analysis of the natural hazards that are affecting humanity. The GAR forms part of the UNISDR and contributes to achieving the HFA. In doing this, the GAR analyses risk patterns and trends, examines progress in disaster risk reduction and provides strategic policy guidance to countries and the international community. The assessment includes the results of probabilistic risk assessments across a range of hazards. The report is produced through collaboration and consultation with a wide range of stakeholders and draws upon academic and research institutions, technical organisations and specialists engaged in natural hazard risk assessment. Geoscience Australia has been one of these collaborators since April 2012.

As part of a review of the GAR13 report, GA highlighted an opportunity for the inclusion of volcanic risk in future assessments of the Asia-Pacific region. GA has developed probabilistic volcanic ash hazard assessments for a number of regional countries through a range of strategies. These have included the engagement and capacity building of volcanologists in counterpart agencies across the region, individually and collectively as expert hazard specific groups through Australian Aid funded projects. This initiative has been taken forward utilising funding from Australian Aid and the UN. This report describes the ensuing development and implementation of PVAHA for the Asia-Pacific region and its outcomes. It complements other GAR activities by GA that are being supported by Australian Aid in vulnerability, tsunami and earthquake hazard assessment.

In this report, background to the GAR15 report is provided and the approach taken by the UNISDR team to develop probabilistic risk information on a global scale is summarised. The implications of this approach to volcanic ash hazard information development are identified and discussed in describing an innovative, new approach for multi-scale PVAHA, developed at GA that is integrated into the GAR15 work. The report separately describes the PVAHA undertaken for the Asia-Pacific, used to inform the volcanic risk assessment for GAR15. Finally recommendations are made for future volcanic ash knowledge development in the region.

1.1 United Nations International Strategy for Disaster Reduction

The probabilistic volcanic ash hazard work reported herein was undertaken to be compatible with and implementable within the risk modelling framework being used for the GAR15. In this chapter, the role of probabilistic volcanic ash hazard assessment in the context of the GAR activity is described along with an overview of how the outcomes of the volcanic ash sub-component will underpin the GAR15 volcanic risk modelling work. Finally, the volcanic ash sub-component contributions made in this research and other supporting work towards GAR15 funded by Australian Aid are outlined.

1.2 GAR 15 Risk Assessment Framework

The global risk modelling used for GAR is based on a probabilistic risk analysis approach which quantifies losses due to possible future events. The aim of the global risk assessment is to provide an overview of the risk (and losses) and encourage countries to act upon this information. The GAR risk

modelling has required the development of a Global Exposure Database (GED). The GED focusses primarily on buildings within communities and enables severe hazard related, physical damage related losses to be assessed. It has been developed to suit the coarse grained type of indicative risk assessment adopted by GAR with exposure aggregated to 5 x 5km grid cells for earthquake, wind and volcanic ash hazards and to 1 x 1km grid cells for the more localised hazards of flood and tsunami.

For the probabilistic risk assessment in GAR15, the vulnerability of exposed elements is assessed using vulnerability functions (Maqsood et al., 2014). These relate the hazard intensity to the expected mean damage index together with the expected variance of this value. The damage index is a measure of the direct physical damage to the building fabric and is the expected outcome for a population of buildings rather than that of an individual building (CIMNE et al., 2013). These functions are called vulnerability curves and they are developed for each building type so that a particular vulnerability curve can be assigned to each one of the building types in the exposure database. Furthermore, when considering earthquake and severe wind hazards, a suite of vulnerability curves is utilised for each building type, one for each of four resistance levels (High, Medium, Low and Poor). Resistance level is a term used to describe local variations in building vulnerability that may occur within a single region due to local construction practices, code compliance level or variable hazard level within a country. For a given building type, the appropriate vulnerability curve relating to High, Medium, Low or Poor resistance level is determined on the basis of Country Development Level (measured by gross national income per capita), Complexity Level of the urban area (measured by settlement population) and local Hazard Level. GA coordinated the development of a heuristic suite of regional vulnerability functions across five hazards (earthquake, severe wind, flood, volcanic ash and tsunami) for GAR15 through collaboration with key experts who have a rich and broad experience in the building types to be assessed and familiarity with local construction practices (Maqsood et al., 2014).

1.3 Australian Aid funded Volcanic Ash Sub-Component

Australia's Aid program within the Department of Foreign Affairs has directly supported GA's contribution to the 2013 and 2015 GARs since April 2012. The overarching aims of this contribution included increasing the scientific and technical rigour in GAR15, and ensuring a greater Asia-Pacific region focus in GAR15. The task to develop a probabilistic volcanic ash hazard assessment for the Asia-Pacific region was a contribution directed at these aims. This entailed establishing a new and innovative framework for assessing and expressing the probability of volcanic ash hazard for a site(s) of interest across multiple spatial scales (PVAHA) based on analogue approaches developed for multi-scale earthquake and tsunami hazard assessments (PSHA and PTHA). In addition, a tool (VAPAHR) was developed as a mechanism for facilitating the analysis of the Asia-Pacific region for GAR15.

Other Australian Aid funded tasks undertaken by GA to achieve the overarching aims, included:

- The development of a heuristic suite of regional vulnerability functions across five hazards (earthquake, severe wind, flood, volcanic ash and tsunami);
- The development of a tsunami hazard analysis for the Asia-Pacific for the tsunami component of GAR15 through engagement between GA and the Norwegian Geological Institute (NGI);
- The development of an upgraded global earthquake analysis for GAR15 through engagements between GA and regional partners in earthquake hazard and risk. These included GNS Science in New Zealand and the Global Earthquake Model (GEM) based in Pavia, Italy.

The hazard results were validated against local and provincial scale studies in the Asia-Pacific already undertaken by GA in order to ensure consistency and validity of GAR15 products. Once quality assured, the scientific outputs from these activities were provided to the CAPRA team who were tasked by UNISDR to conduct the global risk assessment for GAR15.

2 Introduction to volcanic ash

2.1 Background

Volcanic ash represents a serious hazard to many towns, cities and even megacities (population in excess of 10 million) in the vicinity of active volcanoes in developing countries across the Asia-Pacific region. Volcanic ash hazard maps are essential tools for contingency planning and to assist decision makers when establishing mitigation procedures (Costa et al., 2009; Macedonio et al., 2008). Undertaking volcanic ash hazard assessments is an important scientific, economic and political exercise and of great importance to public safety. One-third of the world's largest volcanic eruptions (since 1800) have taken place within the Asia-Pacific region.

Explosive volcanic eruptions eject large quantities of lapilli, coarse ash and fine ash pyroclasts into the atmosphere over relatively long periods of time. Pyroclastic particles can be transported and emplaced close to ground surface through entrainment by pyroclastic density currents or dispersed through the atmosphere as pyroclastic fallout. The largest blocks and bombs typically follow a ballistic trajectory and are deposited close to the eruptive source whereas lapilli, coarse ash and fine ash pyroclasts can remain airborne for hours, days or years (Rose and Durant, 2011). The rate and distance over which pyroclasts are dispersed is dependent on the effects of gravity, wind advection (wind speed and direction) and atmospheric turbulence. Individual pyroclasts are dispersed depending on their terminal settling velocity where coarser-grained pyroclasts (lapilli) settle closer to the source than finer-grained pyroclasts (coarse and fine ash). Pyroclasts dispersed through the atmosphere, collectively referred to here as volcanic ash fallout, affect vast areas proximally (tens km), medially (hundreds km) and distally (thousands km) from the source vent (Folch and Sulpizio, 2010). This has important implications for communities living in the vicinity of active volcanoes.

2.2 Volcanic ash impacts

Volcanic ash is the most widespread of all volcanic hazards and has the potential to affect hundreds of thousands of people in the densely populated islands of the Asia-Pacific region. Volcanic eruptions generate convecting plumes of gas, ash and rock fragments and can distribute large volumes of ash over hundreds of kilometres. The dispersal of volcanic ash is highly dependent on the size of an eruption and the speed and direction of prevailing wind conditions.

Volcanic ash can cause a wide variety of detrimental effects (Figure 1):

- The accumulation of volcanic ash on the roof tops of buildings can cause structural damage/collapse leading to casualties and/or loss of essential services.
- Volcanic ash is abrasive and may be coated with a film of corrosive acid that can damage machinery, corrode metallic surfaces and disrupt electrical systems (i.e. communications)
- Differences in chemical composition between volcanic ash and the surrounding soil can result in soil contamination.
- Volcanic ash deposition on plants can damage/destroy crops (i.e. ash prevents photosynthesis).
- Volcanic ash can contaminate water supplies and ingestion can lead to adverse health effects.

- Volcanic ash in the atmosphere can significantly damage aircraft and result in widespread airport closures.
- Inhalation of volcanic ash can lead to respiratory and ocular problems.
- Fine grained volcanic ash suspended in the atmosphere can reduce visibility conditions leading to traffic disruptions and accidents.

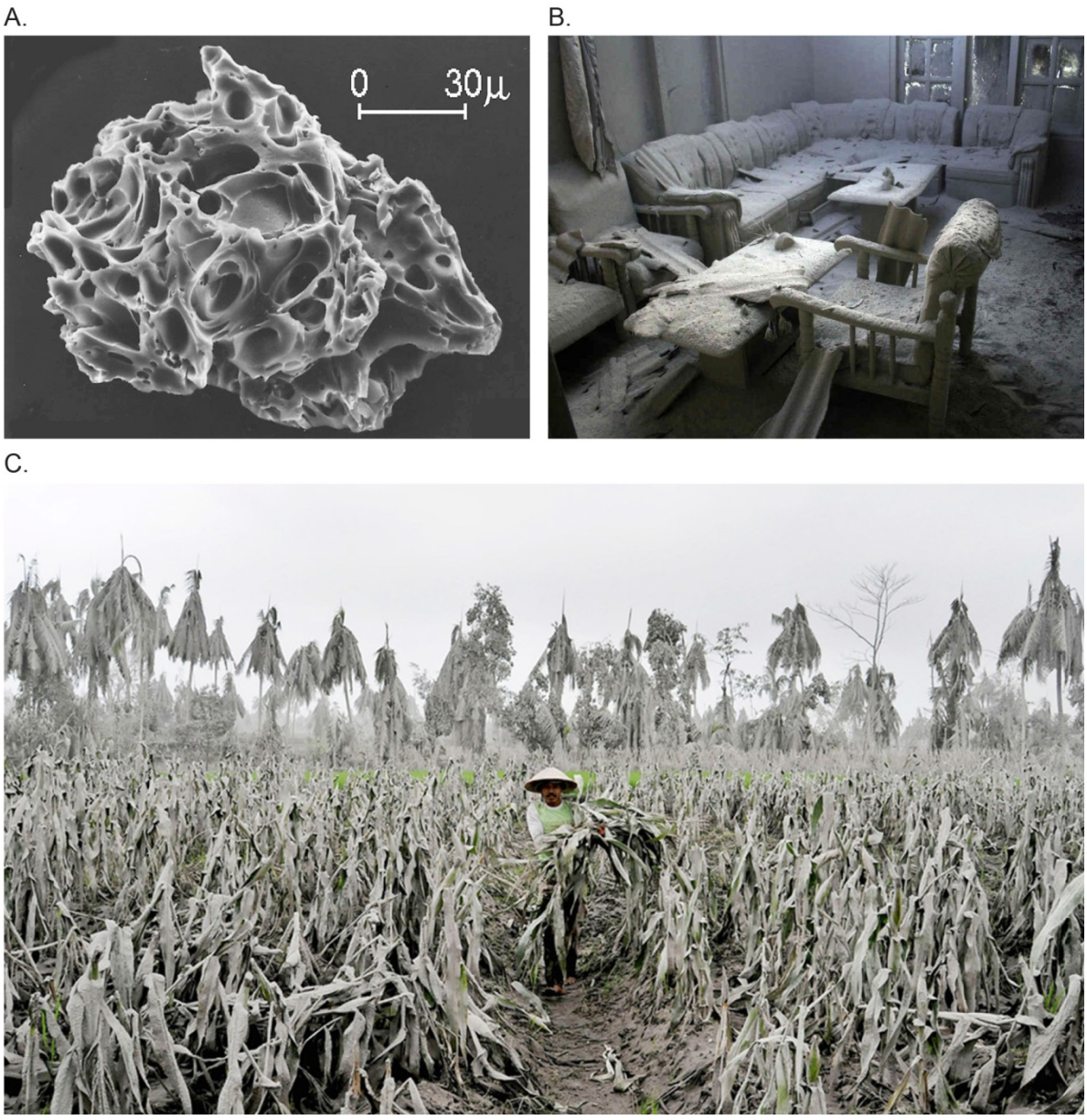

Figure 1 *Volcanic Ash; A. Scanning electron microscopic (SEM) image of a volcanic ash particle featuring the abrasive, angular texture of the clast (Source: A.M Sama-Wojcicki, USGS); B. Furniture covered by volcanic ash in a house in a village during the eruption of Mount Merapi in Kinahrejo, Yogyakarta, Indonesia, Wednesday, Oct. 27, 2010 (Source: Slamet Riyadi/AP).*

2.3 Previous work in volcanic ash hazard analysis

Numerous approaches have been adopted in the past to assess volcanic ash hazard at the local-scale (10s kms) including observational, statistical, deterministic and probabilistic techniques (Bear-Crozier et al., 2012; Blong, 2003; Bonadonna and Houghton, 2005; Bonadonna et al., 2002a; Bonadonna et al., 2002b; Costa et al., 2006; Folch et al., 2009; Folch and Sulpizio, 2010; Jenkins et al., 2012a; Jenkins et al., 2012b; Simpson et al., 2011) (Figure 2). However, incomplete historical data on the magnitude and frequency of eruptions worldwide and the difficulties associated with up-scaling computationally intensive volcanic ash dispersal models have limited regional or global scale assessments (100s kms).

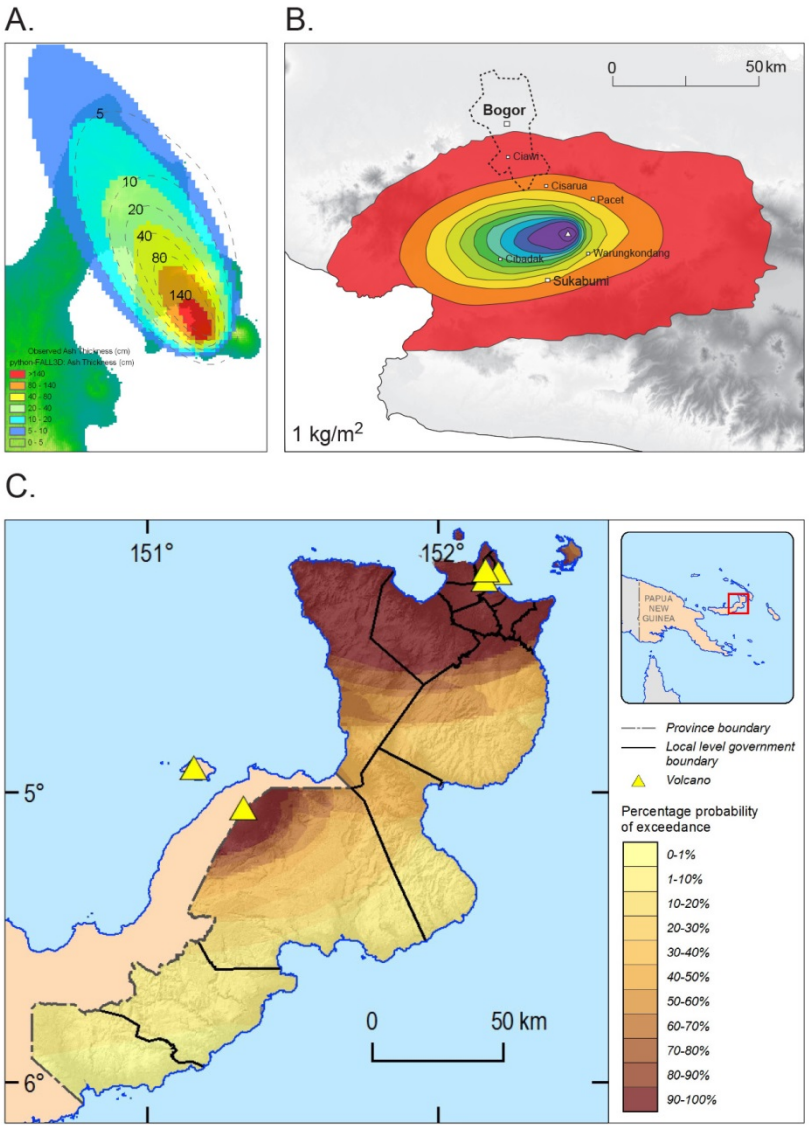

Figure 2 *Examples of volcanic ash hazard maps generated by observational, deterministic and probabilistic methods; A. Isopach (ash thickness) contours (dotted black lines) based on field observations of ash fallout on the ground during the 1994 eruption of Tavurvur, Rabaul. Also depicted in a rainbow colour palette are contours for volcanic ash thickness modelled using a tephra dispersal model for a deterministic scenario (e.g. one eruption, one wind direction) B. Volcanic ash ground load probability map for Gunung Gede, Java Indonesia produced using a tephra dispersal model showing probability in % that the volcanic ash load will exceed 1kg/m^2 for rainy season wind conditions (i.e. one source (Gede), multiple wind profiles) (Bear-Crozier et al., 2012); C. Volcanic*

ash ground load probability map for East New Britain Province, Papua New Guinea produced using a tephra dispersal model showing probability in % that the cumulative volcanic ash load on the ground from five volcanoes of interest will exceed 1kg/m^2 during dry season wind conditions (i.e. multiple sources (Tavurvur, Vulcan, Rabaul, Ulawun and Lolobau) and multiple wind profiles)(Bear-Crozier et al., 2013)

Simple assessments of volcanic ash hazard are based on compiling observations of the distribution of volcanic ash from historical eruptions, an approach that is still adopted worldwide (Barberi et al., 1990; Bonadonna et al., 1998; Costa et al., 2009; McKee et al., 1985). These maps discriminate land areas buried by volcanic ash fallout in the past from those that have not. Building on observational methods, statistical procedures when applied to observed ash fall events are used to estimate ash thickness expected from future events.

Deterministic methods extend the usefulness of statistical and observational methods by utilising the benefits of numerical and computational models and typically consider the causes driving the hazard. The objective of the deterministic approach is usually to address "what is the worst that could happen?" For example, for a particular site of interest, find the nearest volcano, assume that the wind prevails towards this site and calculate what the maximum expected ash load would be for the largest plausible eruption. The advantage of this approach is that it is computationally straightforward and provides a conservative result, which maximises safety. The disadvantage is that subjective and implicit assumptions made on the probability of the chosen scenario commonly result in an over-estimation of conservative hazard values, whereby the largest possible eruption may be possible but highly unlikely.

Probabilistic methods estimate the probability of occurrence of the hazard at a site according to the location, magnitude and frequency of occurrence of hazardous events around that site. They are flexible and can take into account as much data as you have available. Probabilistic methods produce hazard curves, which provide information on the level of expected hazard for any given return period. Incorporating occurrence rate information into hazard analysis is more complex than deterministic, statistical or observational approaches. However, the resulting hazard curve is more useful for prioritising regions where more detailed analysis is needed. Probabilistic approaches to volcanic ash hazard assessment are the focus of this study.

In the past, probabilistic analyses of volcanic ash hazard have focused on quantitative assessments of the frequency and potential consequences of eruptions. Simpson et al. (2011) undertook a quantitative assessment of volcanic ash hazard across the Asia-Pacific region using the Smithsonian Institution's Global Volcanism Program (GVP) database that enabled the straightforward production of magnitude–frequency plots for each country and, to some extent, provinces within countries, in the region. Quantitative approaches have focused on a single source or site of interest at a local scale (10s of km) using tephra dispersal models (e.g. Campi Flegrei, Italy (Costa et al., 2009); Gunung Gede, Indonesia (Bear-Crozier et al., 2012); Okataina, New Zealand (Jenkins et al., 2008); Somma-Vesuvio, Italy (Folch and Sulpizio, 2010) and Tarawera, New Zealand (Bonadonna et al., 2005)). Numerical simulations of volcanic ash fallout generally involve running a deterministic eruptive scenario that represents the most likely event (based on historical investigation and/or modern analogues) over a period of time sufficiently large as to capture all possible meteorological conditions (Bear-Crozier et al., 2012; Folch et al., 2008a; Folch et al., 2008b; Folch and Sulpizio, 2010; Magill et al., 2006).

Regional-scale probabilistic volcanic ash hazard assessments are less common (Hurst and Turner, 1999; Jenkins et al., 2012a; Jenkins et al., 2012b; Magill et al., 2006). Jenkins et al. (2012a; 2012b) developed a probabilistic framework for assessing ash fall hazard at the regional-scale and have

applied this technique to the Asia-Pacific region. This methodology employs a stochastic simulation technique that up-scales implementation of the ash dispersal model ASHFALL for regional-scale assessments (Hurst, 1994; Hurst and Turner, 1999). Ash fall hazard is quantified for each square kilometre grid cell of urban area across a region of interest. Annual Exceedance Probability (AEP), and its inverse, the Average Recurrence Interval (ARI) are generated for ash fall exceeding a targeted threshold thickness of interest. This approach presented a method for assessing regional-scale ash fall hazard which had not been attempted previously and represents an important step forward in the development of techniques of this kind (Jenkins et al., 2012a). However, significant limitations associated with this approach include:

- The computationally intensive nature of up-scaling ash dispersal models for regional-scale applications would require significant high-performance computing resources, long simulation times and could potentially constrain the spatial resolution, geographic extent and number of sources considered;
- Hazard curves of annual exceedance probability versus volcanic ash thickness for individual sites of interest are not generated and therefore;
- Disaggregating the dominant contribution to the hazard at a particular site by magnitude, source or distance is not possible.

2.4 A new approach for GAR15

Workers in other geohazards fields (earthquake, wind, flood etc.) have faced similar limitations associated with quantifying hazard on the regional scale. Major developments were made by seismologists working in this space in the 1960s interested in assessing ground motion hazard at multiple sites associated with potential earthquake activity (Cornell, 1968). A fit-for-purpose methodology was developed for quantifying earthquake hazard at the regional scale named PSHA (Cornell, 1968; McGuire, 1995; McGuire, 2008). PSHA consists of a four-step framework for which uncertainty in size, location and likelihood of plausible earthquakes can be incorporated to model the potential impact of future events (Dhu et al., 2008). An early attempt at adapting part of the PSHA methodology and applying seismologically-based techniques for quantifying hazard to volcanic ash (on a local scale) was reported by Stirling and Wilson (2002) for two volcanic complexes on the North Island of New Zealand (Okataina and Taupo). More recently, tsunami scientists adopted the PSHA technique for tsunami by adapting the procedure to account for the complexities of modelling tsunami propagation (i.e. tsunami wave amplitude).

This record presents a framework for undertaking PVAHA developed at Geoscience Australia based on the PSHA procedure adapted for volcanic ash (Bear-Crozier et al., in revision; Miller et al., in revision). PVAHA considers a multitude of volcanic eruption occurrences and associated volcanic ash load attenuation relationships and produces an integrated description of volcanic ash hazard representing all possible events across a region of interest. The development and implementation of the Volcanic Ash Probabilistic Assessment tool for Hazard and Risk (VAPAHR), as a mechanism for facilitating multi-scale PVAHA, is also presented. VAPAHR outputs can be aggregated to generate maps that visualise the expected volcanic ash hazard for sites across a region at return periods of interest, or disaggregated to determine the causal factors which dominate volcanic ash hazard at individual sites. VAPAHR can be used to identify priority areas for more detailed, local scale ash dispersal modeling that can be used to inform disaster risk reduction efforts.

A regional-scale volcanic ash hazard assessment for the Asia-Pacific was undertaken during the development of the PVAHA methodology and the VAPAHR tool and the results are presented here (Miller et al., in revision). In the Asia-Pacific region, 276 source volcanoes were included, each characterised by their magnitude-frequency relationships. Sites for analysis within the Asia-Pacific region were limited to land-based locations within 500km of a volcanic vent. Results were disaggregated for sites of interest (e.g. Jakarta, Indonesia; Manila, the Philippines; Port Moresby, Papua New Guinea and Tokyo, Japan) in order to demonstrate how this multi-scale event-based approach allows for the rapid dissemination and disaggregation of results to identify priority areas subject to high volcanic ash hazard and the broader implications of this for disaster risk reduction efforts (Miller et al., in revision).

3 Multi-scale probabilistic hazard assessment

3.1 Probabilistic Seismic Hazard Analysis (PSHA)

For decades seismologists have been faced with the inherent difficulty of assessing and expressing the probability of earthquake hazard at a site of interest in terms of maximum credible intensity (Cornell, 1968; McGuire, 1995; McGuire, 2008; Stirling and Wilson, 2002). A fit-for-purpose methodology was developed for quantifying earthquake hazard at the regional-scale (PSHA) (Cornell, 1968; McGuire, 1995; McGuire, 2008; Stirling and Wilson, 2002). PSHA was developed to consider a multitude of earthquake occurrences and ground motions and produce an integrated description of seismic hazard representing all events (Cornell, 1968; McGuire, 1995). The PSHA technique consists of a four-step framework for which uncertainty in size, location and likelihood of plausible earthquakes can be incorporated to model the potential impact of future events (Cornell, 1968; Dhu et al., 2008; McGuire, 1995). Traditional PSHA considers the contribution of magnitude and distance to the hazard at a given site and to produce a uniform hazard spectrum, which represents the ground motion exceedance values as a function of spectral frequency (or period) for a given probability value (McGuire, 1995). Advances in seismic hazard analysis and the proliferation of high-performance computing have led to the development of event-based PSHA (Marrero et al., 2012; Robinson et al., 2006; Robinson et al., 2005).

Event-based PSHA allows for calculation of ground-motion fields from stochastic event sets. Post-processing the set of computed ground-motion fields can generate classical PSHA results, such as hazard curves (Butler et al., 2013). In an earthquake hazard context, stochastic event sets represent collections of earthquakes, where each earthquake is composed of key distinguishing criteria (e.g. magnitude, tectonic region type, source type, rupture geometry etc.).

The four-step procedure for event-based PSHA reported by Musson (2000) is presented in Figure 3A and is summarised below:

1. Seismicity data for the region of interest must be spatially disaggregated into discrete seismic sources.
2. For each seismic source the seismicity is characterised with respect to time (i.e. the annual rate of occurrence of different magnitudes).
3. A stochastic event set is developed which represents the potential realisation of seismicity over time and a realisation of the geographic distribution of ground motion is computed for each event (taking into account the aleatory uncertainties in the ground motion model).
4. This database of ground-motion fields, representative of the possible shaking scenarios that the investigated area can experience over a user-specified time span, are used to compute the corresponding hazard curve for each site. Hazard curves are computed for each event individually and aggregated to form probabilistic estimates.

The PSHA technique has been used to quantify seismic hazard at numerous sites of interest across multiple spatial scales including the Newcastle, region of New South Wales and the Perth region of Western Australia (Fulford et al., 2002; Robinson et al., 2006; Sinadinovski et al., 2005). More recently, the 2012 Australian earthquake hazard map was generated using event-based PSHA facilitated by GA's open-source earthquake hazard and risk model (EQRM) (Burbidge et al., 2012; Robinson et al., 2006) (Figure 3B).

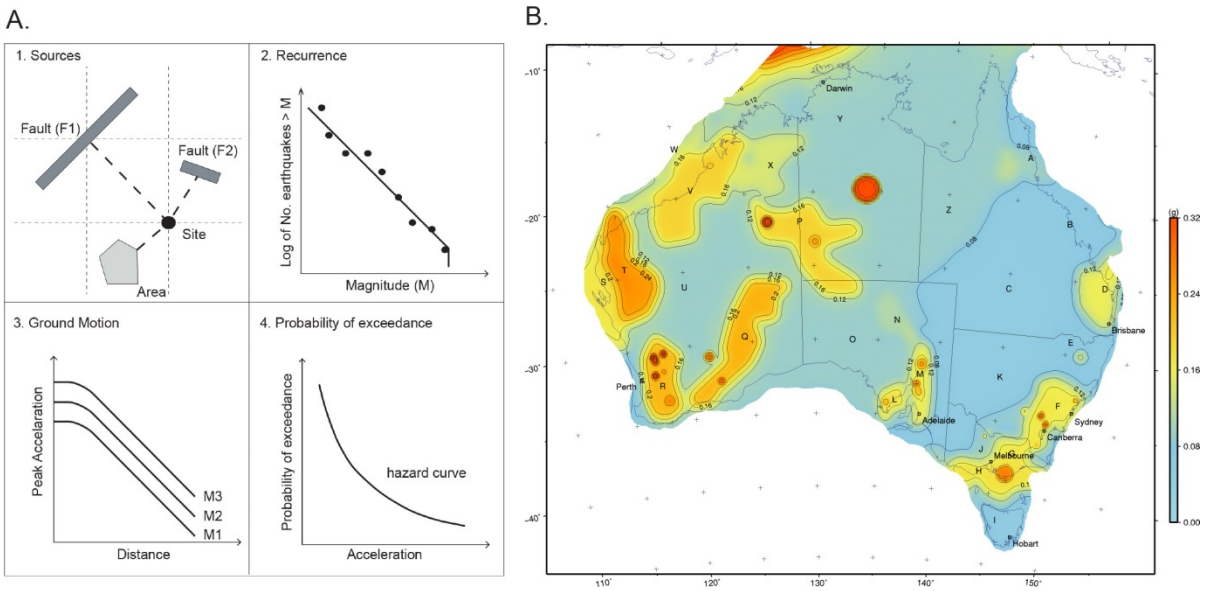

Figure 3 *Probabilistic Seismic Hazard Analysis (PSHA) A. Schematic representation of the four stage procedure for PSHA (modified after (Musson, 2000; TERA, 1980); B. The 500 year return period, Peak Ground Acceleration (PGA) hazard map calculated with a 50/50 weighting smoothed with a 90km wide Gaussian filter. The map is shown in 2D and the State and Territories capital cities are labelled in black. This map is the authors' preferred weighting and smoothing (Burbidge et al., 2012).*

3.2 Probabilistic Tsunami Hazard Analysis (PTHA)

PSHA is considered the global standard for developing seismic hazard information to inform national building codes and underpin seismic risk assessments and has been adapted for assessing other hazard types. Probabilistic Tsunami Hazard Analysis (PTHA) represents a methodology based on the established Monte Carlo approach to PSHA adapted to tsunami (Horspool et al., in press) (Figure 4).PTHA aims to calculate the probability of exceeding a given tsunami wave height over a fixed time period at the coast from tsunami generated by local, regional and distant earthquake sources. PTHA adapts the PSHA framework to account for the complexities of tsunami propagation by incorporating tsunami greens functions that allow rapid computation of the thousands of tsunami events required for probabilistic analysis. GA have undertaken a number of PTHA's both in Australia (e.g. PTHA for Western Australia (Burbidge and Cummins, 2007; Burbidge et al., 2008)) and regionally (e.g. Southwest Pacific PTHA (Thomas and Burbidge, 2009); Indian Ocean PTHA (Burbidge et al., 2009)). More recently, GA has worked with Indonesian scientists to develop the first PTHA for Indonesia (Horspool et al., in press).

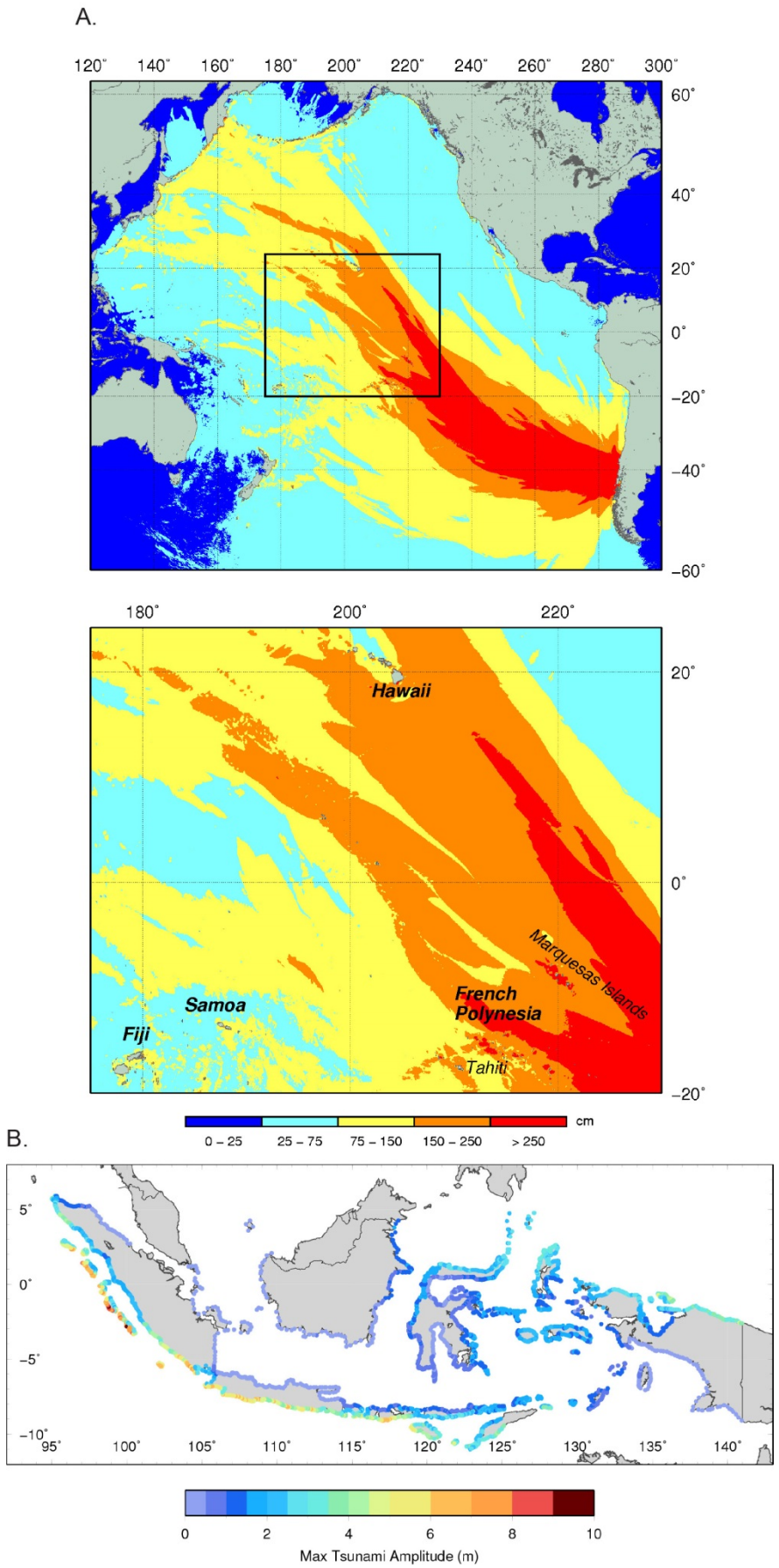
A.
120˚ 140˚ 160˚ 180˚ 200˚ 220˚ 240˚ 260˚ 280˚ 300˚
60˚
40˚
20˚
0˚
−20˚
−40˚
−60˚
180˚ 200˚ 220˚
20˚
0˚
−20˚
Hawaii
Marquesas Islands
French Polynesia
Samoa
Fiji
Tahiti
cm
0 – 25
25 – 75
75 – 150
150 – 250
> 250
B.
5˚
0˚
−5˚
−10˚
95˚ 100˚ 105˚ 110˚ 115˚ 120˚ 125˚ 130˚ 135˚ 140˚
0 2 4 6 8 10
Max Tsunami Amplitude (m)

Figure 4 *Probabilistic Tsunami Hazard Analysis; A. Normalised modelled maximum wave heights of the 1960 Chilean tsunami based on uniform slip model given by Barrientos and Ward (1990). Wave heights have been normalised to 50 metres depth and the maximum is taken over the full time period of the simulation (Thomas and Burbidge, 2009); B. Tsunami hazard map showing maximum tsunami amplitudes at the coast with a 1 in a 100 chance of being exceeded annually (~ 100 year return period; (Horspool et al., in press))*

4 Probabilistic Volcanic Ash Hazard Analysis (PVAHA)

A probabilistic framework for assessing volcanic ash hazard at multiple spatial scales (PVAHA) adapted from the seismologically based PSHA technique for earthquake hazard is presented here (Figure 5). This PVAHA methodology consists of a four-step procedure:

1. Identification of volcanic sources with respect to any given site of interest for a probabilistic assessment of volcanic ash hazard.
2. Assignment of annual eruption probabilities for each volcanic source based on magnitude-frequency relationships.
3. Calculation of volcanic ash load attenuation relationships for a set of stochastic events (synthetic catalogue) using ash load prediction equations (ALPEs) derived from ash dispersal modelling.
4. Calculation of the annual exceedance probability versus volcanic ash hazard for each stochastic event at each site across a region of interest.

The procedures used here for identifying volcanoes of interest (step one), undertaking a statistical analysis of magnitude-frequency relationships for each volcano (step two) and deriving volcanic ash hazard attenuation relationships for a set of stochastic events using ash dispersal modelling (step three) are outlined below. The development and implementation of the VAPAHR tool as a mechanism for undertaking step four is also detailed below.

4.1 Identification of volcanic sources and eruption statistics

The Smithsonian Institution's GVP catalogue of Holocene events was used to identify volcanic sources for analysis (Siebert et al., 2010). The GVP reports on current eruptions from active volcanoes around the world and maintains a database repository on historical eruptions over the past 10,000 years. We acknowledge this database is not a complete record and does contain gaps in the eruption record. Factors that contribute to these gaps, particularly in the Asia-Pacific region include incomplete or non-existent historical record, poor preservation of deposits or lack of accessibility to geographically remote sources. However, the GVP database is widely recognised as the most complete global resource currently available and represents the authoritative source for information of this kind. Other sources of data can be used to augment an analysis of this kind including volcano observatory archive data and other databases including but not limited to the Large Magnitude Explosive Volcanic Eruptions database (Crosweller et al., 2012).

Database fields including volcano ID, region, sub-region, volcano type, volcano name, latitude, longitude, eruption year and VEI (magnitude) were captured for each eruption at each volcano. The data was examined and entries for volcanic sources classified as submarine, hydrothermal, and fumerolic or of unknown type and those with a volcano explosivity index (VEI) of zero, one (non-explosive eruptions) or none were discarded. Sources with no assigned VEI but designated caldera 'C' or Plinian 'P' were included and reclassified as VEI 4 events for the purpose of this analysis.

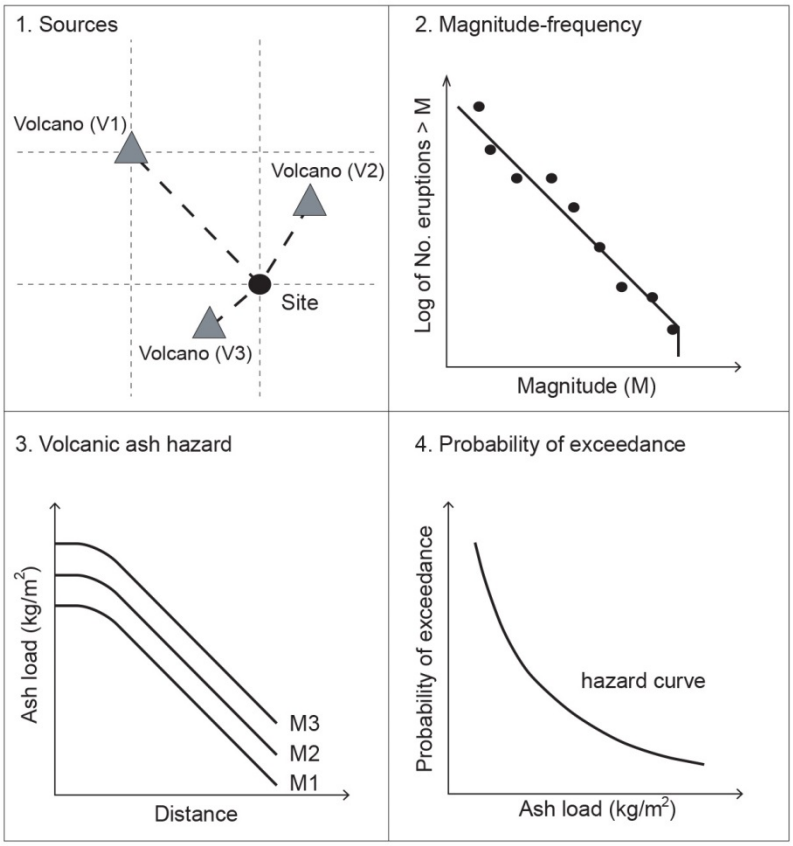

Figure 5 *Schematic representation of the modified PSHA procedure for Probabilistic Volcanic Ash Hazard Analysis (PVAHA).*

4.1.1 Magnitude-frequency relationships

A procedure analogous to developing earthquake magnitude-frequency distributions for PSHA (Musson, 2000) is adopted here to characterise the annual rate of occurrence for eruptions of different magnitudes from each volcanic source. Calculation of these magnitude-frequency relationships for potential sources of volcanic ash hazard follows the methodology outlined by Jenkins et al (2012a) and Simpson et al. (2011). It is important to acknowledge here that volcanic ash hazard at any given site may represent the cumulative hazard from multiple volcanic sources, all of which are likely to have different eruption probabilities, styles and magnitudes (Jenkins et al., 2012a). Therefore, the individual annual eruption probability for each volcanic source is calculated following the procedure outlined below.

4.1.2 Record of completeness

Following assembly of the eruption database it is necessary to assess the eruption record of completeness (ROC). Different magnitude eruptions have different time periods for which the record is relatively complete, and these periods may differ across a region (Simpson et al., 2011). Larger eruptions are better preserved in the record than smaller eruptions and this has important implications for the ROC. A complete record for larger magnitude eruptions might be thousands of years but only tens of years for smaller magnitude eruptions. Magnitude-frequency calculations for the region of interest should reflect this difference.

Eruptions are divided into small magnitude (VEI 2 – 3) and large magnitude (VEI 4 – 7) subsets (Figure 6). Each subset was considered individually by plotting the cumulative number of events against years before present. A 'break in slope' method was used to estimate the ROC for each subset ($ROC_{VEI\ 2\text{-}3}$ and $ROC_{VEI\ 4\text{-}7}$) whereby a complete record is represented by a graph of relatively constant slope leading up to the present time assuming that eruption frequency is relatively constant through time. Only eruptions for a region within the interval deemed to be 'complete' were included in the frequency calculations.

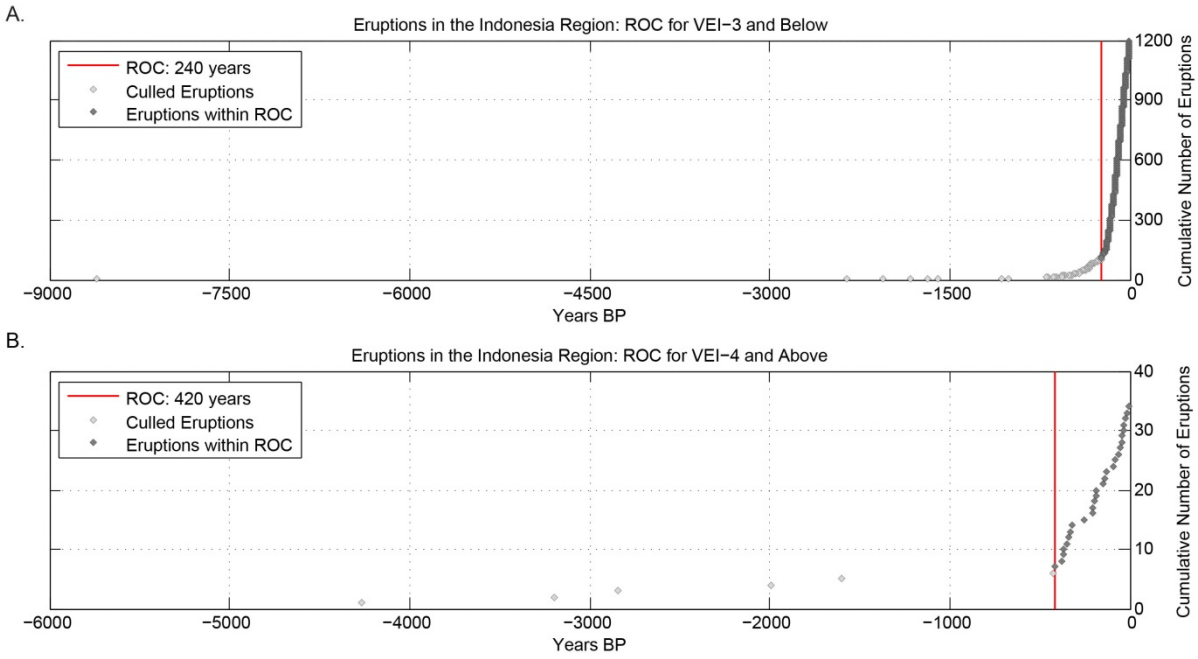

Figure 6 *Example ROC graphs for events in Indonesia; A. Record of completeness (red line) for small magnitude eruptions (ROC VEI 2-3); B. Record of completeness (red line) for large magnitude eruptions (ROC VEI 4-7)*

4.1.3 Probability of an event

The average annual event probability for a volcanic source (λ) is determined by dividing the total number of events (N) by the time period for which the catalogue is thought to be complete (T). This calculation is performed for each source volcano in the small magnitude class (V2-3) to determine the likelihood of an event of any magnitude occurring and under the assumption that past averaged frequency is characteristic of future event frequency. The calculation is repeated for sources in the large magnitude class (V4-7).

$$\lambda = N/T. \quad (1)$$

In order to calculate the likelihood of an event of any magnitude occurring (λV2-7) the ROC for each magnitude class must be aggregated into a single (converted) ROC value (RC) for all magnitudes. This is achieved by normalising the different record lengths to one time period, assuming a constant eruption rate. The factor for converting RV2-3 to RV4-7 is calculated:

$$RC = R_{V4\text{-}7}/R_{V2\text{-}3} \quad (2)$$

The converted number of events for the small magnitude class (NCV2-3) and a normalised total number of events (NV2-7) are calculated:

$$NC_{V2\text{-}3} = N_{V2\text{-}3} * RC \quad (3)$$

$$N_{V2\text{-}7} = NC_{V2\text{-}3} + N_{V4\text{-}7}. \quad (4)$$

Using the normalised total number of events (NV2-7) the likelihood of an event of any magnitude occurring is calculated for each volcanic source:

$$\lambda_{V2\text{-}7} = N_{V2\text{-}7}/R_{V4\text{-}7}. \quad (5)$$

4.1.4 Conditional probability of an event at each magnitude

Having ascertained the probability of an event of any magnitude occurring the conditional probability of that event being VEI 2, 3, 4, 5, 6 or 7 is considered. Each source is assigned a source type related to morphology and previous eruption style (e.g. lava dome, small cone, large cone, shield or caldera).

The conditional probability of each source type erupting at a given magnitude ($P_{VT}|M_{VEI}$) is calculated by dividing the number of events for a given VEI (N_V) by the total number of events for each magnitude class (T_{MC}).

$$P_{VT}|M_{VEI} = N_V/T_{MC}. \quad (6)$$

4.1.5 Annual probability of an event

The annual probability of an event of a given magnitude occurring at each source PEV(x) is calculated by multiplying the annual probability of an event of any magnitude for a source λV2-7 by the probability that the event will be a given magnitude (conditional upon an event of any magnitude) PVT|MV(x):

$$PE_{V(x)} = \lambda_{V2\text{-}7} * P_{VT}|M_{V(x).} \quad (7)$$

Following the methodology of Jenkins et al. (2012a) we use annual probabilities calculated for analogous sources (those of the same source type) as proxies for likely eruption behavior at sources where the record contains few events. For example, the annual probability of a VEI 5 event from a shield type source in Indonesia, calculated based on detailed historical records, can be used as an analogue for other shield-type sources in Indonesia where few or no VEI5 events have been captured in the database. Metadata is developed to preserve the distinction between probability values based on historical data versus analogues.

4.2 Derivation of ash load prediction equations

4.2.1 Stochastic set of events

A stochastic set of events are developed for probabilistic analysis. An estimation of the rate at which volcanic ash load decays with distance from the source, as a function of magnitude, eruptive column height, duration, dispersal model and wind speed is required for the stochastic set of events under consideration. The dispersal of volcanic ash through the atmosphere produces deposits at ground level that diminish gradually in load (kg/m^2) with distance from the source but in directions controlled by the wind. Consequently, ash load attenuation is a complex function of distance and azimuth from source (Stirling and Wilson, 2002). Each event is simulated, using a volcanic ash dispersal model,

forming a synthetic catalogue of events which consider the ground load hazard for all sites of interest, from every possible magnitude, at every possible distance, from every possible volcanic source.

Stochastic events developed here were based on the development of a logic-tree data structure, the purpose of which was to capture and quantify the uncertainty associated with the inputs for each event and thus enable estimation of the resulting uncertainty in the hazard (Bommer and Scherbaum, 2008). The logic tree data structure developed here is presented in Figure 7.

Input parameters include:

- eruption magnitude (VEI between 2 and 7),
- eruption column height (in meters; between 1,000 and 40,000),
- eruption duration (in hours),
- eruption style (from Strombolian through Vulcanian and Sub-Plinian to Plinian) and;
- wind speed (in metres per second and increments of 5, 10, 15 and 20; variations in wind direction are considered in a subsequent step).

A total of 1056 events were developed and each assigned a weighting for probability of occurrence. Events are not volcano specific but rather represent a suite of synthetic eruptions which when coupled with magnitude-frequency statistics can be used to assess a range of potential events at each volcano. It's important to note that assignment of weightings could be refined where detailed knowledge is known about a particular volcanic source or region (i.e. prevailing wind speeds, predominant eruption magnitude etc.) but for the purposes of this study all events are deemed equally probable.

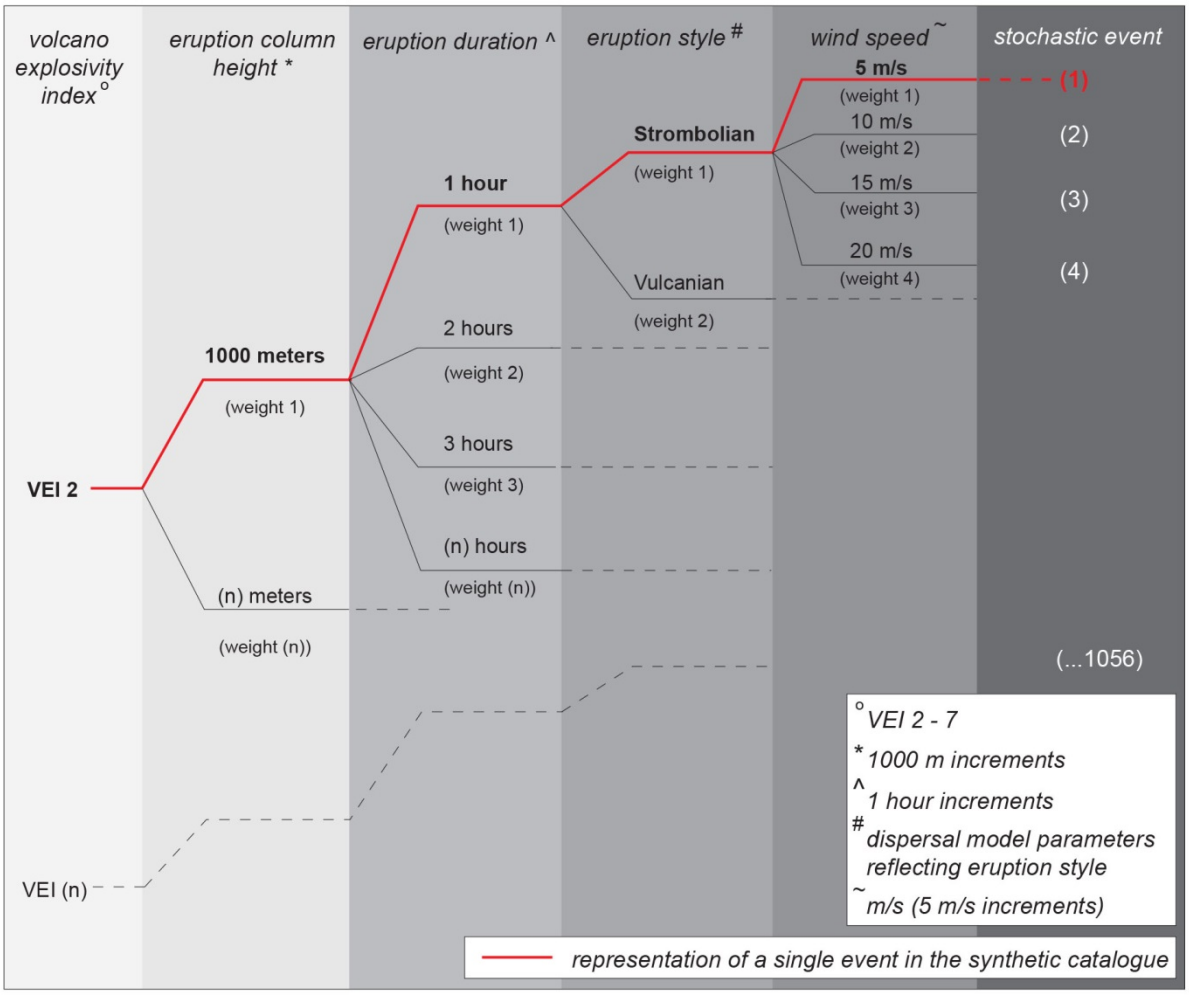

Figure 7 *Schematic representation of the logic tree structure used to develop the stochastic set of events used for PVAHA featuring input parameters for magnitude (VEI), eruption column height, eruption duration, eruption style and wind speed.*

4.2.2 Volcanic ash dispersal modelling

The volcanic ash dispersal model FALL3D was used here to computationally model volcanic ash fall expected for each event in the synthetic catalogue. It is acknowledged that FALL3D is one of a number of suitable ash dispersal models that could be utilised for an analysis of this kind. FALL3D is a time-dependent Eulerian model which solves the advection-diffusion-sedimentation (ADS) equation on a structured terrain-following mesh. FALL3D outputs time-dependent deposit load at ground level as a hazard footprint of changing ash load with distance from source (Folch et al., 2012). It is important to note that any ash dispersal model could be used to develop the hazard footprints used in this modelling framework.

An assessment of the mass eruption rate, height and shape of the eruption column is made for each stochastic event in the catalogue. These parameters together describe the eruptive source term needed to simulate the dispersal of volcanic ash using FALL3D. The source term can be defined as either a 1D buoyant plume model (Bursik, 2001) or as an empirical relationship (Suzuki, 1983). The empirical relationship (Suzuki) used here estimates the mass eruption rate (MER) given an eruption column height (H) using known best-fit relationships of MER versus H (Sparks et al., 1997). A

generalised granulometry profile is developed for each eruption style based on analogue eruptions worldwide which include minimum and maximum grainsize, average grainsize, sorting, density and sphericity of clasts. FALL3D was used to simulate 1056 hazard footprints (one for each stochastic event in the synthetic catalogue). An example hazard footprint for one event is presented in Figure 8A.

4.2.3 Ash load prediction equations

Earthquake hazard is measured in terms of the level of ground motion that has a certain probability of being exceeded over a given time period (Dhu et al., 2008; McGuire, 1995; McGuire, 2008). This relationship is represented numerically through the development of Ground Motion Prediction Equations (GMPEs) or attenuation relationships, which provide a means of predicting the level of ground shaking and its associated uncertainty at any given site or location, based on an earthquake magnitude, source-to-site distance, local soil conditions and fault mechanism.

Similarly here, a python script was developed that derives the mathematical expression for changing volcanic ash load with distance from source from a hazard footprint generated by FALL3D. The script operates by extracting changing ash load with distance from the source at incrementally increasing angles as a series of radial slices through the hazard footprint (Figure 8A). The script extracts the mathematical relationship for changing ash load versus distance along each radial slice and integrates these into an equation which is representative of the hazard footprint as a whole:

Ash Load=a.e^((x(b(y^2)+cy+d)+ey+f)gz) (8)

Where ‘x’ is wind speed (m/s), ‘y’ is the cosine angle between the direction of the wind (degrees) and the location of the site of interest and ‘z’ is the distance of the site from the source (Figure 8B). The resulting equation, named here an Ash Load Prediction Equation (ALPE), statistically emulates the volcanic ash attenuation relationship observed in the hazard footprint and can be used to quantify the volcanic ash hazard from any given event of this kind at any location of interest from any volcanic source as a function of distance of the site from the source. Each ALPE represents one stochastic event in the synthetic catalogue. An example plot which illustrates changing ash load with distance along each radial slice for an example event is presented in Figure 8B.

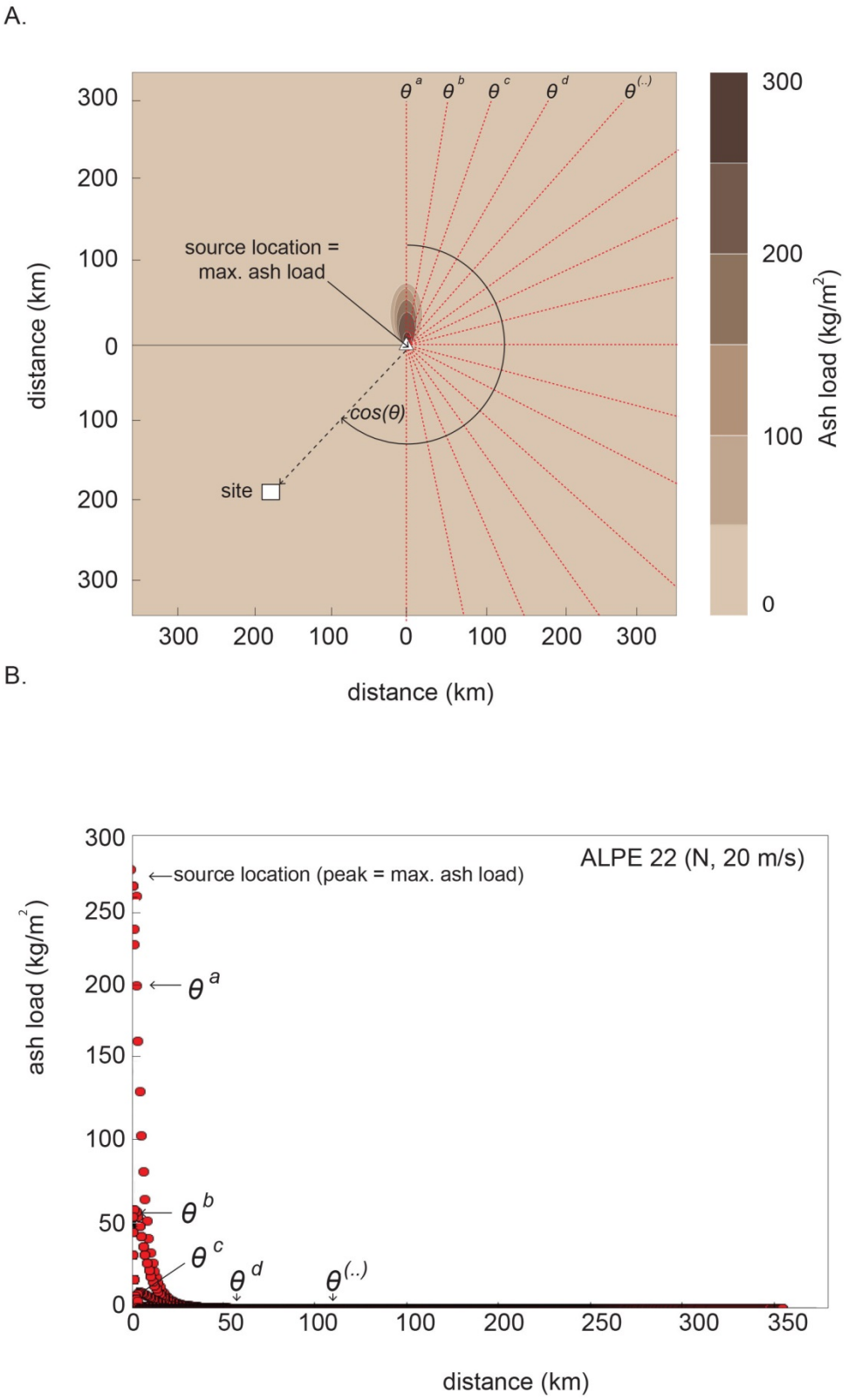

Figure 8 *Schematic representation of the volcanic ash load footprint generated by FALL3D for a randomly selected event in the synthetic catalogue (ALPE 22: wind direction 'N', wind speed 22 m/s) featuring radial slices of decreasing volcanic ash load (kg/m^2) with distance from source at regular intervals and a visual representation of the cosine angle for a random site; B. Composite plot of volcanic ash load versus distance for each radial slice in (A) used to derive the ash load prediction equation for event 22 (N, 20m/s) in the synthetic catalogue.*

The equations developed here are well suited to a regional or global context where the influence of local factors such as variable topography or prevailing wind speeds are not finely resolved or well constrained and are thus simplified. For the purpose of this study, to demonstrate the usefulness of the technique, the wind speed is modelled at five degree increments between 5 and 20 m/s. However, it is acknowledged that other users of the procedure might choose to incorporate detailed topographic information and prevailing wind speeds at varying pressure levels into the development of each ALPE where computational resources are abundant and/or the spatial scale is suitably localised. Not unlike GMPEs used to conduct PSHA, the generation and application of ALPEs will have a considerable influence on the outcome of the PVAHA. The ALPEs developed here use the dispersal model FALL3D however other dispersal models could be used (e.g. (Hurst, 1994; Hurst and Turner, 1999), HAZMAP (Costa et al., 2009), or TEPHRA (Bonadonna et al., 2005)) and the authors would encourage the development of ALPEs using a range of dispersal models currently available to build on and compare/contrast with the current work.

4.3 Volcanic Ash Probabilistic Assessment tool for Hazard and Risk (VAPAHR)

A tool was developed to facilitate the fourth step of the PVAHA framework (Figure 9). This tool, named here, Volcanic Ash Probabilistic Assessment for Hazard and Risk (VAPAHR) was developed in python and utilises a scripted interface and high performance computing technology in order to undertake assessments at multiple spatial scales. The VAPAHR tool emulates a multitude of volcanic eruption occurrences with associated ash fall-load attenuation relationships integrated across all possible events to arrive at a preliminary AEP for each site across the region of interest. Other tools of this kind have been developed for probabilistic earthquake hazard assessment (e.g. the Earthquake Risk Model (EQRM) (Robinson et al., 2005)). Inputs for the VAPAHR tool include:

1. Volcanic sources identified for analysis and associated annual probabilities (developed in steps one and two);
2. Ash load prediction equations for each stochastic event in the synthetic catalogue which represent the volcanic ash load attenuation relationship (developed in step 3) and;
3. A hazard grid of pre-determined resolution clipped to the domain extent.

A configuration file is used to customise the extent of the assessment. Geographic co-ordinates for the region of interest, resolution of the hazard grid, return periods of interest and instructions for generating outputs are user-specified fields. The configuration file, importantly, is where variations in wind direction are captured in the analysis. The user can specify all wind directions (e.g. 1 degree increments = 1056 events * 360 wind directions = 380,160 events per source) or choose to assess larger increments (e.g. every 5 degrees = 76,032 events) or only the 16 cardinal wind directions (e.g. 22.5 degrees = 23,760). The decision will ultimately depend on the purpose of the assessment, the size of the region of interest and the time and computational resources available (i.e. a resolution fit-for-purpose should be selected). A default profile is generated by VAPAHR where no user-defined wind conditions are specified. This approach is useful for assessing regions where the prevailing wind directions are not well constrained or highly variable. However it is recommended that future users of the VAPAHR tool incorporate region-specific, prevailing wind directions whenever this data exists if it is fit-for-purpose (i.e. suitable for use at the spatial scale being investigated) and the likelihood of occurrence is well documented.

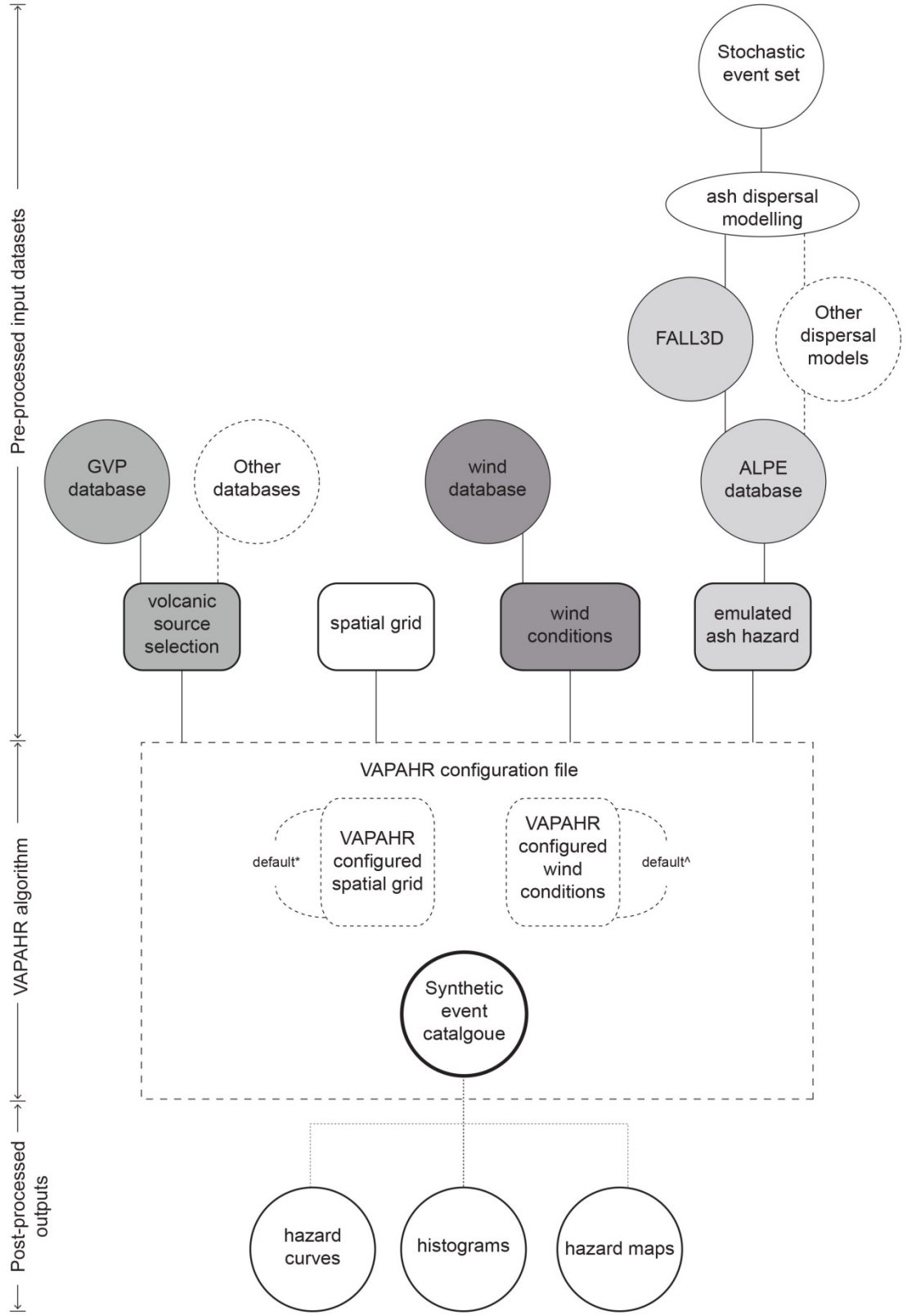

Figure 9 *Schematic representation of the operational procedure for the VAPAHR tool. * VAPAHR will auto-generate a spatial grid using user-specified parameters in the configuration file if one is not provided as a pre-processed input. ^ VAPAHR will auto-generate wind conditions using user-specified parameters in the configuration file if they are not provided as a pre-processed input.*

4.3.1 VAPAHR tool procedure

The VAPAHR tool can be run in both serial and parallel environments (i.e. on one or many processors simultaneously) on high performance computing platforms or standard PC equipment. Simulation time will vary according to the number of events, the number of sources, the resolution of the hazard grid and the number of wind directions investigated. For example, a regional scale assessment (e.g. Asia Pacific region) undertaken on a 1km resolution grid with >20,000 events results in a simulation time in the order of several days whereas undertaking the same assessment using a conventional ash dispersal model would almost certainly take weeks to months. A python script is used to execute the procedure as follows:

1. The first site is located on the hazard grid and the distance is calculated in kilometres between this site and the first source in the catalogue.
2. The distance value is then used to evaluate the ALPE for the first stochastic event in the catalogue in order to derive the expected ash load (kg/m^2) at that site for the first event.
3. The calculated ash load for the first event and its associated probability derived from the magnitude-frequency relationships for the first source in the catalogue are written to a database file.
4. The algorithm then moves to the next source in the catalogue and repeats steps (2) and (3) until all sources have been assessed for the first site. This process will capture all instances where the site might experience multiple ash load hazards from more than one source.
5. The algorithm will then calculate the cumulative probability of each event (e.g. each instance where a volcanic ash load was recorded from one or more sources) for the site and generate a hazard curve of volcanic ash load (kg/m^2) versus annual probability of exceedance and the maximum expected ash load hazard for return periods of interest (specified by the user in the configuration file).
6. The algorithm then loops to the next site and repeats steps (1) – (5) until all sites have been evaluated.

4.3.2 Visualisation of VAPAHR output

VAPAHR integrates across all possible events (incorporating the relative frequencies of occurrence) and expected ash load (using a spectrum of eruption parameters) to arrive at a combined probability of exceedance for a site(s) of interest (e.g., a densely populated city or critical infrastructure). The result is a synthetic catalogue of events which can be used for the rapid dissemination and disaggregation of results and the identification of priority areas subject to high volcanic ash hazard.

VAPAHR can be configured to automatically generate AEP curves for a site(s) of interest. The maximum expected ash load (kg/m^2) at return periods of interest derived from the data can also be automatically generated. An example AEP curve and maximum expected ash load values for a series of return periods is presented in Figure 10.

By aggregating the hazard data developed for each site, VAPAHR can also be configured to generate cumulative hazard maps which display the maximum expected volcanic ash load (kg/m^2) at each site across a region at a return period of interest (e.g. 1-in-100 year event). It's important to clarify here that a 1-in-100 year event does not suggest that the maximum expected ash load for a site will occur regularly every 100 years, or only once in 100 years but rather given any 100 year period, the maximum expected ash load for a particular site may occur once, twice, more, or not at all.

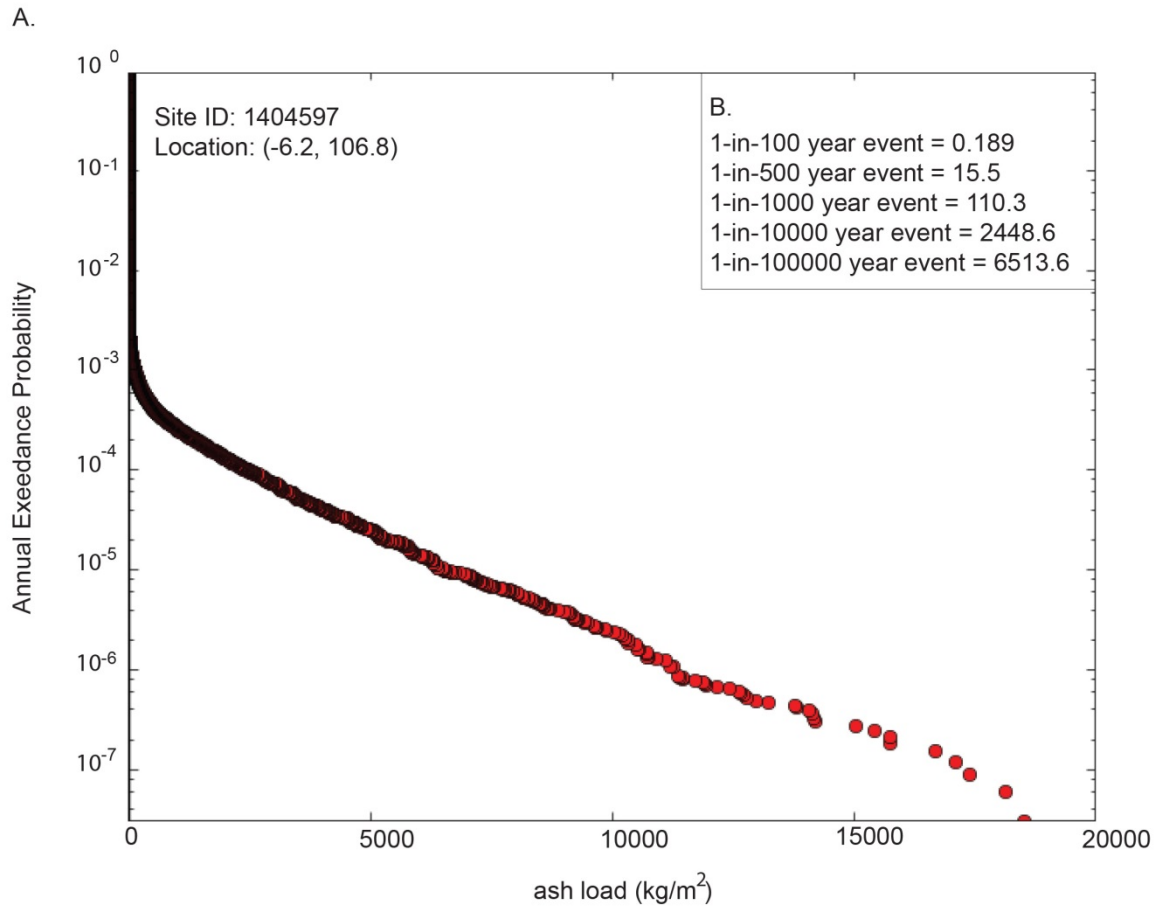

Figure 10 *Example annual exceedance probability curve versus ash load for a site of interest generated by VAPAHR; B. (inset) volcanic ash load values (kg/m^2) for the site at several return periods.*

Traditional assessments for volcanic ash hazard typically focus on one volcanic source where the maximum expected ash load will be concentrated at sites proximal to volcanic sources, decreasing with distance from source. In addition to this, VAPAHR captures the cumulative ash load hazard for each site (i.e. all events from multiple volcanic sources with eruption probabilities, styles and magnitudes that impact a given site for a return period of interest). This information is stored in the synthetic event catalogue of events and is easily accessible for further study.

Disaggregation is a technique used widely in PSHA and PTHA to ascertain which events dominate the hazard at a particular site. The ability to disaggregate the primary causal factors contributing to the hazard at a given site (i.e. magnitude, source, distance, ash load etc.) is an inherent strength of this approach. Disaggregation parameters are specified in the VAPAHR configuration file prior to undertaking an assessment. The VAPAHR tool will automatically generate histograms which visualise the requested disaggregated data for further analysis. For example, the user might be interested in demonstrating what the percentage contribution to hazard of different volcanic sources on a site of interest might be, and for each volcanic source, what proportion of eruptions are VEI 2, 3, 4, 5, 6 and 7? The VAPAHR tool can be configured to generate and visualize this type of information. An example histogram which disaggregates the % contribution to ash load hazard by magnitude (VEI) for each source at a randomly selected site of interest is presented in Figure 11. Alternatively, histograms can be produced post-assessment using an existing synthetic catalogue of events. This feature enables

new questions to be investigated without running the assessment again which would be time consuming and require computational resources.

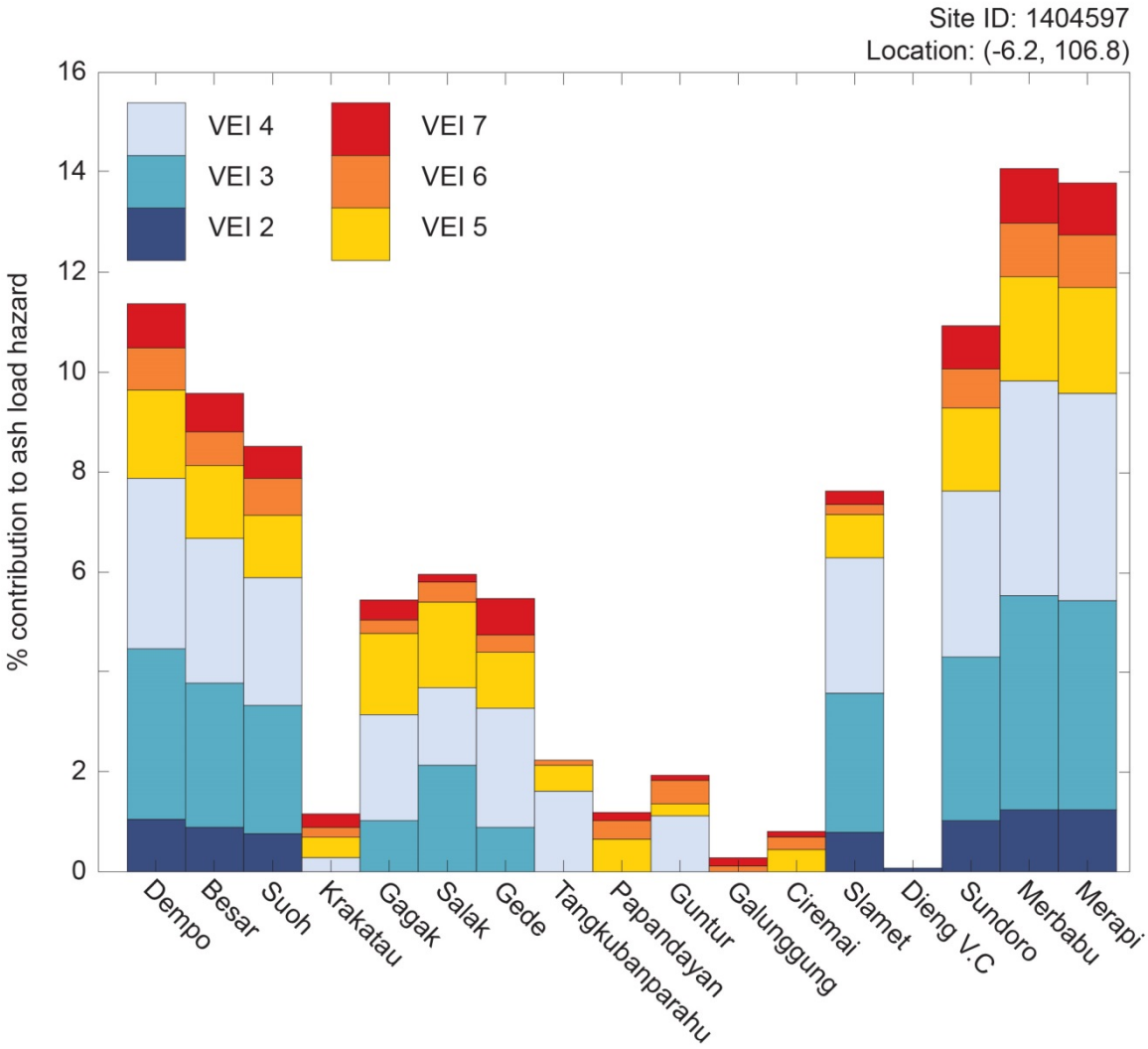

Figure 11 *Example histogram disaggregating the percentage contribution of magnitude (VEI) to volcanic ash load hazard for each source at a site of interest.*

4.4 Advantages

The PVAHA methodology presented here integrates across all possible events and expected volcanic ash loads to arrive at a combined probability of exceedance for a site of interest. The analysis incorporates the relative frequencies of occurrence of different events and a wide range of volcanic ash dispersal characteristics. Like PSHA, this quantitative method of estimating volcanic ash load hazard has the advantage of providing consistent estimates of hazard and can be prepared for one site or many, all in the same region but in significantly different geographic orientations with respect to potential hazard sources (McGuire, 1995; McGuire, 2008).

The methodology is highly customisable allowing for the flexible integration of ALPEs generated using numerous ash dispersal models and eruption statistics derived from a variety of sources. Capacity to build in flexibility in input assumptions highlights the power of this approach for quantifying uncertainty.

The VAPAHR tool, through the integration of ALPEs, effectively replaces the need to up-scale computationally intensive and time-consuming ash dispersal modelling in order to assess larger spatial scales.

While the PVAHA procedure, through application of the VAPAHR tool, is primarily concerned with aggregating the hazard contributions from all sources, disaggregating the volcanic ash hazard has two important implications for the usefulness of the technique over other approaches to multi-scale assessments. Firstly, the causal factors, which dominate the volcanic ash hazard for each site including magnitude, distance and source, are captured in a database that can be easily interrogated (a limitation of dispersal modeling outputs typically generated as gridded data). Second, disaggregation can be used to identify priority areas (sites or sources) from the multitude of volcanic events, for subsequent, more detailed analysis at the local scale that could be used to inform decision-making (e.g. targeted ash modelling at sites identified as subject to potentially high hazard). The benefit of disaggregating the analysis is a better overall understanding of the contributing factors to volcanic ash hazard for a region and evidence-based targeting of disaster risk reduction efforts.

4.5 Addressing uncertainty

The quality and value of the resulting assessment is controlled by the quality of the input models and it is critical that the uncertainties in parameter values, as well as those associated with the dispersal model itself are suitably accounted for. Uncertainty is addressed here through the development of a suite of ALPEs that account for the full spectrum of input parameters and the associated uncertainty of the dispersal model in use. This process also allows multiple competing hypotheses on models and parameters to be incorporated into the analysis (i.e. ALPEs based on other ash dispersal models). Integrating the stochastic set of events generated in the synthetic catalogue with magnitude-frequency relationships derived for each source and carrying those probabilities through to the analysis outputs using the VAPAHR tool also mitigates the uncertainty in assumptions made for annual eruption probability. Sensitivity analyses should be periodically carried out for all parameters and models and updated as new data and information become available in order to refine the resulting assessment.

4.6 Limitations, assumptions and caveats

The PVAHA methodology presented here incorporates a number of assumptions and is subject to limitations on what is produced and how the information should be interpreted and used. All assumptions are made explicit and are open to review and refinement with new evidence. Key assumptions made, limitations and caveats on the resulting assessment include the following:

1. Determination of the record of completeness for a sub-region is difficult to identify and can have a significant impact on the probability values derived for those sources (e.g. volcanoes with long repose periods might be under-represented).
2. The probability of an event is based on the type of source (e.g. caldera, large cone etc.) and this study assumes a static source type (i.e. a caldera remains a caldera) however morphologies are typically dynamic and evolve over the history of a source (e.g. large cones can become calderas). This has implications for estimating the probability of events.
3. All events are assumed to follow a memory-less Poisson process meaning the probability of an event occurring today is not contingent on whether or not an event occurred yesterday.

4. A 2km radii is applied to each source area and volcanic ash load estimates within this zone are not utilised due to over-estimations of proximal deposits (a feature of the dispersal model and considered acceptable due to the general absence of population, buildings and infrastructure within 2km of a source (i.e. on the edifice slopes)
5. This procedure and the VAPAHR tool are intended to be one in a range of tools and techniques used to provide a consistent fit-for-purpose approach to hazard assessment across multiple spatial scales.

5 Probabilistic volcanic ash hazard assessment of the Asia-Pacific region using VAPAHR

This section outlines the implementation of the PVAHA framework described previously in the Asia Pacific region using the VAPAHR tool (Miller et al., in revision).

5.1 Preparation of input datasets for the Asia-Pacific regional study

In order to characterise the volcanic ash hazard for an area of interest it is important to ascertain which volcanoes have the potential to erupt, the expected frequency of events and what kind of eruption might occur (e.g. style, magnitude, composition). Given that wind at the vent (e.g. speed and direction) can influence the final ash distribution patterns once an event occurs (e.g. distance and area), it is also important to account for the local wind conditions.

The VAPAHR tool requires the user to provide five key input datasets:

1. Volcanic sources identified for analysis combined with;
2. A-priori characterisation of volcanic sources using associated annual probabilities (magnitude-frequency relationships);
3. Ash load prediction equations for each event in the stochastic event set, which represent the volcanic ash load attenuation relationship;
4. Characterisation of the sites of interest: Either a database containing a pre-determined hazard grid of required resolution clipped to the domain extent, or a grid created by VAPAHR when indicated in the configuration file;
5. Characterisation of the local wind field: Either pre-determined values of wind direction and speed, or a simplified characterisation created by VAPAHR when indicated in the configuration file.

Other factors that can contribute to the final ash distribution following an eruption include topography and more detailed meteorological conditions (e.g., temperature and humidity). These variables are not considered in this instance as they are influenced heavily by locally varying factors that are not easily resolved at the regional-scale.

5.1.1 Identification of volcanic sources for the Asia-Pacific region

The volcanoes of the Asia-Pacific region were identified using the Smithsonian Institution's GVP database of current and past eruptive activity (Siebert et al., 2010), following the procedure outlined by Bear-Crozier et al. (in revision). The selective process of eruptive sources for this study was limited according to the following criteria:

- At least one recorded eruption during the last 10,000 years;
- Sources recorded as submarine, hydrothermal, fumerolic, or of unknown type were excluded;
- Eruptions with no assigned VEI were excluded;

- Sources with no assigned VEI, but recorded as caldera or Plinian in the database, were classified as VEI-4 events.

A total of 276 eruptive source volcanoes were identified across the Asia-Pacific region and then characterised by their statistical eruption frequency using a total of 3997 historical eruptions (Figure 12; Table 1).

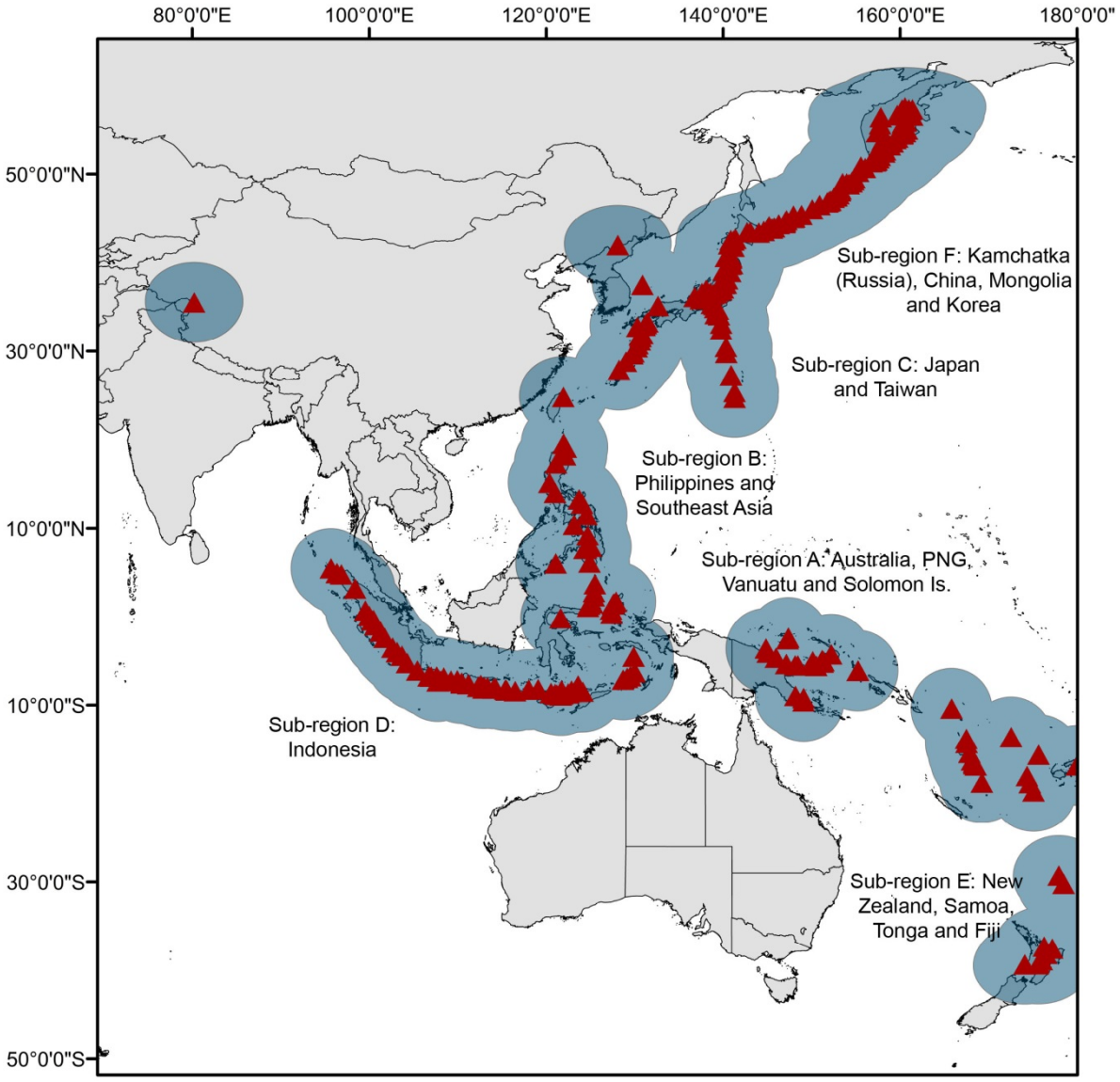

Figure 12 *Map showing study region of the Asia-Pacific; potential volcanic sources are indicated as red triangles. The 500km buffered region used for the extent of the site grid is shown in blue.*

Table 1 *The 276 volcanoes utilised for the Asia-Pacific regional ash hazard assessment, grouped by sub-region and country. Volcanoes highlighted in bold were assigned proxy values for annual rate of occurrence.*

Sub-region	Country	Volcanoes
A	Papua New Guinea	Bagana, Baluan, Bam, Bamus, Billy Mitchell, Dakataua, Garbuna Group, Karkar, Lamington, Langila, Lolobau, Long Island, Manam, Pago, Rabaul, Ritter Island, St. Andrew Strait, Ulawun, Victory, Waiowa
	Vanuatu	Ambrym, Aoba, Epi, Gaua, Kuwae, Lopevi, Suretamatai, Traitor's Head
	Solomon Islands	Tinakula
B	Philippines	Ambalatungan Group, Babuyan Claro, Biliran, Bulusan, Cagua, Camiguin, Didicas, Jolo, Kanlaon, Makaturing, Mayon, Musuan, **Parker**, Pinatubo, Ragang, Taal
C	Japan	Adatara, **Akagi**, Akan, Akita-Komaga-take, Akita-Yake-yama, Aoga-shima, Asama, Aso, Azuma, Bandai, Chokai, E-san, Fuji, Hachijo-jima, Hakkoda Group, **Hakone**, Haku-san, Haruna, Hiuchi, Ibusuki Volcanic Field, Ioto [Iwo-jima], Iwaki, Iwate, Iwo-Tori-shima, Izu-Tobu, Kikai, Kirishima, Kita-Iwo-jima, Komaga-take, Kozu-shima, Kuchinoerabu-jima, Kuju, Kurikoma, Kusatsu-Shirane, Kuttara, Mashu, Miyake-jima, **Myoko**, Nakano-shima, Nasu, Niigata-Yake-yama, Nii-jima, Nikko-Shirane, Nipesotsu-Maruyama, Nishino-shima, **Norikura**, **Numazawa**, On-take, Oshima, Rausu, Sakura-jima, **Sanbe**, Shikotsu, Shiretoko-Iwo-zan, Sofugan, **Sumiyoshi-ike**, Suwanose-jima, **Takahara**, Tate-yama, Tokachi, Tori-shima, Towada, Tsurumi, Unzen, Usu, Yake-dake, Yokoate-jima, Zao
D	Indonesia	Agung, Arjuno-Welirang, Awu Banda Api, Batu Tara, Batur, **Besar**, Bur ni Telong, Cereme, Colo [Una Una], Dempo, Dieng Volcanic Complex, Dukono, Ebulobo, Egon, Galunggung, Gamalama, Gamkonora, Gede, Guntur, Ibu, Ijen, Iliboleng, Iliwerung, Inielika, Iya, Kaba, Karangetang [Api Siau], Kelimutu, Kelut, Kerinci, Krakatau, Lamongan, Lawu, Leroboleng, Lewotobi, Lewotolo, Lokon-Empung, Mahawu, Makian, Marapi, Merapi, Merbabu, Nila, Paluweh, Papandayan, Perbakti-Gagak, Peuet Sague, Ranakah, Raung, Rinjani, Ruang, Salak, Sangeang Api, Semeru, Serua, Seulawah Agam, Sinabung, Sirung, Slamet, Soputan, Sorikmarapi, Sumbing, Sundoro, Suoh, Talakmau, Talang, Tambora, Tandikat, Tangkubanparahu, Tengger Caldera, Teon, Tongkoko, Wurlali
E	New Zealand	Late, Macauley Island, Mayor Island, Okataina, Raoul Island, Ruapehu, Taranaki, Taupo, Tongariro, White Island
	Samoa	Savai'i
	Tonga	Fonualei, Niuafo'ou, Tofua
	Fiji	**Taveuni**
F	Russia (Kamchatka)	Akademia Nauk, Alaid, **Alney-Chashakondzha**, Atsonupuri, Avachinsky, **Bakening**, Baransky, Berutarube, Bezymianny, **Bliznetsy**, **Bolshoi-Kekuknaysky**, Chikurachki, Chirinkotan, Chirip, Chirpoi, Ebeko, Ekarma, Elovsky, Fuss Peak, Golovnin, Gorely, Goriaschaia Sopka, **Gorny Institute**, Grozny Group, Ichinsky, Ilyinsky, Karymsky, **Ketoi**, Khangar, Kharimkotan, Khodutka, Kikhpinych, Kinenin, Kizimen, Kliuchevskoi, Kolokol Group, **Komarov**, Koryaksky, Koshelev, **Kostakan**, Krasheninnikov, Kronotsky, Ksudach, Kunlun Volcanic Group, Kurile Lake, Lvinaya Past, Maly Semiachik, Medvezhia, Mendeleev, Mutnovsky, Nemo Peak, Opala, Prevo Peak, Raikoke, Rasshua, Sarychev Peak, Shiveluch, Sinarka, Tao-Rusyr Caldera, Tiatia, Tolbachik, Tolmachev Dol, Ulreung, Ushkovsky, **Veer**, **Vilyuchik**, **Vysoky**, Zavaritsky, Zavaritzki Caldera, Zheltovsky, Zhupanovsky
	China	Changbaishan
	Korea	Ushishur
	Taiwan	Kueishantao

5.1.2 Characterisation of magnitude-frequency relationships

The annual rate of occurrence of eruptions for each magnitude are utilised to characterise the magnitude-frequency relationships. The annual rate of occurrence is the total number of eruptions from a given volcano divided by the length of time for which the record is deemed complete (ROC). The GVP database described above is used for this study, and source volcanoes are grouped for a more robust statistical analysis. The Asia-Pacific region volcanic sources are divided into six sub-regions based on their eruptive behaviour, in accordance with the Smithsonian catalogue: A – Papua New Guinea (PNG), Vanuatu, the Solomon Islands and Australia; B – Philippines and Southeast Asia; C – Japan and Taiwan; D – Indonesia; E – New Zealand, Samoa, Tonga, and Fiji and F – Kamchatka (Russia), China, Mongolia, and Korea (Table 1).

The level of detailed knowledge and records for a given volcano, and hence the completeness of the eruption record, is highly variable. For each sub-region, a ROC is established for both smaller (VEI 3 and below) and larger (VEI 4 and above) eruption magnitude classes using the break in slope method (Figure 13; Table 2). All eruptions for source volcanoes in a given sub are ordered by time-before-present and plotted. The record of completeness is assumed to be similar for segments with similar slopes. Each slope break was manually identified , however, recent work has identified ways to automate this process (e.g., Mead and Magill, in revision) . Eruptions that fell within the ROC for each sub-region were included in the magnitude-frequency relationship calculations (Electronic Attachment 1). For each volcanic source, the probability of an eruption occurring, regardless of magnitude, is calculated using the two magnitude-based subsets (VEI 3 and below; VEI 4 and above). The combined ROC for each volcano is calculated by normalising the occurrence interval for each of the two subsets to a single interval, with an assumed constant eruption rate.

Each source volcano is classified according to morphology and previous eruption style (caldera, large cone, shield, lava dome, small cone), following Jenkins et al. (2012a; 2012b). These five categories allow analogous proxies to be used to determine the probability of an eruption for volcanic sources without eruption records or eruptions falling beyond the ROC. Additionally, the typologies are used for the conditional probabilities. In this study 22 volcanoes were assigned proxy values for annual rate of occurrence (highlighted in bold, Table 1). An average value for all volcanoes in a given category (i.e., large cone) was used as a proxy ROC. In this way, volcanoes that have more detailed historical records are used to compensate for those that are underrepresented in the eruption database. The eruptions for each sub-region ROC calculation is outlined in Table 2.

Once ROCs are calculated for every possible eruption from a given source, the conditional probability of that eruption being of a given VEI is calculated. We assign the generic probability that a given category of volcano will produce a certain size eruption by calculating the number of events of a given VEI from each typology, divided by the total number of events in each magnitude class. We avoid assigning volcano types that show no historic evidence for larger magnitude eruptions (e.g., shield, small cone) with a likelihood of VEI-7 eruption at any given volcanic source. This type based generic probability is multiplied by the probability of any eruption occurring at a specific volcanic source to arrive at the annual probability of an event occurring at each VEI for each volcanic source. The final probabilities for each source volcano are provided in Electronic Attachment 2(A-F).

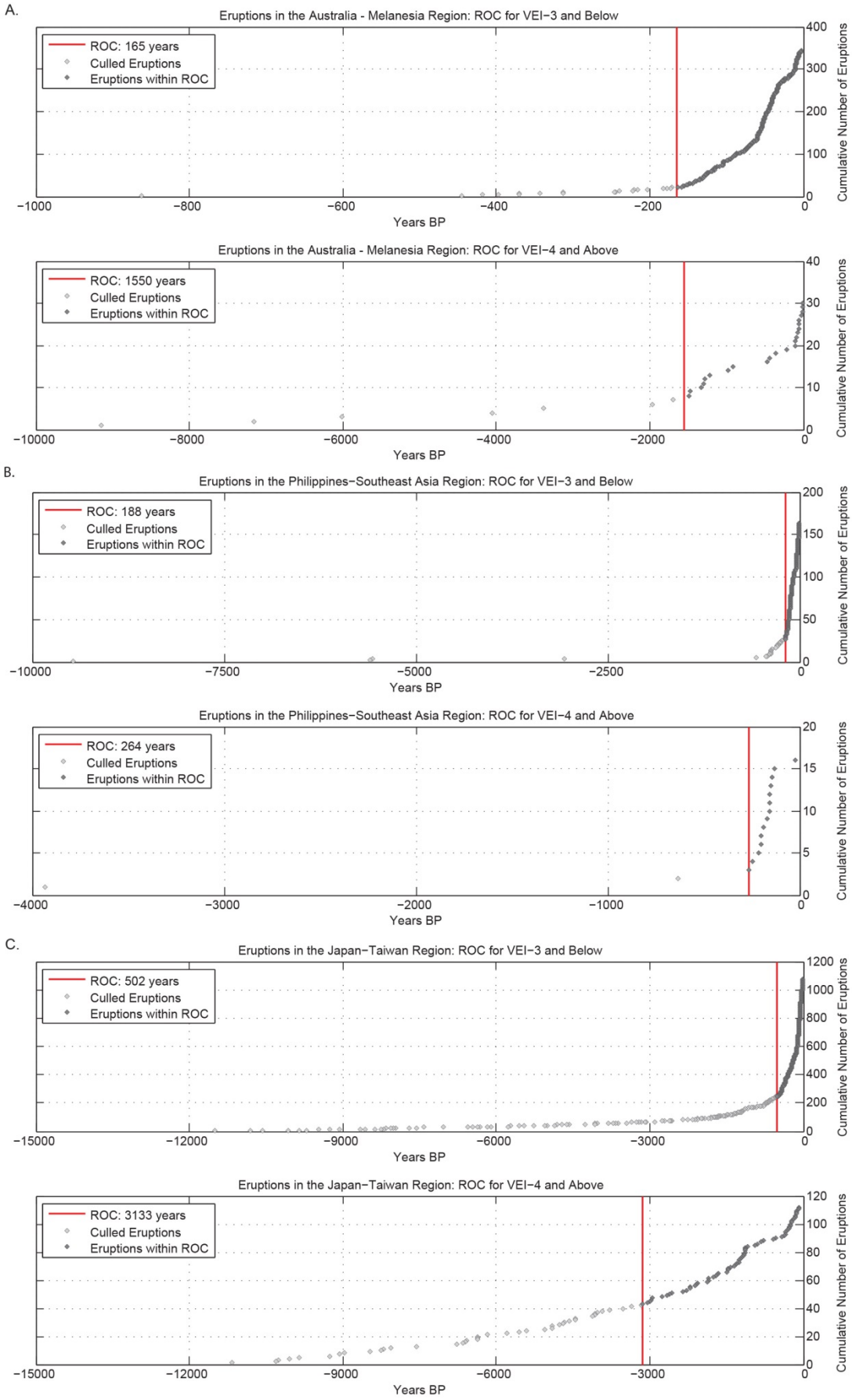
A.
Eruptions in the Australia - Melanesia Region: ROC for VEI−3 and Below
ROC: 165 years
Culled Eruptions
Eruptions within ROC
Years BP
Cumulative Number of Eruptions
Eruptions in the Australia - Melanesia Region: ROC for VEI−4 and Above
ROC: 1550 years
Culled Eruptions
Eruptions within ROC
Years BP
Cumulative Number of Eruptions
B.
Eruptions in the Philippines−Southeast Asia Region: ROC for VEI−3 and Below
ROC: 188 years
Culled Eruptions
Eruptions within ROC
Years BP
Cumulative Number of Eruptions
Eruptions in the Philippines−Southeast Asia Region: ROC for VEI−4 and Above
ROC: 264 years
Culled Eruptions
Eruptions within ROC
Years BP
Cumulative Number of Eruptions
C.
Eruptions in the Japan−Taiwan Region: ROC for VEI−3 and Below
ROC: 502 years
Culled Eruptions
Eruptions within ROC
Years BP
Cumulative Number of Eruptions
Eruptions in the Japan−Taiwan Region: ROC for VEI−4 and Above
ROC: 3133 years
Culled Eruptions
Eruptions within ROC
Years BP
Cumulative Number of Eruptions

D.

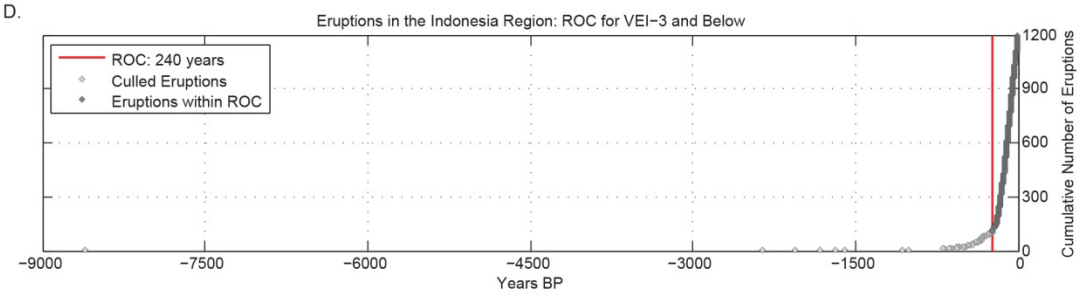
Eruptions in the Indonesia Region: ROC for VEI−3 and Below
ROC: 240 years
Culled Eruptions
Eruptions within ROC
−9000
−7500
−6000
−4500
−3000
−1500
0
Years BP
1200
900
600
300
0
Cumulative Number of Eruptions

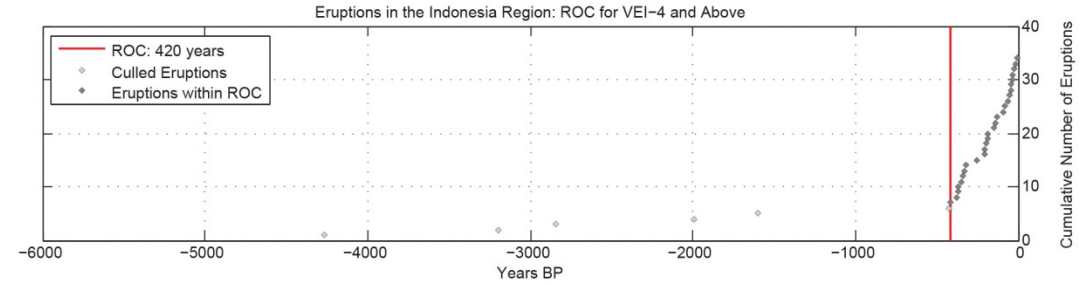
Eruptions in the Indonesia Region: ROC for VEI−4 and Above
ROC: 420 years
Culled Eruptions
Eruptions within ROC
−6000
−5000
−4000
−3000
−2000
−1000
0
Years BP
40
30
20
10
0
Cumulative Number of Eruptions

E.

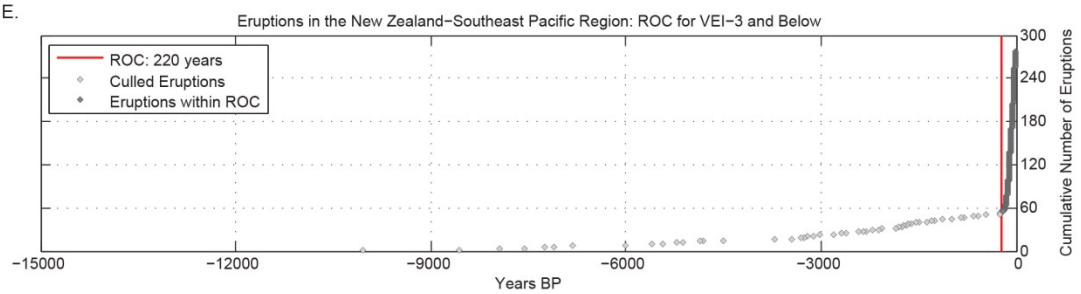
Eruptions in the New Zealand−Southeast Pacific Region: ROC for VEI−3 and Below
ROC: 220 years
Culled Eruptions
Eruptions within ROC
−15000
−12000
−9000
−6000
−3000
0
Years BP
300
240
180
120
60
0
Cumulative Number of Eruptions

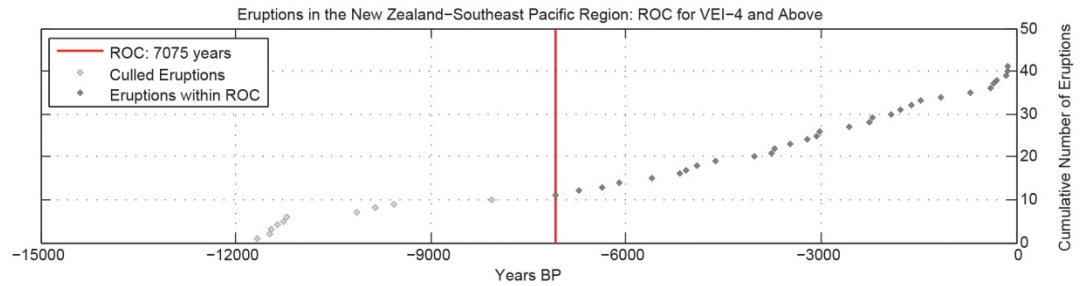
Eruptions in the New Zealand−Southeast Pacific Region: ROC for VEI−4 and Above
ROC: 7075 years
Culled Eruptions
Eruptions within ROC
−15000
−12000
−9000
−6000
−3000
0
Years BP
50
40
30
20
10
0
Cumulative Number of Eruptions

F.

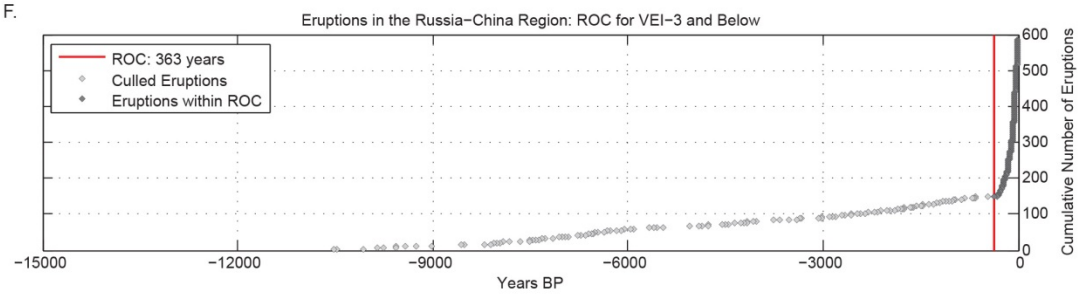
Eruptions in the Russia−China Region: ROC for VEI−3 and Below
ROC: 363 years
Culled Eruptions
Eruptions within ROC
−15000
−12000
−9000
−6000
−3000
0
Years BP
600
500
400
300
200
100
0
Cumulative Number of Eruptions

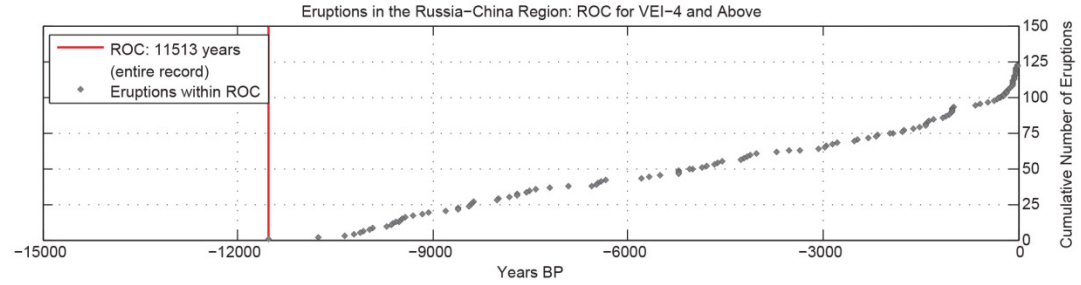
Eruptions in the Russia−China Region: ROC for VEI−4 and Above
ROC: 11513 years
(entire record)
Eruptions within ROC
−15000
−12000
−9000
−6000
−3000
0
Years BP
150
125
100
75
50
25
0
Cumulative Number of Eruptions

Figure 13 *Cumulative number of small (VEI 3 and below; top) and large (VEI4 and above; bottom) eruptions over time for each sub-region a) Australia, PNG, Vanuatu, Solomon Islands; b) Philippines, Southeast Asia; c) Japan, Taiwan; d) Indonesia; e) New Zealand, Samoa, Tonga, Fiji; f) Kamchatka (Russia), China, Mongolia, Korea.*

Table 2 *Sub-region record of completeness (total number of eruptions included in each sub-region)*

Sub-region	ROC <VEI 3 (Year B.P)	No. eruptions <VEI 3 (within ROC)	No. eruptions <VEI 3 (Total)	ROC >VEI 4 (Years B.P)	No. eruptions >VEI 4 (within ROC)	No. eruptions >VEI 4 (Total)	No. eruptions in sub-region (within ROC)	No. eruptions in sub-region (Total)
A - Australia, Papua New Guinea, Vanuatu, Solomon Islands	165	324	345	1550	23	30	347	375
B - Philippines, Southeast Asia	188	138	164	264	14	16	152	180
C - Japan, Taiwan	502	828	1073	3133	70	112	898	1185
D - Indonesia	240	1090	1198	420	28	34	1118	1232
E - New Zealand, Samoa, Tonga, Fiji	220	222	277	7075	31	41	253	318
F - Kamchatka (Russia), China, Mongolia, Korea	363	436	585	11513 (whole record)	122	122	558	707

5.1.3 ALPEs for the Asia-Pacific region

The ALPEs for this study were determined using the volcanic ash hazard outputs generated by the 3D time-dependent Eulerian model FALL3D (Folch et al., 2012). The database of 1056 ALPEs was generated according to the following range of parameters from the stochastic event set:

- Eruption magnitude, VEI 2-7;
- Eruption column height, 1000 – 40000 m;
- Eruption duration (1 – 12 hours);
- The Suzuki parameters (commonly accepted ash dispersal parameters for a spectrum of eruption styles; (Suzuki, 1983));
- Simplified wind profiles (5-20 m/s).

The volcanic ash load (kg/m^2) at ground level with distance is predicted for each parameter combination in the catalogue. The ALPEs are used by VAPAHR to quantify the volcanic ash hazard through the generation of a synthetic catalogue of events for each of the volcanic sources in the Asia-Pacific region by coupling ALPEs with the magnitude-frequency relationships for the region (Bear-Crozier et al., in revision).

5.1.4 Identification of sites of interest for the Asia-Pacific region

The spatial extent of the volcanic ash assessment domain can be customised for the area of interest and available resources. Defining the full extent of the Asia-Pacific region resulted in the creation of a grid enclosing an area of 111 x 107 degrees. This gridded area was then clipped to include only land-based nodes that are located in areas within 500km of a volcanic vent (a conservative distal limit imposed by the authors for estimating ground loading of volcanic ash using dispersal models; refer Figure 12). Working at a 0.05 x 0.05 degree resolution (approximately 5km^2), the analysis covered 178,935 gridded nodes, translating to a region of approximately 4,600,000 km^2(Figure 12).

5.1.5 Representation of wind for the Asia-Pacific region

Ash accumulation is greatly influenced by meteorological conditions. Ash is primarily dispersed in the direction of the prevailing wind at the time of eruption, with the distance of dispersal influenced by wind velocity. The influence of wind direction on the distribution of the ash load can be customised and provided as an input to VAPAHR using the same file as the volcano source probabilities. Development of wind customised for each volcano location takes time, but is recommended for sub-regional case studies. Here a simplified representation using the VAPAHR defaults is utilised using the pre-determined ALPEs developed for four wind speed profiles (5, 10, 15, and 20 m/s). For the Asia-Pacific regional study we characterised wind by applying the ALPEs at 5 degree increments, with each combination having an equal likelihood in the logic tree (Bear-Crozier et al., in review).

5.2 Execution of the VAPAHR tool for the Asia-Pacific region

5.2.1 Configuring VAPAHR for the Asia-Pacific region

The case-study for the Asia-Pacific region was tailored using the following configuration (refer to Figure 14):

- Magnitude-frequency relationships developed for 276 volcanoes in the Asia-Pacific region– Volcano Source database, loaded into VAPAHR;
- Predetermined ALPEs developed using FALL3D - ALPE database, loaded into VAPAHR;
- Customised site files in order to reduce the computational redundancy. The 0.05 degree grid clipped to land only sites within 500km of a source volcano – Site Location database, loaded into VAPAHR;
- Wind represented using VAPAHR default values at four wind speeds at 5 degree increments with equal likelihood – no database loaded into VAPAHR, use of VAPAHR defaults specified in the configuration file.

5.2.2 Running VAPAHR for the Asia-Pacific region

The workflow undertaken in VAPAHR for the Asia-Pacific regional case study includes the following steps (summarised in Figure 14):

- Develop input datasets
  - Volcano source database with characterisation of magnitude-frequency relationships
  - ALPE database with footprints determined using FALL3D dispersal modelling and then emulated using statistical relationship
  - Site location database with customisation appropriate to assessment purpose.
- Tailor the configuration file to indicate
  - Where customised input databases are available versus default values (e.g. here a customised site location database is used, but default wind determination is used in lieu of a wind database)
  - Appropriate settings when defaults are used (e.g. for wind determination)
  - Number of return periods for ash calculations
  - Thresholds for ash calculations
  - Thresholds for creation of associated plots.
- Optional customisation of files for use on super-computer facilities.

The ALPE database is used by VAPAHR to quantify the volcanic ash hazard through the generation of a synthetic catalogue of simulated events for each of the volcanic sources in the region of interest. The ALPE database is coupled with the magnitude-frequency relationships for the Asia-Pacific region (Bear-Crozier et al., in revision) using parameters applicable to the given volcanic sources and wind speed applied at each wind direction, resulting in a total of 20,535,552 individual scenarios. VAPAHR then integrates the volcanic ash hazard for each scenario at every site in the region generating annual probability of exceedance curves for each site (Figure 15).

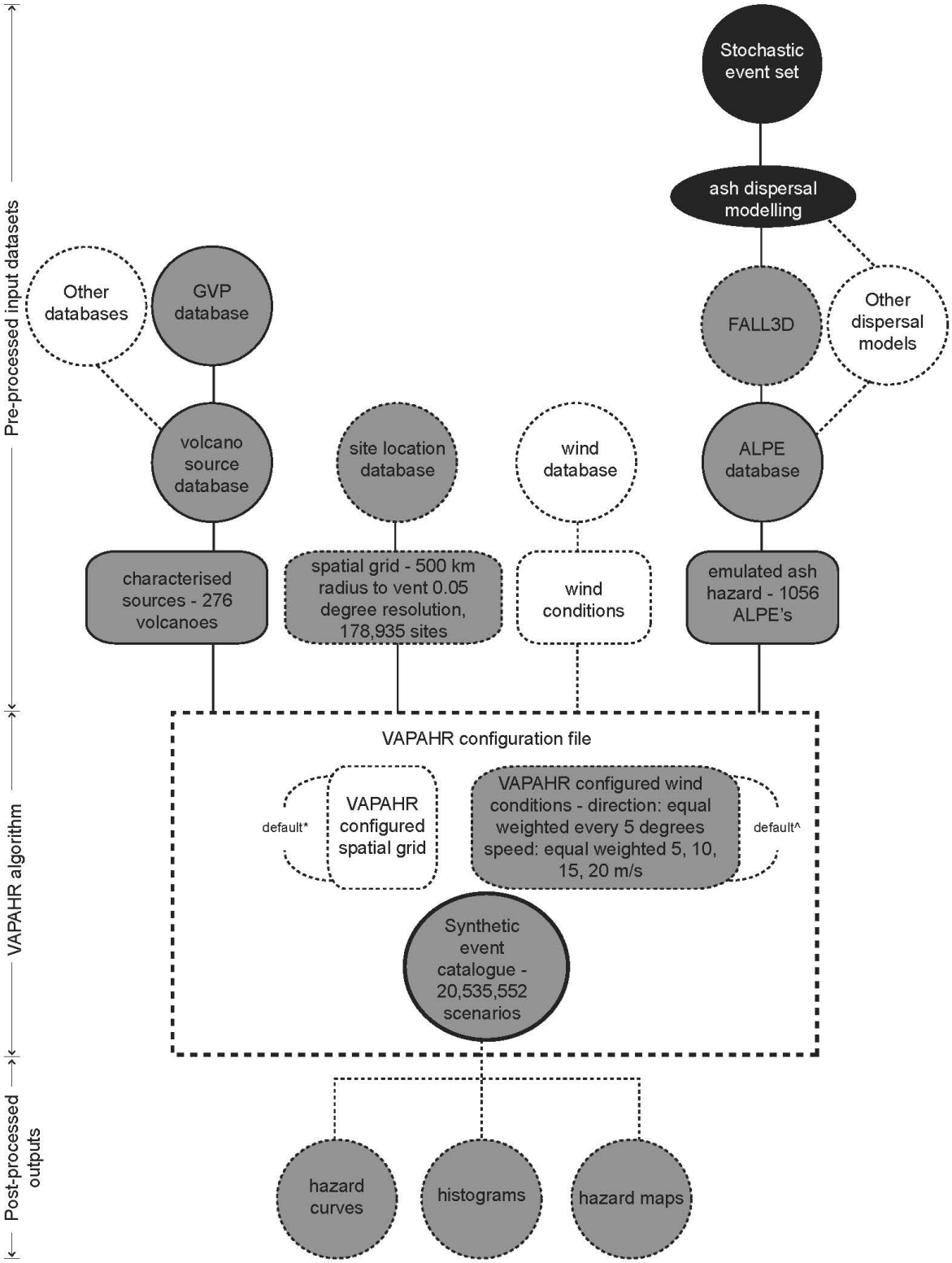
Pre-processed input datasets
VAPAHR algorithm
Post-processed outputs
Stochastic event set
ash dispersal modelling
Other databases
GVP database
FALL3D
Other dispersal models
volcano source database
site location database
wind database
ALPE database
characterised sources - 276 volcanoes
spatial grid - 500 km radius to vent 0.05 degree resolution, 178,935 sites
wind conditions
emulated ash hazard - 1056 ALPE's
VAPAHR configuration file
default*
VAPAHR configured spatial grid
VAPAHR configured wind conditions - direction: equal weighted every 5 degrees speed: equal weighted 5, 10, 15, 20 m/s
default^
Synthetic event catalogue - 20,535,552 scenarios
hazard curves
histograms
hazard maps

Figure 14 *Schematic representation of the PVAHA workflow undertaken for the Asia-Pacific regional analysis. The pre-determined stochastic event set is indicated in black. Non-optional aspects are indicated by black outline. Optional aspects are indicated by dashed outline, with options used in the Asia-Pacific regional analysis indicated in dark grey. Adapted from the operational procedure for the VAPAHR tool (Bear-Crozier et al., in revision)* VAPAHR will auto-generate a spatial grid using user-specified parameters in the configuration file if one is not provided as a pre-processed input. ^ VAPAHR will auto-generate wind conditions using user-specified parameters in the configuration file if they are not provided as a pre-processed input.*

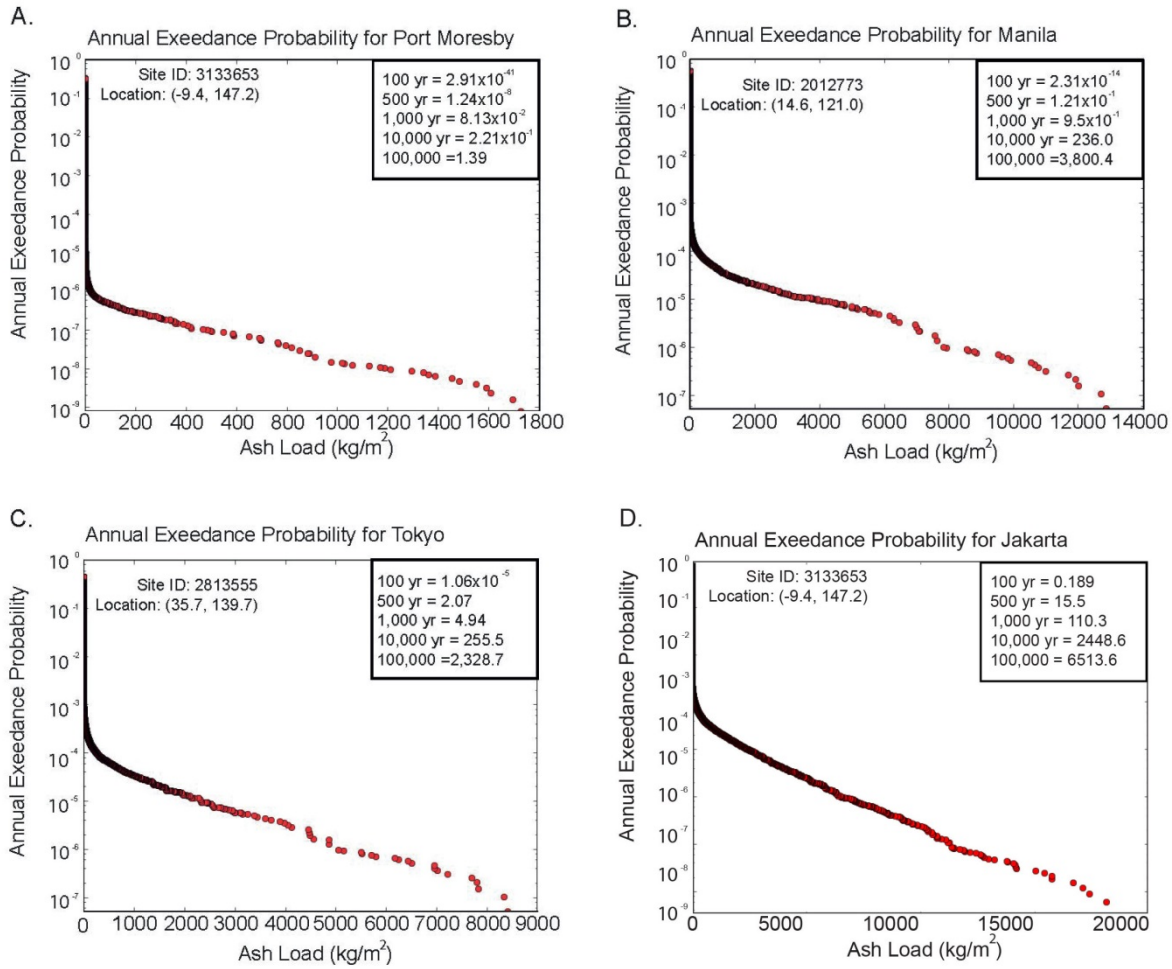

Figure 15 *Annual exceedance probability curves for sites in A. Port Moresby, PNG; B. Manila, the Philippines; C. Tokyo, Japan; D. Jakarta, Indonesia. Maximum ash load in kg/m^2*

For the Asia-Pacific regional study (276 volcanoes, 0.05 degree site grid, 5 degree wind spacing, including a total of 20,535,552 individual scenarios), 60 CPUs were utilised on a local computing cluster and the analysis took approximately three days. By optimising for use on super-computing facilities the VAPAHR tool can be configured to run the same analysis for the full Asia-Pacific region in less than one day using 240 CPUs on the National Computational Infrastructure (NCI). In comparison, FALL3D utilises one CPU to run just one eruption from one volcano and can take up to three days to simulate a larger magnitude (VEI 7) eruption.

In this study the inverse of probability of exceedance is determined to establish hazard curves for 12 average return periods (50, 100, 500, 1,000, 5,000, 10,000, 50,000, 100,000, 500,000, 1,000,000, 50,000,000, 10,000,000 years) versus volcanic ash load (kg/m^2).

5.3 Results – Asia Pacific region

The estimated maximum volcanic ash load for the Asia-Pacific region is presented here for the 100-year return period (Figure 16), the 1,000-year return period (Figure 17) and the 10,000-year return period (Figure 18).

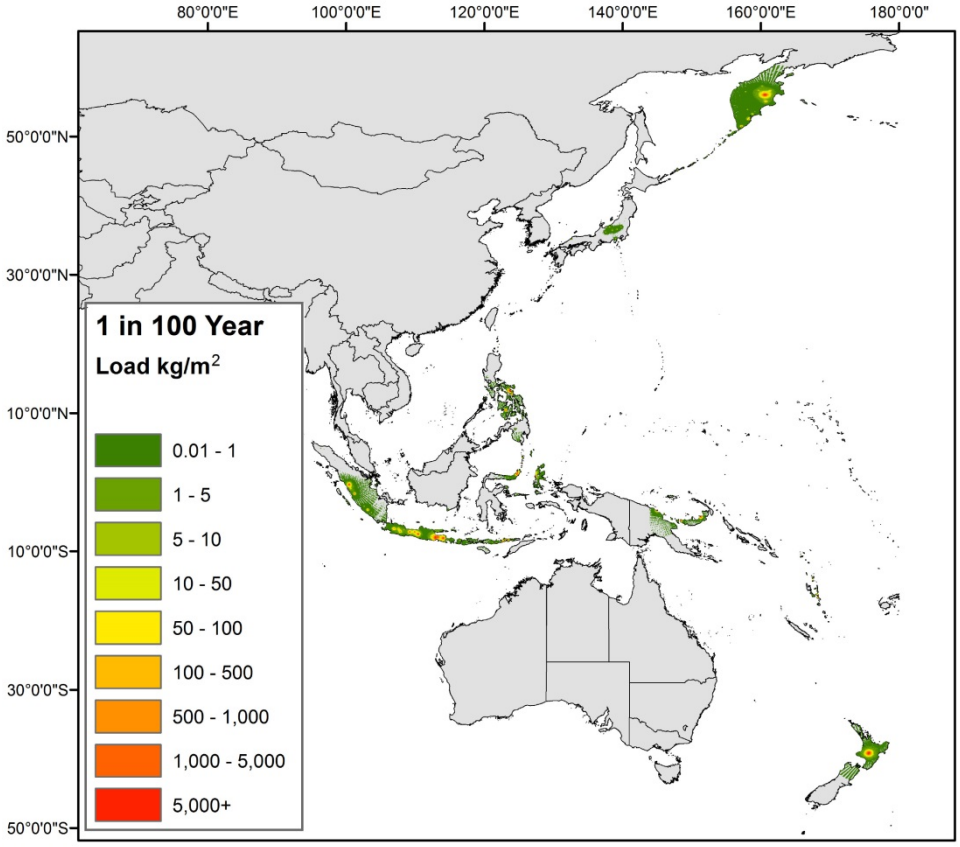

Figure 16 *Estimated maximum volcanic ash load for the Asia-Pacific region at the 100 year return period. The colour bar indicates the maximum ash load in kg/m^2.*

The Indonesian Island Arc system exhibits the greatest volcanic ash hazard in the entire Asia-Pacific region for all observable return periods, with the other volcanic arc systems across the region, particularly Japan, the Philippines, PNG, the Kamchatka peninsula (Russia), and the north island of New Zealand, exhibiting increased volcanic ash hazard at the longer return periods. Indonesia has 74 active volcanoes contributing to this hazard analysis, more than any other sub-region. Coupled with the fact that several of these volcanoes have high eruption recurrence rates across the entire VEI range, 10-20% of the Indonesian land mass has estimates of volcanic ash loads >1 kg/m^2, even at the 100-year return period; this proportion is greater for the island of Java. For higher ash loads, capable of causing building damage and collapse (100-500 kg/m^2), the hazard is focused on the volcanic

centers, with the greatest hazard in east Java (Tengger Caldera, Semeru, Lamongan centres), where these volcanoes combine to create a higher load value zone 80-120km in diameter. Japan (Northeast Honshu Arc), the Philippines (Mayon, Kanlaon, Bulusan volcanoes), PNG (Bismarck Volcanic Arc), New Zealand (central Taupo Volcanic Zone) and the Kamchatka peninsula (dominated by Kluchevskoi volcano) also reveal localised high estimates of volcanic ash loads (>100 kg/m^2) at this low return period (Figure 16).

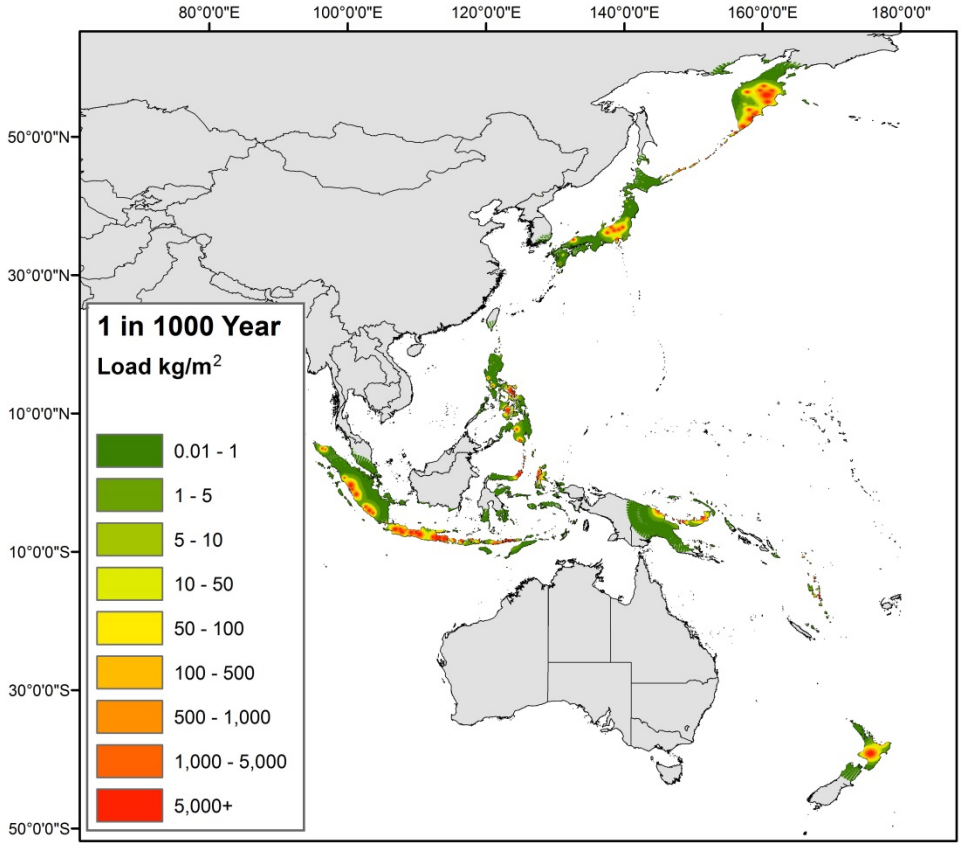

Figure 17 *Estimated maximum volcanic ash load for the Asia-Pacific region at the 1000 year return period. The colour bar indicates the maximum ash load in kg/m^2.*

As the return period increases, the level of volcanic ash hazard in the Asia-Pacific region increases. At the 1,000-year return period, widespread regions of Indonesia, Japan, the Philippines, PNG, the Kamchatka peninsula and New Zealand show elevated estimates of maximum ash load above the threshold of 1 kg/m^2 (Figure 17); the ash loads at the 1,000-year return period highlight an increased risk of serious disruption and at least minor damage to buildings (load 100-500 kg/m^2) throughout the Asia-Pacific region. By the 10,000-year return period, all countries along the island arcs and plate boundaries of the region show widespread and high volcanic ash hazard (Figure 18).

It should also be noted that there are areas of high ash hazard observed in some of the smaller Pacific island nations, such as Vanuatu. The hazard here is more difficult to observe at the regional-scale, given the small area of these island land masses and the larger regional groupings in this analysis. Whilst the total area likely to be impacted by these levels of ash may be small, it will comprise a larger percentage of the land mass available to the populations living in these nations.

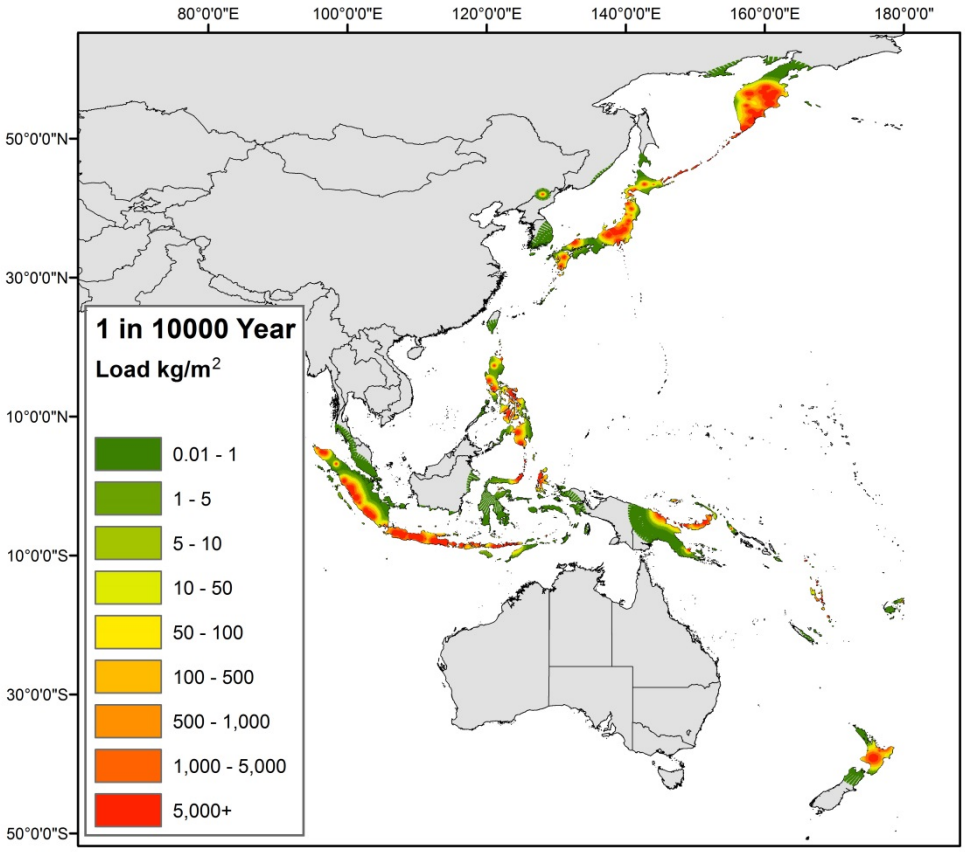

Figure 18 *Estimated maximum volcanic ash load for the Asia-Pacific region at the 10000 year return period. The colour bar indicates the maximum ash load in kg/m^2.*

Here we focus on several other sites of interest in the region with high population densities that are exposed to volcanic ash hazard to various degrees. VAPAHR is used to disaggregate the ash hazard as a function of volcanic source for three sites of interest; Port Moresby, PNG, Manila, in the Philippines, Tokyo, Japan and Jakarta, Indonesia.

5.3.1 Port Moresby, PNG

The volcanic ash hazard map for Papua New Guinea at the 1,000-year return period is presented in Figure 19.There are six volcanoes (Long Island, Ritter Island, Langila, Lamington, Victory, and Waiowa) contributing to the calculated ash accumulation for the site interest, Port Moresby (Figure 19; Figure 20). The maximum calculated ash load for Port Moresby at the 100-year return period is only ~2.9 x 10^{-41} kg/m^2. The volcano contributing the most ash at this scale is Lamington, with potential eruptions at all magnitudes amounting to approximately 40% of the anticipated ash load for this site (Figure 20). At the 1,000-year return period, the estimated ash load increases to ~0.1 kg/m^2. Long Island is now seen as the greatest ash load contributor at ~60%, with VEI 3 and 4 eruptions contributing >30% of the estimated ash load (Figure 20). The estimated ash load increases to ~1.4 kg/m^2 at the 10,000-year return period, enough to cause disruption to crops, roads and critical infrastructure, but not enough to cause building collapse. Long Island and Ritter Island each contribute >30% of the total anticipated ash load (Figure 20) at this scale. This fluctuation in source volcano contributions to the estimated ash load at each return period highlights how the inputs (namely eruption strength and frequency) influence the estimated ash load over time.

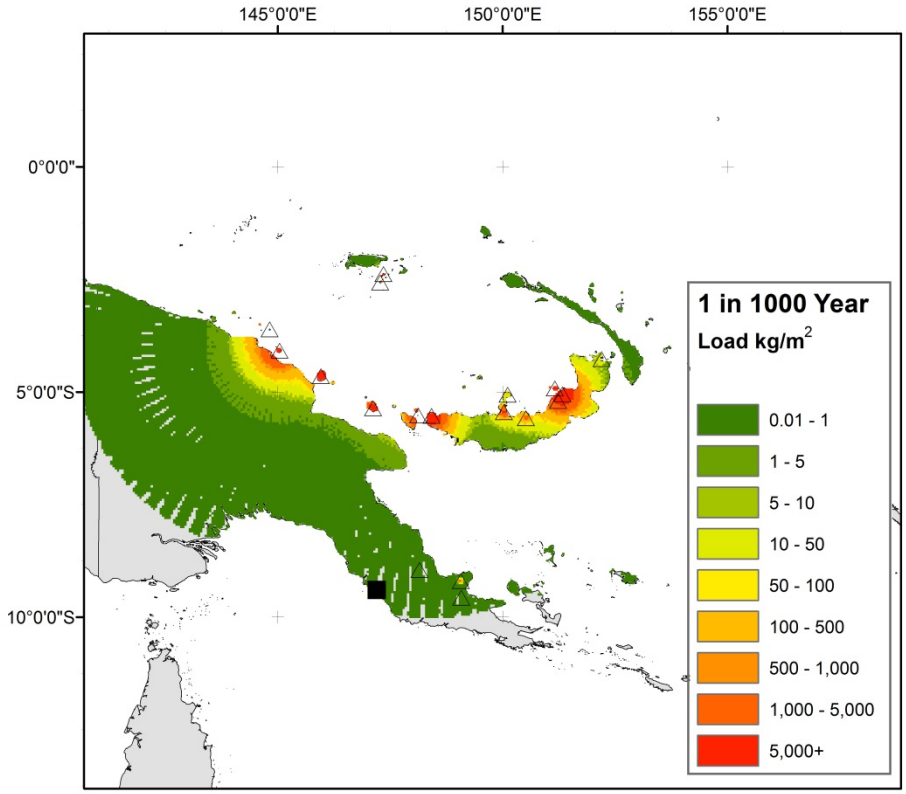

Figure 19 *Estimated maximum ash load for sites in Papua New Guinea at the 1000 year return period. The colour bar indicates the maximum ash load in kg/m^2. Port Moresby's location is indicated by the black square, volcanoes indicated by the black-outlined triangles.*

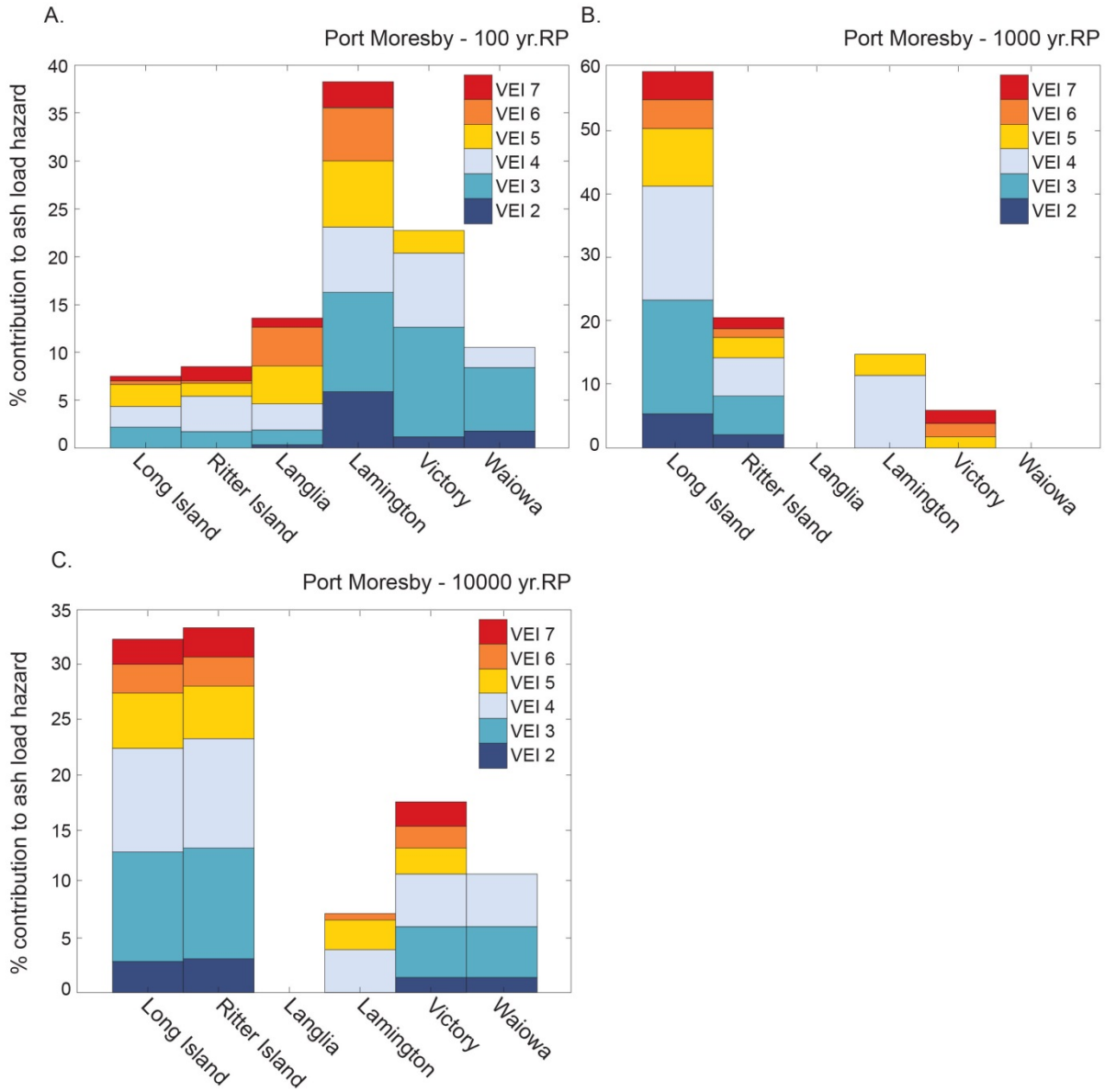

Figure 20 *Estimated maximum ash load % contributions disaggregated by volcanic source and magnitude of eruption (VEI – as indicated by the colour bar) for Port Moresby at the a) 100 year return period; b) 1,000 year return period and c) 10,000 year return period.*

5.3.2 Manila, the Philippines

The volcanic ash hazard map for the Philippines at the 1,000-year return period is presented in Figure 21. In the Philippines six volcanoes (Bulusan, Mayon, Taal, Pinatubo, Ambalatungan Group, Cagua) contribute to the calculated ash hazard accumulation for Manila (Figure 22). The maximum calculated ash load for Manila at the 100-year return period is ~2.3 x 10^{-14} kg/m^2. The volcano contributing the most ash at this scale is Pinatubo, with potential eruptions at all magnitudes (mostly VEI3 and VEI4) amounting to >35% of the anticipated ash load for this site (Figure 22). This is closely followed by Taal volcano with potential ash contributions also coming from all VEIs (again mostly VEI3 and VEI4). Taal volcano contributes approximately 35%. At the 1,000-year return period, the estimated ash load increases to ~0.9 kg/m^2, with a potential to cause disruption. Taal is now seen as

the greatest ash load contributor at ~35% contribution (Figure 22). Pinatubo's contribution has dropped to just under 20% with Cagua and Bulusan volcanoes contributing slightly greater percentages in the 20-25% range. The estimated ash load increases to ~236.0 kg/m^2 at the 10,000-year return period, with Taal volcano dominating the contribution at almost 70% of the total anticipated ash load (Figure 22) from eruptions of VEI 4 and above. The rest of the ash contribution at this return period is mostly from Pinatubo at ~30%, with other volcanoes having little contribution.

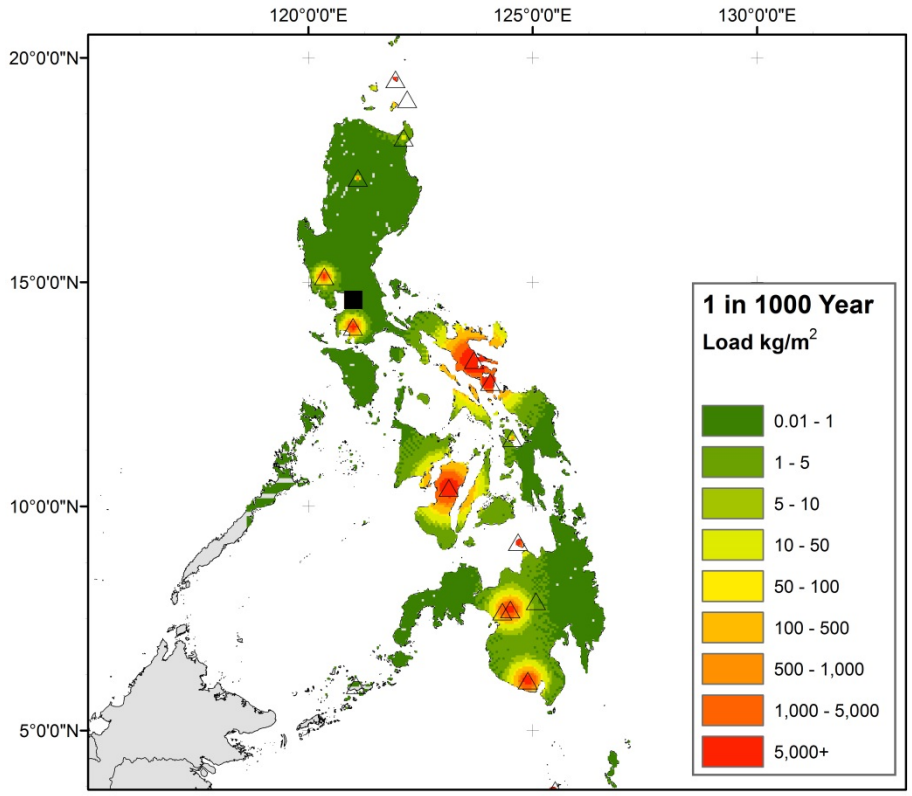

Figure 21 *Estimated maximum ash load for sites in the Philippines at the 1000 year return period. The colour bar indicates the maximum ash load in kg/m^2. Manila's location is indicated by the black square, volcanoes indicated by the black-outlined triangles.*

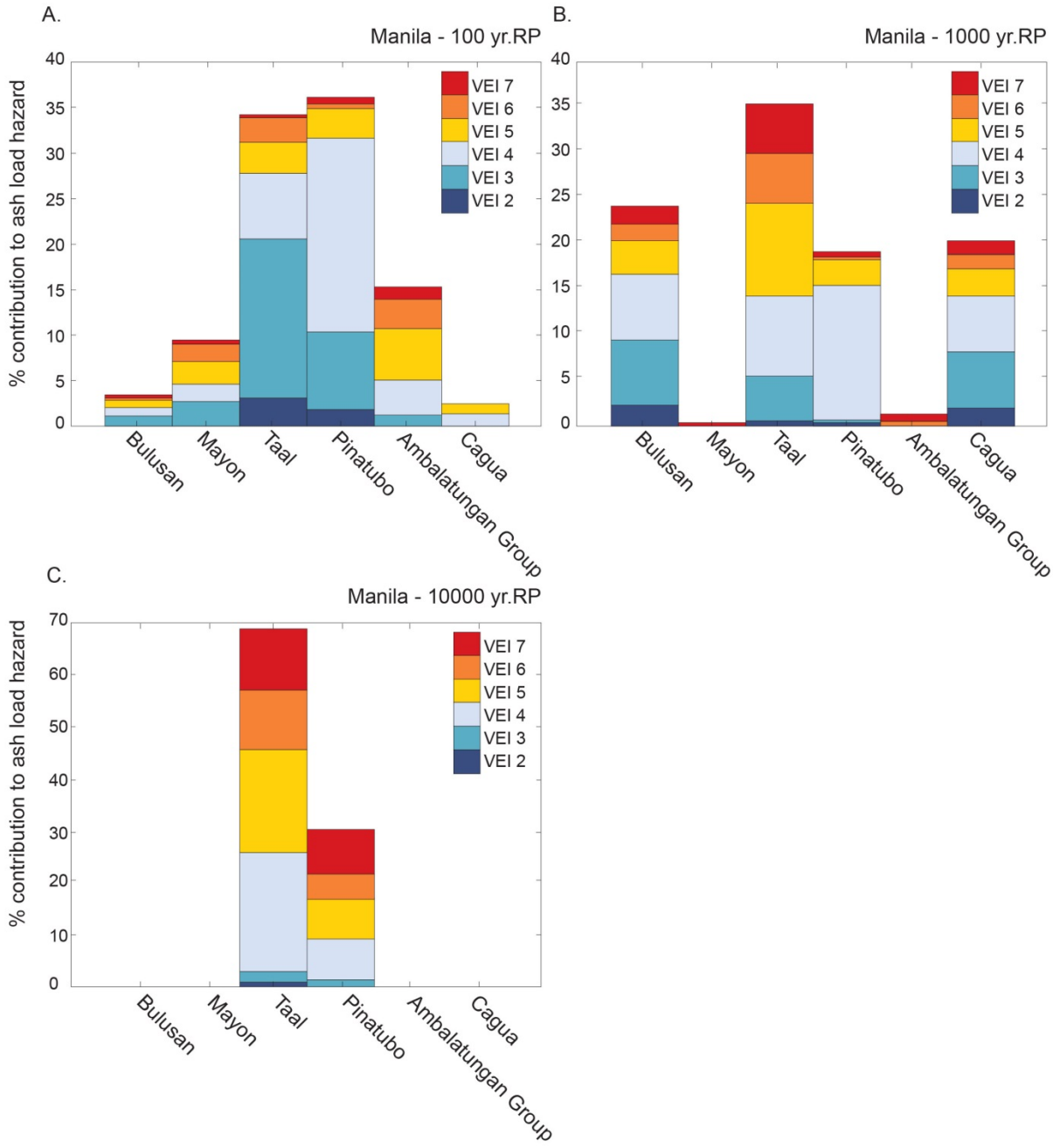

Figure 22 *Estimated maximum ash load % contributions disaggregated by volcanic source and magnitude of eruption (VEI – as indicated by the colour bar) for Manila at the a) 100 year return period; b) 1,000 year return period and c) 10,000 year return period.*

5.3.3 Tokyo, Japan

The volcanic ash hazard map for Japan at the 1,000-year return period is presented in Figure 23. More than 30 volcanoes contribute to the ash hazard for Tokyo at all timescales (Isu-Tobu, Hakone, Fuji, On-take, Haku-san, Norikura, Yake-dake, Niigata-Yake-yama, Tate-yama, Myoko, Asama, Kusatsu-Shirane, Haruna, Akagi, Hiuchi, Nikko-Shirane, Takahara, Nasu, Numazawa, Bandai, Adatara, Azuma, Zao, Kurikoma, Chokai, Akita-Komaga-take, Iwate, Akita-Yake-yama, Oshima, Nii-jima, Kozu-shima, Miyake-jima, Hachijo-jima, Aoga-shima; Figure 24). The maximum calculated ash

load for Tokyo at the 100-year return period is ~1.1 x 10^{-5} kg/m^2. There are so many volcanoes contributing to the ash accumulation that the volcano contributing the most ash at this scale, Hakone, amounts to less than 10%. There are eight volcanoes contributing >5% to the ash accumulation (Hakone, Fuji, Asama, Haruna, Akagi, Kusatsu-Shirane, Takahara, Oshima), with potential eruptions at all magnitudes (Figure 24). At the 1,000-year return period, the estimated ash load increases to ~4.9 kg/m^2. Similarly Hakone is the greatest ash load contributor, but again there are still several volcanoes contributing in the 5-10% range (Figure 24). The estimated ash load increases to ~255.5 kg/m^2 at the 10,000-year return period, on the same order of magnitude as for Manila at this timescale, with Hakone volcano now the dominant contributor at almost 25% of the total anticipated ash load mostly from eruptions of VEI 4 and above. The next highest contributor at almost 15% is Fuji volcano. There are additional volcanoes contributing 5-10% towards the ash accumulation.

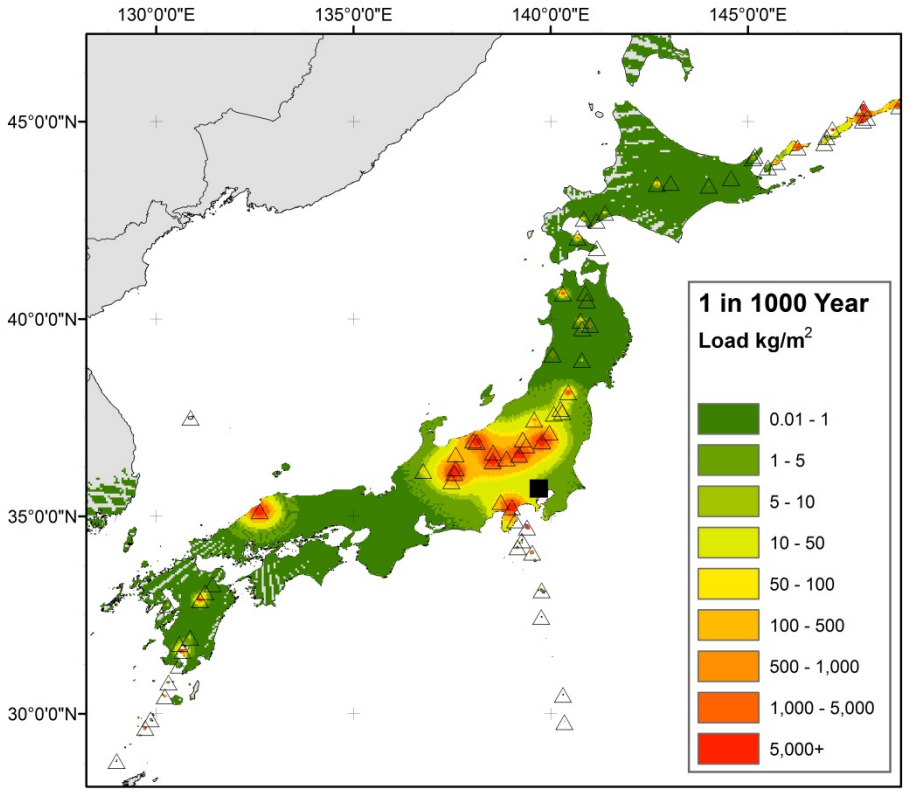

Figure 23 *Estimated maximum ash load for sites in Japan at the 1000 year return period. The colour bar indicates the maximum ash load in kg/m^2. Tokyo's location indicated by the black square, volcanoes indicated by the black-outlined triangles.*

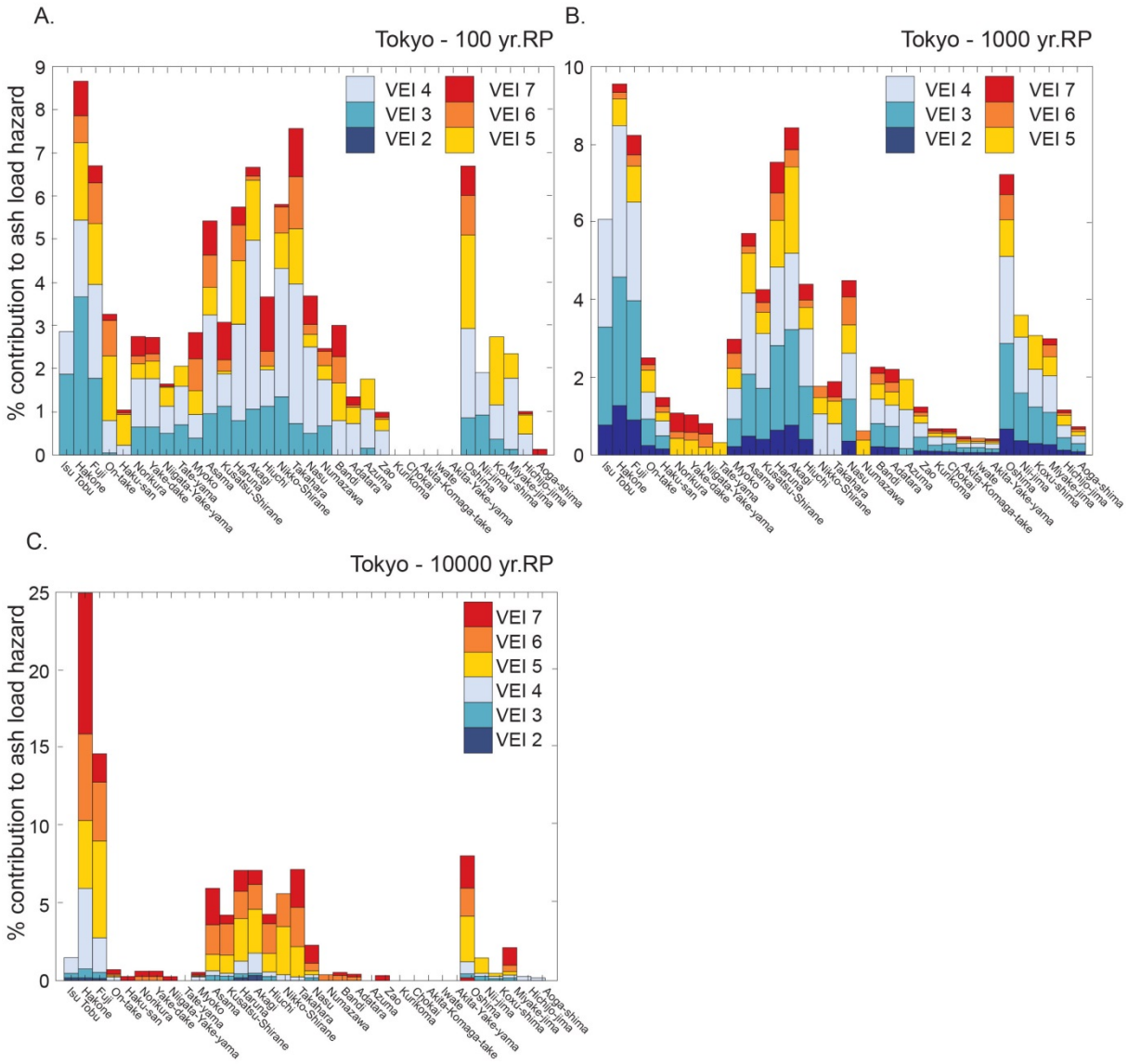

Figure 24 *Estimated maximum ash load % contributions disaggregated by volcanic source and magnitude of eruption (VEI – as indicated by the colour bar) for Tokyo at the a) 100 year return period; b) 1,000 year return period and c) 10,000 year return period.*

5.3.4 Jakarta, Indonesia

The volcanic ash hazard map for Indonesia at the 1,000-year return period is presented in Figure 25. In Indonesia, 17 volcanoes contribute to the ash hazard for Jakarta at all timescales (Dempo, Besar, Suoh, Krakatau, Gagak, Gede, Tangkubanparahu, Papandayan, Guntur, Galunngung, Ciremai, Slamet, Dieng V.C, Sundoro, Merbabu and Merapi; Figure 25). The maximum calculated volcanic ash load for Jakarta at the 100-year return period is 1.89 x 10^{-1} kg/m^2. Volcanoes contributing to the ash load hazard in Jakarta at this return period are widely dispersed across the island of Java (West, Central and East). The volcano contributing the most ash at this scale is Merbabu in Central Java, with potential eruptions at all magnitudes (mostly VEI3 and VEI4) amounting to >14% of the anticipated ash load for this site (Figure 26). This is closely followed by Merapi volcano, also in Central Java, with potential ash contributions also coming from all VEIs (again mostly VEI3 and VEI4). Merapi volcano

contributes approximately 13% of the hazard at this return period. At the 1000-year return period the maximum ash load increased to 110.3 kg/m^2. Volcanoes contributing to the ash load hazard in Jakarta are concentrated in West Java with influences from volcanoes in Central and East Java considerably diminished. Salak in West Java is now seen as the greatest ash load contributor at ~29% (mostly VEI 4) contribution (Figure 26). The contributions from Merbabu and Merapi are negligible at this return period and contributions from Gagak and Gede (also in West Java) significantly increase (24 and 19% respectively; mostly VEI 4; Figure 26). At the 10,000-year return period the maximum ash load increased to 2448.6 kg/m^2. Again volcanoes in West Java dominate the hazard for Jakarta at this return period with influences from volcanoes in Central and East Java no longer present. Salak remains the dominant contributor increasing to ~34%. The dominant eruption magnitude generated at Salak also increased from VEI 4 to VEI 5. Similarly, Gagak and Gede remain significant contributors to ash load in Jakarta at this return period, both increasing to ~27%. The proportion of VEI 4 eruptions at Gagak and Gede have also decreased and the proportion of VEI 5, 6 and 7 eruptions have increased at the 10,000-year return period.

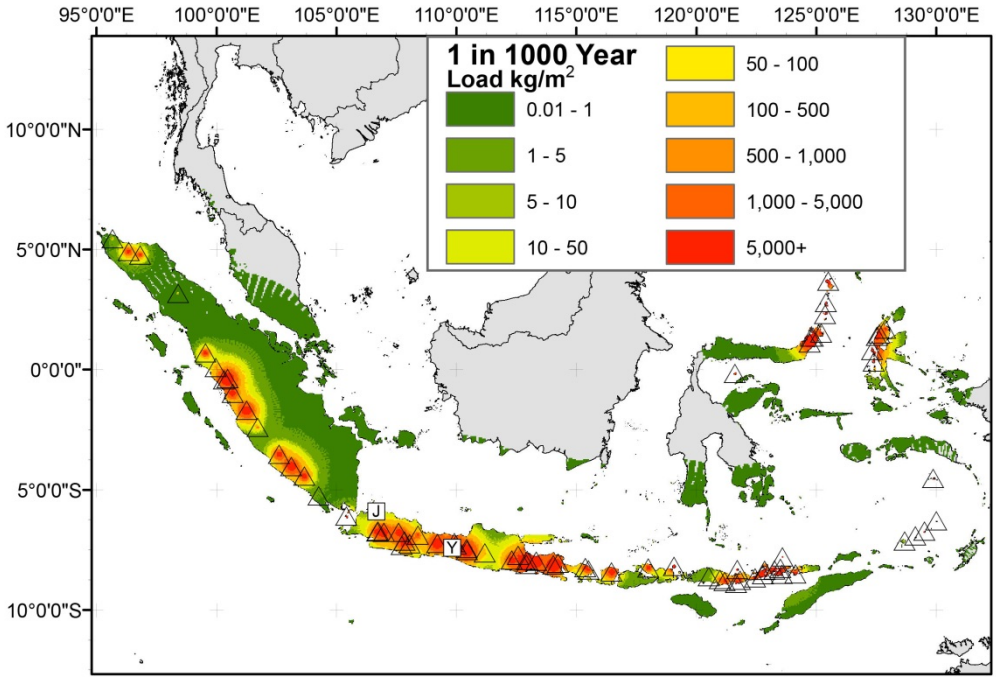

Figure 25 *Estimated maximum ash load for sites in Indonesia at the 1000 year return period. The colour bar indicates the maximum ash load in kg/m^2. Jakarta's location is indicated by the white square with the 'J' at the centre, volcanoes indicated by the black-outlined triangles.*

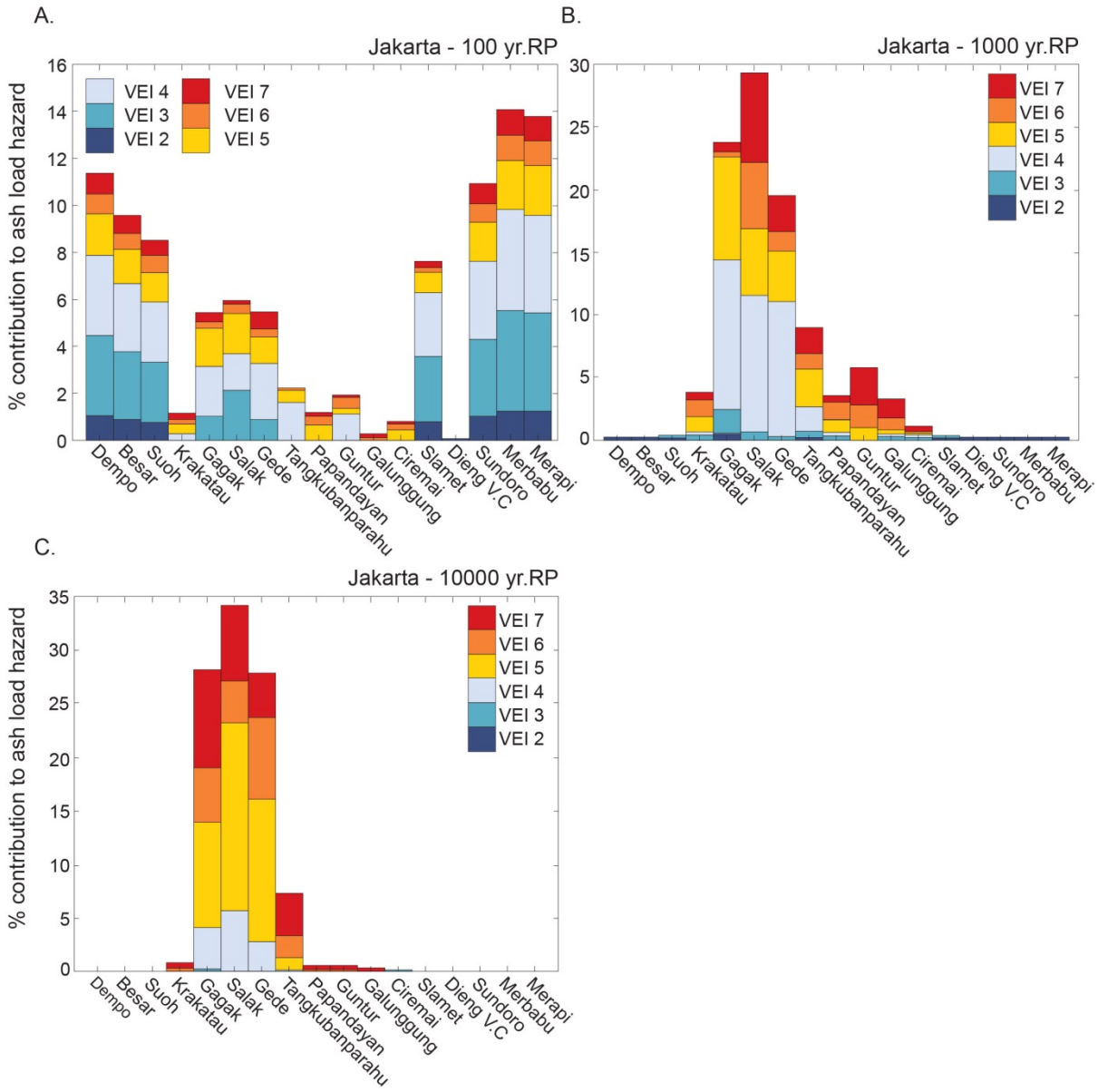

Figure 26 *Estimated maximum ash load % contributions disaggregated by volcanic source and magnitude of eruption (VEI – as indicated by the colour bar) for Jakarta at the a) 100 year return period; b) 1,000 year return period and c) 10,000 year return period.*

6 Discussion

6.1 Probabilistic Volcanic Ash Hazard Analysis for the Asia-Pacific

This PVAHA developed for the Asia-Pacific region using VAPAHR highlights the degree of volcanic ash hazard across the region as a function of return period; we identify the greatest hazard present in Indonesia at the 100-year return period, with all volcanic centers along the regional plate boundaries presenting considerable hazard at the 10,000-year return period. This PVAHA, which employed all available eruption data for the Asia-Pacific region, allows us to quickly gauge the relative ash hazard across the region and identify volcanic sources and sites that should be prioritised for more detailed analysis.

PNG, the Philippines and Japan are all countries which exhibit a high density of active volcanoes. The volcanic ash hazard maps developed in this study highlight the potential exposure of communities in these countries to volcanic ash hazard. To evaluate the risk from volcanic ash hazard for a given population, we must also consider where the populations (and their corresponding infrastructure) are located. By focusing on the capital cities for these three countries to examine the hazard, our results indicate that Port Moresby has the lowest ash hazard of the three. In this case, if Port Moresby were the only location of interest within the country, it would appear that PNG can consider lower hazard with respect to volcanic ash. However, it can be seen from the ash hazard maps that there are other areas of PNG with greater hazard, and it would be important to assess the ash hazard for towns and infrastructure within these zones (e.g. Kimbe, West New Britain).

At the 100-year and 1,000-year timescales, it can be seen that Tokyo has the highest anticipated hazard, primarily a function of the density of volcanoes in the surrounding region that are contributing to a likely ash hazard. At the 10,000-year timescale, the hazard for Tokyo is of the same order as Manila. The different ways that this hazard is shaped by source volcanoes has important implications for planning, depending on the focus of the disaster risk reduction strategy. For instance, if the goal were to target emergency management planning for a maximum likelihood event (e.g., using the 10,000-year return period), this understanding of individual volcanic contributions is critical in developing evacuation maps and monitoring strategies. In Manila, one could develop one map based upon more detailed modelling from Taal volcano, as it is likely that 70% of the ash hazard contributed at this timescale would be from this source. However, in Tokyo, whilst there is a 25% likelihood that maximum ash hazard would come from Hakone, there is still a significant likelihood that Fuji would be a contributor. This may indicate that resources for monitoring and planning should be distributed amongst the contributing volcanoes and would suggest that detailed local-scale probabilistic modelling would need to be undertaken to fully understand the hazard for Tokyo. If, for example, a global business is investigating which of their capital offices might be more prone to volcanic ash hazard in the shorter term, the focus might be directed from Manila to Tokyo, because of the higher likelihood of experiencing ash at all-time scales. To address questions at the local scale, such as the level of detail required to make evacuation maps, it is recommended that local-scale probabilistic dispersal modelling be undertaken which accounts for local variations in wind and topography.

VAPAHR integrates across all possible events (incorporating the relative frequencies of occurrence) and expected ash load (using a spectrum of eruption parameters) to arrive at a combined probability

of exceedance for a site(s) of interest (e.g., a densely populated city or critical infrastructure). There were several advantages of adopting this framework for the Asia-Pacific region case study:

- VAPAHR uses emulated volcanic ash load decay relationships, removing the need to undertake large-scale ash dispersal modelling for every source across the Asia-Pacific region, which would be time consuming and computationally intensive;
- The large-scale analyses for the Asia-Pacific region can be undertaken quickly and easily, making it possible to run new analyses as needed (e.g. as new data for the region becomes available, or a different resolution is required);
- PVAHA is advantageous for quantifying the uncertainty in our modelling of the volcanic ash hazard. The stochastic set of events represents the full spectrum of input parameters and together with the associated probabilities this enables the uncertainty assumptions to be incorporated into the final results;
- The event-based approach, which calculates hazard curves of annual probability of exceedance versus volcanic ash load at individual sites, allows for disaggregation of the hazard results (e.g., by magnitude, distance or source) at each site. This ability to easily interrogate and understand the contributing factors is a useful tool for determining risk at a site of interest (e.g., a densely populated city or piece of critical infrastructure), and for identifying priority areas for more detailed dispersal modelling at the local-scale;
- The VAPAHR tool is adaptable and can be run in serial (using a single CPU) on a desktop computer (with the timeline dependant on required resolution); it has also been optimised to run in parallel on super computer facilities. For this study we were able to utilise both forms of computation;
- VAPAHR outputs are designed to be compatible with and incorporated into risk modules such as the CAPRA/CIMNE risk-modelling platform (CIMNE et al., 2013). PVAHA outputs from this study were designed to be integrated with vulnerability and exposure information for buildings across the Asia-Pacific region (at the 5 x 5km resolution; De Bono (2013)) using the CAPRA risk engine to provide an assessment of volcanic ash risk (the results of which will be presented as part of GAR 2015 Global Assessment Report on Disaster Risk Reduction 2015). The VAPAHR tool simplified the process of tailoring outputs for this application (e.g. scale and setting of return periods). However the tool can be configured to just as easily run at 1 x 1km resolution if needed for integration with global population datasets (e.g., GPW3 data – CIESIN-CIAT, 2005).

VAPAHR establishes the integrated volcanic ash hazard for each scenario in the catalogue for a location (or region) of interest. The ability to disaggregate the results of the analysis can be beneficial when it comes to prioritising funding or developing mitigation strategies, particularly for sites with multiple volcanic sources contributing to the anticipated hazard, when emergency planning will need to be more complex and will need to be tailored appropriately.

6.2 Addressing uncertainty

It is acknowledged that volcanic ash dispersal models have inherent limitations including their ability to accurately resolve ash accumulation at ground level at great distances (i.e. >500km), the overestimation of ash accumulations close to vent (i.e. 0-2km) and uncertainty associated with meteorological controls on the dispersal of ash particles. The PVAHA framework adopted here acknowledges these limitations and seeks to address each by promoting a transparent methodology

for identifying and carrying through these uncertainties in the resulting analysis. The implications of this approach are discussed here.

The ability of dispersal modelling to adequately represent ash fall hazard on the ground at increasing distances is not well validated. Ash accumulation at ground level, more than 1,000km from source is rare (Blong, 1994). It is acknowledged that ash accumulation at ground level does occur at great distances (i.e. 500 -1000 km) however the ability of dispersal models to resolve this is not well tested. Therefore a 500km distance threshold is imposed here as a confidence limit for estimating ground loading of volcanic ash using dispersal models at the regional-scale. As a consequence, volcanic ash accumulation beyond 500km in mapped ash deposits may not be captured. For example the results from Western New Guinea (Irian Jaya) and Kalimantan show no ash hazard at any return period. This is an artefact of the imposed 500km distal limit. Instances such as this have important implications for the hazard assessment such that at longer time scales, the footprint for a given threshold of ash loading might be expected to increase beyond the imposed 500km limit, meaning that the distribution of ash at the longer return periods (e.g. 10,000 years) may be underestimated. Dispersal models typically overestimate the ash accumulation at proximal locations (0-2km from vent). Therefore calculated values within a 0-2km radius applied to each volcano are excluded from the analysis as these values are most certainly exaggerated due to simplifications in the dispersal modelling.

Wind is considered one of the major controls on short to medium range ash fall deposits, particularly for small to moderate eruptions (e.g., Mortazavi et al., (2009)) . Whilst the effect of wind direction has been recognized for some time, the complex interactions of eruption plumes and meteorological conditions are still an active area of research (Woodhouse et al., 2013). To adequately represent wind at a given volcano location for the purpose of fully probabilistic analysis it is necessary to interrogate the full range of meteorological data, in order to incorporate the uncertainty in any particular set of conditions, over a period of years and for temporal ranges that sufficiently characterize the seasonal variations. For a regional-scale study it would require both time and computational resources to fully capture ‘all wind’ scenarios, rather than just subsets of data. In this study, a greatly simplified representation of the wind field was implemented, and each wind direction is given an equal weighting in the calculation process and as such does not account for prevailing wind conditions. It is acknowledged that this will lead to an underestimation of volcanic ash hazard at sites located in line with prevailing winds and an overestimation of hazard in other directions, particularly at shorter return periods. Consider PNG, where prevailing winds are from the southeast. Rabaul volcano is located northwest of the town of Kokopo (East New Britain). In this instance volcanic ash hazard at sites in Kokopo may be overestimated using this model. Given the simplified meteorological input, the results of the Asia-Pacific region modelling are intended to provide a broad overview of regional scale volcanic ash hazard for informing a partial volcanic ash risk assessment for the GAR15 and more generally for prioritising areas for more detailed local-scale dispersal modelling. Development of wind customised for each volcano location is recommended for any future sub-regional case studies and hazard results presented here should not be used as an alternative to tested and accepted methods of undertaking local scale hazard modelling (e.g., dispersal modelling) or for local-scale decision-making.

6.3 Future directions

The PVAHA methodology presented here is fully customisable and can be modified to reflect advances in our understanding of the dynamics of volcanic ash dispersal, improvement of statistical analysis techniques for historical eruptive events and ever increasing capabilities in high-performance computing. There is no limit to the number of ash dispersal models which could be used to generate

ALPEs for consideration and this allows multiple competing hypotheses on models and parameters to be incorporated into the analysis.

The VAPAHR tool currently addresses hazard, however the modular nature of the tool supports a framework for risk analysis. For example, a python module for damage (i.e. building damage, infrastructure damage or agricultural crop damage), containing vulnerability functions for volcanic ash could be developed and integrated into the VAPAHR tool. Vulnerability functions are defined here as the relationship between the potential damage to exposed elements (e.g. buildings, agricultural crops, critical infrastructure) and the amount of ash load (Blong, 2003; Blong, 1980; Spence et al., 2005; Wilson et al., 2012). Through integrating the hazard module (presented here) with a damage module, the conditional probability of damage (or loss in dollars) for an exposed element could be calculated for a given threshold of volcanic ash load. The resulting damage curves could be integrated with an exposure data module (e.g. population density, building footprints and crop extents) for the region of interest and the potential impact of events could be quantified in a risk framework.

Determination of the record of completeness for the Asia-Pacific region is difficult and can have a significant impact on the probability values derived for those sources (e.g., volcanoes with long repose periods might be under-represented and uncertainty in estimating the completeness of eruption data will affect the probabilities). The results of this analysis are highly sensitive to the accuracy of the statistical characterisation of the volcanic sources and thus are susceptible to gaps in the eruption database. This is demonstrated by high ash hazard for the Kamchatka area that is clearly dominated by the Kluchevskoi cluster, which has been very active in recent times. The preservation of eruption deposits is inherently biased by the size of the eruption (larger eruptions are more likely to be preserved in the record (Simpson et al., 2011). The record completeness is also influenced by country specific factors such as the population and record keeping procedures. This highlights that the magnitude-frequency relationships for volcanic sources in the region need to be refined and updated as new information becomes available, such as sustained programs of field studies and lab analysis aimed at better characterisation of individual volcano histories.

Whilst gaps in the database of volcanic eruptions (in this case GVP) and bias from well-documented eruptions exist, these known limitations highlight the need to continually update hazard assessments. The advantage of the PVAHA framework and the VAPAHR tool used here for the regional-scale analysis is that it can be quickly (on the order of days depending on the required resolution and available resources) re-run once an eruption occurs in the Asia-Pacific region, or further data are collected and compiled, with probabilities updated. The ability to quickly run the tool opens the door to exploring anticipated hazard using different catalogues of information. For example, we can employ more detailed catalogues where the data exists or predictive catalogues where the current catalogue represents a conservative approach (e.g., the current catalogue represents a minimum level of completeness and we assume that there has been a higher level of activity). The stochastic approach means that alternating hypotheses could be represented in the analysis and explored.

7 Concluding Remarks

The management of natural hazard risk is central to ensuring the sustainability of communities and economic activity within a country. This risk is particularly high in some developing nations as a result of the nature of local building stock, the size of human populations and a high natural hazard. This risk is manifested in severe events which inflict considerable damage, loss of life, socio-economic disruption and place acute demands on emergency services. Ultimately, these often devastating consequences can only be addressed with the uptake of effective and targeted disaster risk reduction strategies based on reliable risk information. Consistent information of this kind can enable decision makers to identify, quantify and manage risk with the objective of reducing it at a national scale.

The Asia-Pacific region is highly susceptible to volcanic ash hazard, with this hazard duly corresponding to the most active volcanic arc systems across the region, particularly Japan, the Philippines, PNG, the Kamchatka peninsula (Russia), and the north island of New Zealand. The greatest volcanic ash hazard is exhibited by the Indonesian Island Arc system at all observable return periods. Volcanic ash is a hazard that does not confine itself within national borders. Even small amounts of ash can cause disruption to civil aviation routes, critical infrastructure and other exposed elements. Countries without volcanoes still need to be aware of the hazard that might exist. Given the extensive nature of the impacts from ash hazard and the increasing interconnectivity and globalisation of communication, transport and economies, it is important to understand the hazard on the breadth of scales used for long-term strategic planning.

When examining hazard on a regional to global scale, methods and tools that are employed for local-scale analysis may not be suitable due to computational or time constraints. Quantifying volcanic ash hazard on a large scale will at present require simplified approaches and coarser input datasets. Here we demonstrate an application of the PVAHA methodology for the Asia-Pacific region, using the recently developed VAPAHR tool for emulating multi-scale volcanic ash load hazard. This PVAHA, which employed all available eruption data for the Asia-Pacific region, allows us to quickly gauge the relative ash hazard across the region and identify volcanic sources and sites that should be prioritised for more detailed analysis. Results were disaggregated for sites of interest (e.g. Jakarta, Indonesia; Manila, the Philippines; Port Moresby, Papua New Guinea and Tokyo, Japan) in order to demonstrate how this multi-scale event-based approach allows for the rapid dissemination and disaggregation of results to identify priority areas subject to high volcanic ash hazard and the broader implications of this for disaster risk reduction efforts. This first step towards a fully probabilistic model of volcanic ash hazard for the Asia-Pacific region will be refined through the incorporation of updated eruption data when manifested and the inclusion of finer resolution meteorological models. In this manner, we can move towards a better understanding of the relative volcanic ash hazard in the Asia-Pacific region that can be updated quickly and easily as new information becomes available.

This PVAHA was delivered to our GAR partners in the CAPRA team for integration with vulnerability and exposure information using the CAPRA risk engine to provide a partial assessment of volcanic ash risk for the Asia-Pacific region, the results of which will be presented as part of GAR 2015 Global Assessment Report on Disaster Risk Reduction 2015.

References

Barberi, F., Macedonio, G., Pareshci, M.T. and R, S., 1990. Mapping tephra fallout risk: an example from Vesuvius, Italy. Nature, 344: 142-144.

Barrientos, S.E. and Ward, S.N., 1990. The 1960 Chile earthquake: inversion for slip distribution from surface deformation Geophysical Journal International, 103(3): 589-598.

Bear-Crozier, A.N., Davies, G., Dunford, M.A., Ghasemi, H., Horspool, N., Jakab, M., Metz, L., Miller, V., Power, L. and Robinson, D., 2013. Integrating hazard and exposure for East New Britain. Geoscience Australia Professional Opinion, 2013/07(GeoCat 75462): 238.

Bear-Crozier, A.N., Kartadinata, N., Heriwaseso, A. and Nielsen, O., 2012. Development of python-FALL3D: a modified procedure for modelling volcanic ash dispersal in the Asia-Pacific region. Natural Hazards, 64: 821-838.

Bear-Crozier, A.N., Miller, V., Newey, V., Horspool, N. and Weber, R., in revision. Probabilistic Volcanic Ash Hazard Analysis (PVAHA) I: Development of the VAPAHR tool for emulating multi-scale volcanic ash fall analysis. Submitted to Journal of Applied Volcanology.

Blong, R., 1994. The Rabaul eruption, 1994. Australian Geographer, 25(2): 186-190.

Blong, R., 2003. Building damage in Rabaul, Papua New Guinea, 1994. Bulletin of Volcanology, 65(1): 43-54.

Blong, R.J., 1980. Some effects of tephra falls on buildings. In: S. Self and R.S.J. Sparks (Editors), Tephra studies. Proc NATO Advanced Studies Institute, Laugarvatn and Reykjavik, pp. 405–420.

Bommer, J.J. and Scherbaum, F., 2008. The Use and Misuse of Logic Trees in Probabilistic Seismic Hazard Analysis. Earthquake Spectra, 24(4): 997-1009.

Bonadonna, C., Connor, C.B., Houghton, B.F., Connor, L., Byrne, M., Laing, A. and Hincks, T.K., 2005. Probabalistic modelling of tephra dispersal: Hazard assessment of a multiphase rhyolitic eruption at Tarawera, New Zealand. Journal of Geophysical Research, 110(B3).

Bonadonna, C., Ernst, G.G.J. and Sparks, R.S.J., 1998. Thickness variations and volume estimates of tephra fall deposits: the importance of particle Reynolds number. Journal of Volcanology and Geothermal Research, 81(3–4): 173-187.

Bonadonna, C. and Houghton, B.F., 2005. Total grain-size distribution and volume of tephra-fall deposits. Bulletin of Volcanology, 67: 441-456.

Bonadonna, C., Macedonio, G. and Sparks, R.S.J., 2002a. Numerical modelling of tephra fallout associated with dome collapses and Vulcanian explosions: application to hazard assessment on Montserrat. In: T.H. Druitt and B.P. Kokelaar (Editors), The eruption of Soufrière Hills Volcano, Montserrat, from 1995 to 1999. Geological Society London Memoir, pp. 517-537.

Bonadonna, C., Mayberry, G.C., Calder, E.S., Sparks, R.S.J., Choux, C., Jackson, P., Lejeune, A.M., Loughlin, S.C., Norton, G.E., Rose, W.I., Ryan, G. and Young, S.R., 2002b. Tephra fallout in theeruption of Soufrière Hills Volcano, Montserrat. In: T.H. Druitt and B.P. Kokelaar (Editors), The eruption of Soufrière Hills Volcano, Montserrat, from 1995 to 1999. Geological Society London, Memoir, pp. 483-516.

Burbidge, D. and Cummins, P., 2007. Assessing the threat to Western Australia from tsunami generated by earthqaukes along the Sunda Arc. Natural Hazards, 43: 319-331.

Burbidge, D., Cummins, P., Mleczko, R., Latief, H., Mokhtari, M., Natawidjaja, D., Rajendran, C.P. and Thomas, C., 2009. A probabilistic tsunami hazard assessment of Indian Ocean nations. Geoscience Australia Record, 2009/11.

Burbidge, D., Cummins, P., Mleczko, R. and Thio, H., 2008. A probabilistic tsunami hazard assessment for Western Australia Pure and Applied Geophysics 165: 2059-2088.

Burbidge, D., Leonard, M., Allen, T., Collins, C. and Volti, T., 2012. The 2012 National Earthquake Hazard Map of Australia. Australian Earthquake Engineering Society 2012 Conference

Bursik, M., 2001. Effect of wind on the rise height of volcanic plumes. Geophysical Research Letters, 18: 3621-3624.

Butler, L., Crowley, H., Henshaw, P., Monelli, D., Nastasi, M., Panseri, L., Pagani, M., Silva, V., Simionato, M., Vigan`o, D., Weatherill, G. and Wyss, B., 2013. OpenQuake Engine User Manual Version 1.0.0 Beta. Global Earthquake Model Pavia, Italy.

CIMNE, SAS, I., LTDA, I. and SA, E., 2013. Probabilistic modelling on natural risks at the global level: Global Risk Model 2013. .

Cornell, C., 1968. Engineering seismic risk analysis. Bulletin of the Seismological Society of America, 58: 1583-1606.

Costa, A., Dell'Erba, F., Di Vito, M.A., Isaia, R., Macedonio, G., Orsi, G. and Pfeiffer, T., 2009. Tephra fallout hazard assessment at Campi Flegrei caldera (Italy). Bulletin of Volcanology, 71: 259-273.

Costa, A., Macedonio, G. and Folch, A., 2006. A three-dimensional Eulerian model for transport and deposition of volcanic ashes. Earth and Planetary Science Letters, 241: 634-647.

Crosweller, S., Arora, B., Brown, S.K., Cottrell, E., Deligne, N.I., Ortiz Guerrero, N., Hobbs, L., Kiyosugi, K., Loughlin, S.C., Lowndes, J., Nayembil, M., Siebert, L., Sparks, R.S.J., Takarada, S. and Venzke, E., 2012. Global database on large magnitude explosibe voclanic eruptions (LaMEVE). Journal of Applied Volcanology, 1(4): doi:10.1186/2191-5040-1181-1184

De Bono, A., 2013. The Global Exposure Database for GAR 2013. Geneva, Switzerland.

Dhu, T., Robinson, D., Clark, D., Gray, D. and Row, P., 2008. Event based earthquake risk modelling, The 14th World Conference on Earthquake Engineering, Beijing, China

Folch, A., Cavazzoni, C., Costa, A. and Macedonio, G., 2008a. An automatic procedure to forecast tephra fallout. Journal of Volcanology and Geothermal Research, 177: 767-777.

Folch, A., Costa, A. and Basart, S., 2012. Validation of the FALL3D ash dispersion model using obsrvations of the 2010 Eyjafjallajokull volcanic ash clouds. Atmospheric Environment, 48: 165-183.

Folch, A., Costa, A. and Macedonio, G., 2009. FALL3D: A computational model for transport and deposition of volcanic ash. Computers and Geosciences, 35: 1334-1342.

Folch, A., Jorba, O. and Viramonte, J., 2008b. Volcanic ash forecast - application to the May 2008 Chaiten eruption. Natural Hazards and Earth System Sciences, 8: 927-940.

Folch, A. and Sulpizio, R., 2010. Evaluating long-range volcanic ash hazard using supercomputing facilities: application to Somma-Vesuvius (Itay), and consequences for civil aviation over the Central Mediterranean Area. Bulletin of Volcanology, 72: 1039-1059.

Fulford, G., Jones, T., Stehle, J., Corby, N., Robinson, D., Schneider, J. and Dhu, T., 2002. Earthquake risk in Newcastle and Lake Macquarie. Geoscience Australia Record 2002/15: 103–122.

Horspool, N., Pranantyo, I., Griffin, J., Latief, H., Natawidjaja, D., Kongko, W., Cipta, A., Anugrah, S. and Thio, H., in press. A probabilistic tsunami hazard assessment for Indonesia Natural Hazards Earth System Sciences.

Hurst, A.W., 1994. ASHFALL - A computer program for estimating volcanic ash fallout (Report and User Guide). Institute of Geological & Nuclear Sciences science report 94(23).

Hurst, A.W. and Turner, R., 1999. Performance of the program ASHFALL for forecasting ashfall during the 1995 and 1996 eruptions of Ruapehu volcano. New Zealand Journal of Geology and Geophysics, 42: 615-622.

Jenkins, S., Magill, C., McAneney, J. and Blong, R., 2012a. Regional ash fall hazard I: a probabilistic approach methodology. Bulletin of Volcanology, 74: 1699-1712.

Jenkins, S., Magill, C., McAneney, J. and Hurst, A.W., 2008. Multi-stage volcanic events: tephra hazard simulations for the Okataina Volcanic Centre, New Zealand. Journal of Geophysical Research, 113(F04012).

Jenkins, S., McAneney, J., Magill, C. and Blong, R., 2012b. Regional ash fall hazard II: Asia-Pacific modelling results and implications. Bulletin of Volcanology, 74: 1713-1727.

Macedonio, G., Costa, A. and Folch, A., 2008. Ash fallout scenarios at Vesuvius: Numerical simulations and implications for hazard assessment. Journal of Volcanology and Geothermal Research, 178: 366-377.

Magill, C.R., Hurst, A.W., Hunter, L.J. and Blong, R.J., 2006. Probabilistic tephra fall simulation for the Auckland Region, New Zealand. Journal of Volcanology and Geothermal Research, 153(3-4): 370-386.

Maqsood, T., Wehner, M., Ryu, H., Edwards, M., Dale, K. and Miller, V., 2014. GAR15 Regional Vulnerability Functions: Reporting on the UNISDR/GA SE Asian Regional Workshop on Structural Vulnerability Models for the GAR Global Risk Assessment, 11–14 November, 2013, Geoscience Australia, Canberra, Australia. Geoscience Australia Record, 2014/38.

Marrero, J.M., Garcia, A., Llinares, A., Rodriguez-Losada, J.A. and Ortiz, R., 2012. A direct approach to estimating the number of potential fatalities from an eruption: Application to the Central Volcanic Complex of Tenerife Island. Journal of Volcanology and Geothermal Research, 219-220: 33-40.

McGuire, R., 1995. Probabilistic seismic hazard analysis and design earthquakes: Closing the loop. Bulletin of the Seismological Society of America, 85: 1275-1284.

McGuire, R., 2008. Review - Probabilistic Seismic Hazard Analysis: Early History. Earthquake Engineering and Structural Dynamics, 37: 329-338.

McKee, C., Johnson, R.W., Lowenstein, P.L., Riley, S.J., Blong, R.J., De Saint Ours, P. and Talai, B., 1985. Rabaul Caldera, Papua New Guinea: volcanic hazards, surveillance, and eruption contingency planning. Journal of Volcanology and Geothermal Research, 23: 195-237.

Mead, S.R. and Magill, C., in revision. Determining change points in data completeness for the Holocene eruption record. Submitted to Bulletin of Volcanology.

Miller, V., Bear-Crozier, A.N., Newey, V., Horspool, N. and Weber, R., in revision. Probabilistic Volcanic Ash Hazard Analysis (PVAHA) II : Assessment of the Asia-Pacific region using VAPAHR. Journal of Applied Volcanology.

Mortazavi, M., Sparks, R.S.J. and Amigo, A., 2009. Evidence for Recent Large Magnitude Explosive Eruptions at Damavan Volcano, Iran, with Implications for Volcanic Hazards.

Musson, R.M.W., 2000. The use of Monte Carlo simulations for seismic hazard assessment in the U.K. Annals of Geophysics, 43(1).

Robinson, D., Dhu, T. and Schneider, J., 2006. Practical probabilistic seismic risk analysis: A demonstration of capability. Seismological research letters, 77(4): 453-459.

Robinson, D., Fulford, G. and Dhu, T., 2005. EQRM: Geoscience Australia's Earthquake Risk Model. Technical Manual Version 3.0. Geoscience Australia Record 2005(1).

Rose, W.I. and Durant, A., 2011. Fate of volcanic ash: Aggregation and fallout. Geology, 39(9): 895-896.

Siebert, L., Simkin, T. and Kimberley, P., 2010. Volcanoes of the world (3rd Edition), Berkley: Univ California 551 pp.

Simpson, A., Johnson, R.W. and Cummins, P., 2011. Volcanic threat in developing countries of the Asia-Pacific region: probabilistic hazard assessment, population risks, and information gaps. Natural Hazards, 57: 151-165.

Sinadinovski, C., Edwards, M., Corby, N., Milne, M., Dale, K., Dhu, T., Jones, A., McPherson, A., Jones, T., Gray, D., Robinson, D. and White, J., 2005. Earthquake Risk, Natural hazard risk in Perth, Western Australia - A Comprehensive Report. Geoscience Australia Report pp. 143-208.

Sparks, R.S.J., Bursik, M., Carey, S., Gilbert, J.S., Graze, L.S., Sigurdsson, H. and Woods, A.W., 1997. Volcanic Plumes. Wiley and Sons, Chichester, 574 pp.

Spence, R.J.S., Kelman, I., Baxter, P.J., Zuccaro, G. and Petrazzuoli, S., 2005. Residential building and occupant vulnerability to tephra fall. Natural Hazards and Earth System Sciences, 5(4): 477-494.

Stirling, M.W. and Wilson, C.J.N., 2002. Development of a volcanic hazard model for New Zealand: First approaches from the methods of probabilistic seismic hazard analysis. Bulletin of the New Zealand Society for Earthquake Engineering 35(4): 266-277.

Suzuki, T., 1983. A theoretical model for dispersion of tephra. In: D. Shimozuru and Y. I (Editors), Arc volcanism: Physics and tectonics. Terra Scientific Publishing Company, Tokyo.

TERA, 1980. Seismic hazard analysis: a methodology for the Eastern United States, US Nuclear Regulatory Commision Report No. NURED/CR-1582

Thomas, C. and Burbidge, D., 2009. A probabilisic tsuanmi hazard assessment of the Southwest Pacific nations. Geoscience Australia Record, 2009/02.

Wilson, T.M., Stewart, C., Sword-Daniels, V., Leonard, G., Johnston, D., Cole, J.W., Wardman, J., Wilson, G. and Barnard, S., 2012. Volcanic ash impacts on critical infrastructure. Physics and Chemistry of the Earth Parts A/B/C, 45-46: 5-23.

Woodhouse, M.J., Hogg, A.J., Phillips, J.C. and Sparks, R.S.J., 2013. Interaction between volcanic plumes and wind during the 2010 Eyjafjallajokull eruption, Iceland. Journal of Geophysical Research, 118: 92-109.